Investigation of Catalytic Activity and Selectivity of Pd and Ni Loaded Clinoptilolite Rich Natural Zeolite for Citral Hydrogenation

By

Şule UÇAR

A Dissertation Submitted to the
Graduate School in Partial Fulfillment of the
Requirements for the Degree of

MASTER OF SCIENCE

Department: Chemical Engineering
Major: Chemical Engineering

Izmir Institute of Technology
Izmir, Turkey

October, 2002

We approve the thesis of **Şule UÇAR**

Date of Signature

…….. **24.10.2002**

Assist. Prof. Dr. Selahattin YILMAZ

Supervisor

Department of Chemical Engineering

…….. **24.10.2002**

Prof. Dr. Levent ARTOK

Co-Supervisor

Department of Chemistry

…….. **24.10.2002**

Prof. Dr. Gönül GÜNDÜZ

Department of Chemical Engineering

Ege University

…….. **24.10.2002**

Prof. Dr. Devrim BALKÖSE

Department of Chemical Engineering

…….. **24.10.2002**

Assist. Prof. Dr. Oğuz BAYRAKTAR

Department of Chemical Engineering

…….. **24.10.2002**

Prof. Dr. Devrim BALKÖSE

Head of Department

ACKNOWLEDGEMENTS

I would like to thank my thesis advisors, Assist. Prof. Selahattin Yılmaz and Prof. Dr. Levent Artok for their help, support and encouragement throughout the course of this study.

Special thanks to Prof. Dr. Semra Ülkü for providing the Gas Chromatography and zeolites.

Thanks to Korhan Demirkan for his help and support during construction of the experimental set-up.

I would like to thank Güler Narin and Nesrin Tatlıdil for their assistance during performing gas chromatography experiments. I also wish to thank to the research assistants for their assistance in characterization studies.

Additionally, my deepest thanks to my officemates: Berna Topuz, Hacer Yenal, Deniz Şimşek, Sevdiye Atakul, Metin Becer and Mehmet Gönen for their friendship, help and supports. I also present my special thanks to my family for their patients and love especially to my husband, Arda Samık for his great encouragement.

ABSRACT

The preparation of active and selective clinoptilolite rich natural zeolite supported palladium and nickel catalysts for the liquid phase hydrogenation of citral was investigated. The catalysts were prepared by impregnation and ion exchange methods. Catalytic activity and selectivity tests were performed in a semi-batch reactor for different calcination temperatures, pressures, stirring rates, reaction temperatures, amount of catalysts, ethanol sources, catalyst metal loadings and catalysts preparation methods. Catalyst deactivation was also investigated.

The characterization results showed that clinoptilolite was the major mineral in natural zeolite used as catalyst and catalyst support. It was thermally stable up to 440°C and its stability improved with Pd and Ni loading. Catalysts with loading of 0.72, 2.42, 5.63 % Pd and 3.12 % Ni were prepared by impregnation method. One catalyst was prepared by Pd ion exchange (5.66 %). Surface areas of the catalyst samples changed with calcination temperature, method of metal loading, amount of metal loading. A calcination temperature of 430°C and catalyst metal loading of 2.42 % Pd provided the largest surface area (38.96 m^2/g) among the catalysts prepared by impregnation. The catalyst prepared by ion exchange had a much more larger surface area (49.46 m^2/g) than those prepared by impregnation.

The product distribution changed with catalysts prepared by different methods, catalyst metal loadings, catalyst calcination temperatures and reaction temperatures. The results showed that the Pd catalyst prepared by impregnation favoured the hydrogenation of the conjugated double bond of citral, giving citronellal as the primary hydrogenation products, whereas the amounts of unsaturated alcohols were very minor. High selectivity to citronellal was obtained for the catalyst calcined at 430°C containing 2.42 % Pd. The product distribution and the reaction rates were affected significantly by the reaction temperature (80, 100 and 120°C). The highest selectivity to citronellal (88 %) and the yield of citronellal (87 %) were obtained at 120°C. Higher reaction rates were observed as temperature increased.

Increasing the amount of the catalyst in the reaction medium (150, 250 and 400 mg/100mL) affected the reaction rates, selectivity and the yield of citronellal. The highest amount of citronellal yield (91 %) was obtained when the reaction was carried out in the presence of the largest amount of the catalyst (400 mg/100 mL) used in this study. Different product distributions were obtained with various ethanol sources. Higher yields and selectivities were obtained with more pure solvent.

Product distribution changed with catalyst metal loading. First increased significantly by changing catalyst loading from 0.72 to 2.42 % Pd and then rised slowly when metal loading changed from 2.42 to 5.63 % Pd. This was attributed to active metal surface area and its dispersion. Impregnated Pd catalysts regained their activities and selectivities upon regeneration.

Ni impregnated catalyst showed a different product distribution. It showed a lower activity for a given temperature. Overall selectivities of the best Pd catalyst and Ni catalysts were similar.

Pd catalyst prepared by ion exchange gave different products and its selectivity to citronellal was the lowest. This was attributed to the metal and catalyst surface interactions.

ÖZ

Bu çalışmada paladyum ve nikel yüklü klinoptilolitçe zengin doğal zeolitlerin sıvı fazda sitral hidrojenasyon tepkimelerinde katalizör olarak kullanımı araştırılmıştır. Katalizörler emdirme ve iyon değiştirme metotları ile hazırlanmışlardır. Katalizörlerin aktiviteleri ve seçiciliklerine; kalsine sıcaklığı, basınç, karıştırma hızı, reaksiyon sıcaklığı, katalizör miktarı, etanol kaynağı gibi tepkime parametrelerinin etkileri incelenmiştir. Tepkimeler karıştırmalı ve yarı kesikli bir reaktörde gerçekleştirilmiştir. Katalizör deaktivitasyonu da incelenmiştir.

Karakterizasyon sonuçları katalizör ve katalizör destek malzemesi olarak kullanılan doğal zeolitte, klinoptilolitin başlıca mineral olduğunu göstermiştir. Klinoptilolit 440°C'ye kadar ısıl kararlılık göstermektedir ve kararlılığı Pd ve Ni yüklenmesiyle artış göstermiştir. % 0.72, 2.42, 5.63 Pd ve % 3.12 Ni içeren katalizörler emdirme metoduyla hazırlanmıştır. % 5.66 Pd içeren katalizör de iyon değiştirme metoduyla hazırlanmıştır. Katalizör örneklerinin yüzey alanı kalsinasyon sıcaklığı, metal yükleme metodu ve yüklenen metal miktarı ile değişmiştir. Emdirme metoduyla hazırlanan katalizörler arasında 430°C kalsinasyon sıcaklığındaki katalizör ve % 2.42 Pd yüklü katalizör en yüksek yüzey alanını (38.96 m^2/g) sağlamıştır. İyon değiştirme metoduyla hazırlanan katalizörün emdirme metoduyla hazırlanan katalizörden daha büyük yüzey alanına (49.46 m^2/g) sahip olduğu bulunmuştur.

Ürün dağılımı farklı metotlarla hazırlanan katalizörlerle, katalizöre metal yüklemesiyle, katalizör kalsinasyon sıcaklıklarıyla ve reaksiyon sıcaklıklarıyla değişmiştir. Sonuçlar, emdirme metoduyla hazırlanan Pd katalizörlerle doymamış alkol oluşumunun çok düşük olduğunu göstermektedir. Pd katalizörlerinin sitralin konjuge çift bağlarının hidrojenasyonuyla sitronelal dönüşümünde çok etkin olduğu saptanmıştır. 430°C sıcaklıkla kalsine edilmiş, %2.42 Pd içeren katalizör en yüksek sitronelal seçiciliği ile elde edilmiştir. Ürün dağılımı ve reaksiyon hızı reaksiyon sıcaklığından (80, 100 ve 120°C) etkilenmiştir. Sitronelala en yüksek seçicilik (% 88) ve verim (% 87) 120°C'de gözlenmiştir. Sıcaklığın artmasıyla reaksiyon hızı artış göstermiştir.

Reaksiyon ortamında katalizör miktarının (150, 250 ve 400 mg/100 ml) artması reaksiyon hızlarını, seçiciliği ve sitronelal verimini etkilemiştir. En fazla katalizör miktarıyla gerçekleşen reaksiyon ile sitronelala verim maksimum değerine (% 91) ulaşmıştır. Az yan ürün oluşmuştur. Değişik etanol kaynaklarıyla farklı ürün dağılımları elde edilmiştir. Daha saf solvent ile daha yüksek seçicilik ve verim sağlanmıştır.

Katalizör üzerindeki metal miktarı ürün dağılımını değiştirmiştir. Katalizör üzerindeki Pd miktarının % 0.72'den % 2.42'ye artması katalizör aktivitesini önemli bir miktarda arttırmıştır. Fakat katalizöre yüklenen metal miktarı % 5.63'e çıkarıldığında reaksiyon hızında çok az bir artış gözlenmiştir. Bu da aktif metal yüzey alanına ve dağılımına bağlanmıştır. Pd emdirilmiş katalizörler aktivite ve seçiciliklerini rejenerasyonla geri kazanmışlardır.

Ni emdirilmiş katalizör faklı bir ürün dağılımı ve aynı sıcaklık için daha düşük aktivite göstermiştir. En iyi Pd ve Ni katalizörlerinin seçicilikleri benzer bulunmuştur.

İyon değiştirmeyle hazırlanan Pd katalizörü farklı ürünler vermiş ve sitronelala en düşük seçicilik bu katalizörlerle gözlenmiştir. Bu durum metal ve katalizör yüzey etkileşimlerine bağlanmıştır.

TABLE OF CONTENTS

LIST OF FIGURES

LIST OF TABLES

CHAPTER 1

INTRODUCTION

Hydrogenation reactions are widely used in petroleum, petrochemical, margarine and oil industries for the production of many basic organic chemicals. The organic chemicals industry is based on the manufacture and processing of a great number of compounds. Their chemical formulas have several reactive groups and their production is consequently complicated and costly [1]. Approximately 50-100 kg of by-product can be produced for a single kilogram of product in the fine chemicals [2].

The role of heterogeneous catalysis in the production of fine chemicals is becoming increasingly more important. One important reaction is the selective hydrogenation of α, β unsaturated aldehydes [3]. Citral is an unsaturated aldehyde, which contains both an isolated and conjugated double bond and a carbonyl group. Citral and citral hydrogenation products are important intermediates for production of perfumes, fragrance and pharmaceuticals [4]. The selective hydrogenation is a challenge since the C=C bond is much easily attacked than the C=O bond when a conventional heterogeneous catalyst is used. Therefore, many studies have been made to develop a suitable industrial catalyst that would be able to lead a very high selectivity at total conversion [5].

Many factors have been reported to influence the selectivity of the reaction, among them the nature and particle size of the metal catalyst, the presence of promoters and the catalyst support [6].

The effects of reaction conditions on the selectivity were rarely studied systematically for a given catalyst and reaction, particularly for reactions conducted in liquid phase. Therefore, only fragmentary information is available on the influence of reaction parameters such as prereduction of the catalyst, nature of the solvent, temperature, pressure and concentration of reactant [7].

In literature; promoted, unpromoted metals, metal oxides, carbon based support and microporous supports have been used as catalysts [8]. The active metal component can be loaded by various methods, the most widely used ones are impregnation and ion exchange. The selective properties of the supported metal catalyst depend strongly on the state and dispersion of a metal component.

The use of zeolite catalysts in the production of organic fine chemicals is appearing as a major new direction recently [9]. Because of their properties, including high and adjustable acidity, well defined pore structures with channels and cavities of molecular dimensions, high thermal stability, ion exchange ability and shape selectivity, zeolites are suitable for using as a support and as catalyst [10]. Therefore, the investigation of the use of the natural zeolite rich in clinoptilolite, which is available in large amounts in Turkey as catalyst and catalysts support is important.

In this thesis study, the use of clinoptilolite rich natural zeolite as catalyst and catalyst support for citral hydrogenation was investigated. Catalysts were prepared by impregnation and ion exchange methods with palladium and nickel compounds. The prepared catalysts were characterized with different characterization techniques and tested for citral hydrogenation reactions for different reaction conditions.

CHAPTER 2

HYDROGENATION

2.1. Hydrogenation Reactions

Hydrogenation is a chemical reaction of hydrogen with another substance, generally an unsaturated organic compound. Hydrogenation of organic functional groups can be categorized into (i) addition of hydrogen across single bonds leading to cleavage of functional groups (hydrogenolysis) and (ii) addition of hydrogen to unsaturated groups. Unsaturated organic compounds have at least one pair of carbon atoms connected by a double or triple bond. When an unsaturated compound is treated with hydrogen at a suitable temperature and in the presence of catalyst, the multiple bond between the carbon atoms is broken and a hydrogen atom attaches itself to each carbon atoms.

Hydrogenation is used extensively in industrial processes. Important examples are the chemical and petrochemical industry (e.g. removal of benzene from fuels, oils), the food processing industry (fat hardening), fine chemicals and pharmaceutical industries and in many laboratory-scale operations [11].

2.2. Hydrogenation Catalysts

The most common hydrogenation catalysts are nickel and the platinum metals; platinum, palladium, rhodium, and ruthenium. Cobalt and copper chromium oxide are also used and current exploratory work indicates that rhenium has catalytic properties which make it useful for the hydrogenation of some functional groups. Other metals such as thallium, osmium, iridium and copper have been reported to behave as catalysts for some hydrogenations but, for the most part, these metals are either inferior catalysts or are quite limited in their usefulness [11].

Palladium is a very good catalyst for the C=C bond hydrogenations but, a very bad catalyst for hydrogenation of carbonyl groups [11]. Nickel catalysts favour the hydrogenation of the conjugated double bond and the carbonyl group giving citronellal and citronellol as main products [12].

2.3. Selective Hydrogenation of α-β Unsaturated Aldehydes

The selective hydrogenation of α-β unsaturated aldehydes is an important step in the synthesis of a large number of fine chemicals, particularly in the field of flavour and fragrance chemistry and pharmaceuticals.

The hydrogenation of α-β unsaturated aldehydes proceeds different reaction pathways given schematically in Figure 2.1. The 1,2-addition of hydrogen gives the unsaturated alcohol, the 3,4-addition gives the saturated aldehyde and 1,4-addition gives the enol, which isomerizes into a saturated aldehyde. Subsequent hydrogenation of the C=C or C=O bonds leads to the saturated alcohol. The reaction scheme given in Figure 2.1 can be further complicated by side reactions occurring either on metals or on supports [7].

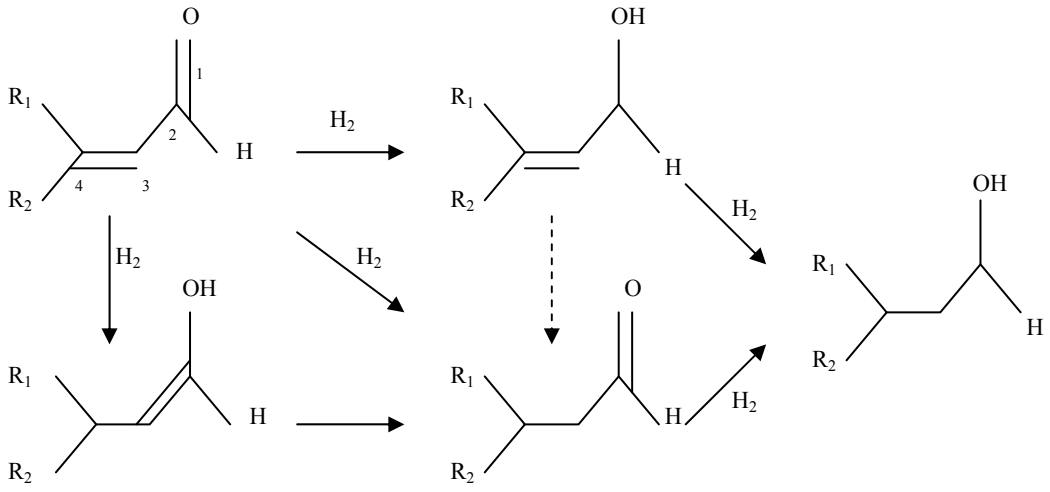

Figure 2.1. Scheme of the reaction pathways in the hydrogenation of α,β-unsaturated aldehydes

The C=C double bond is hydrogenated giving a saturated aldehydes or the C=O double bond is involved yielding an unsaturated alcohol. Finally, a total hydrogenation can occur and a saturated alcohol is obtained. The most important product is an unsaturated

alcohol [13]. This compound is also the most difficult to obtain since the bond energy of a C=C double bond is about 615 kj/mol, compared with the C=O double bond energy of about 715 kj/mol [14]. This is much less than the C=O double bond energy, making the C=C double bonds more reactive than the C=O double bonds. In the case of catalytic hydrogenation, it is assumed that the reactive bond is the one involved in chemisorption on the surface.

According to literature [13], the following adsorption states of the α-β unsaturated aldehyde functionality are possible on a catalyst metal surface as shown in Figure 2.2.

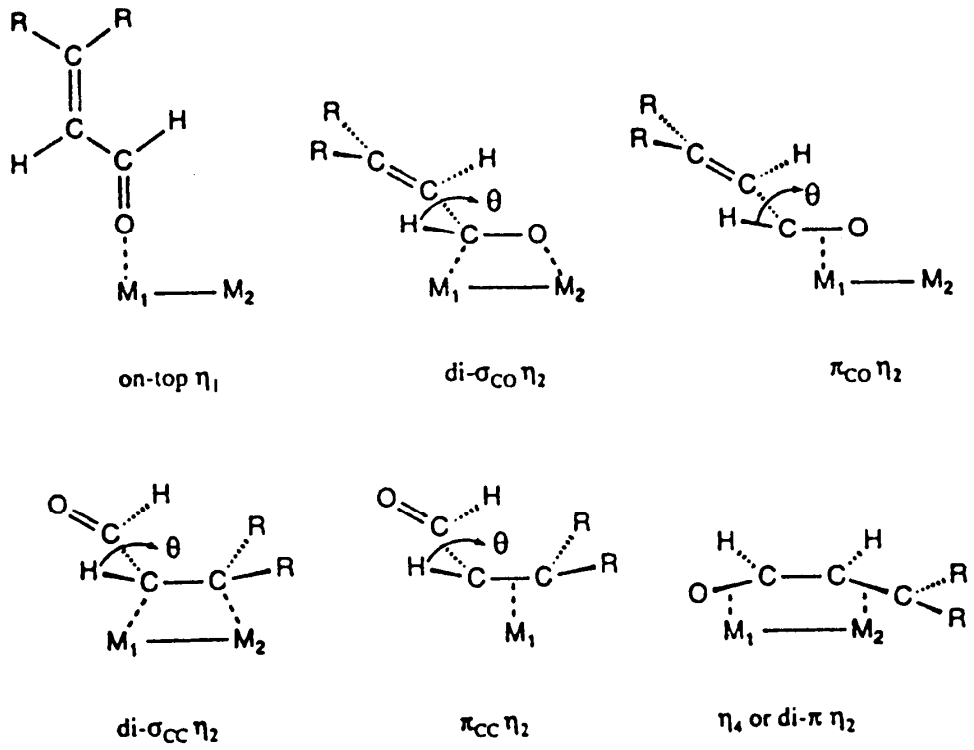

Figure 2.2. Adsorption states of α-β unsaturated aldehydes

2.3.1. Citral Hydrogenation Mechanism

Citral is an α-β unsaturated aldehyde, containing an isolated and a conjugated double bond, as well as a carbonyl group and it exists as cis and trans isomers. The molecular structure is shown below:

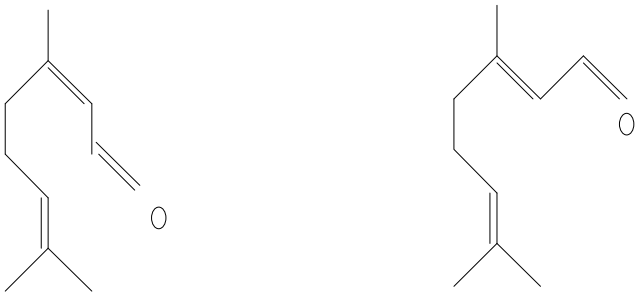

Citral, cis Citral, trans

The carbonyl group and the double bonds of the citral molecule are hydrogenated in a series-parallel sequence. The reaction scheme is illustrated in Figure 2.3. [12].

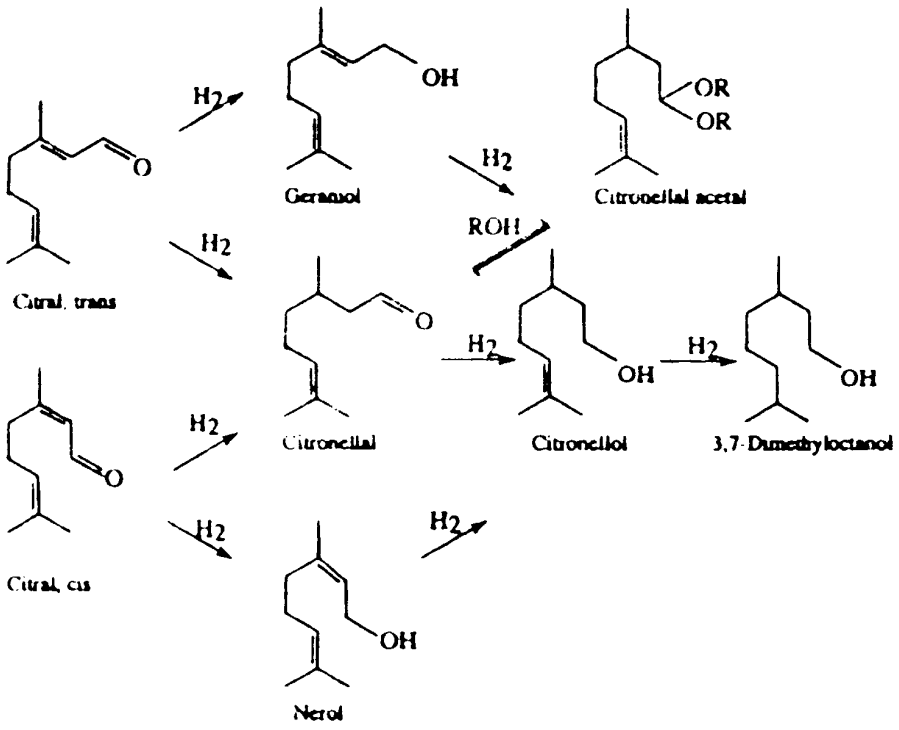

Figure 2.3. Reaction scheme of citral hydrogenation

Citral can be hydrogenated in an alcohol solvent in the presence of a metallic catalyst. Citral and its hydrogenation products are important chemicals used in the perfumery industry. The primary hydrogenation product is citronellal, which reacts further to citronellol and 3,7-dimethyloctanol. There also exist other products formed in this system, namely the unsaturated alcohols (nerol and geraniol). When citral is hydrogenated in the solvent, citronellal acetals can be formed.

CHAPTER 3

CATALYSIS

The catalysis history is as old as more than a century. Berzelius, who in 1835 first introduced the terms catalysis, defined that "The phenomenon whereby the rate of a chemical reaction may be significantly increased by the presence of a substance that ***is not part of the reactants*** and hence (ideally) can continue to exist and accelerate the reaction for infitely long periods".

Catalytic phenomena affect virtually all aspect of our lives. They are crucial in many processes occurring in living things, where enzymes are the catalysts. They are important in the processing of foods and the production of medicines, in the refining of petroleum and the manufacture of synthetic fibers and plastics, and in the production of many different chemicals (fine and heavy chemicals) with all kinds of uses. Moreover, catalysts play an important role in the preservation of our environment, as demonstrated by their vital contributions in making lead-free gasoline a reality and in decreasing pollution from automobile exhaust gases [15].

3.1. Definitions

The basic concept of a catalyst is a substance, that in a small amount causes a large change [16]. The other definition is that: A catalyst is a substance that accelerates a chemical reaction but is not consumed in the reaction and does not affect its equlibrium. Catalysts cause reactions to proceed faster than they would otherwise, and they can be used over and over again [17]. Without catalysts, various chemical reactions of great importance would proceed so slowly that they could not even be detected, although the reactions conditions (temperature and pressure) are thermodynamically favorable for the occurrence of the reactions. Suitable catalysts provide a solution to this problem. They make it possible for the reactions to proceed at rates high enough to permit their

commercial exploitation on a large scale, with resulting economic benefits for everyone [15].

Catalysis is that a reaction involves a cyclic process in which a site on a catalyst forms a complex with reactants, from which products are desorbed, thereby restoring the original site and continuing the cycle. This concept may lead to the idea that a catalyst is unaltered by the reaction it catalyzes, but this is misleading. A catalyst may undergo major changes in its structure and composition as a result of the mechanism of its participation in the reaction [16].

3.2. Catalysis Classification

Catalytic reactions are often classified as heterogeneous, homogeneous and enzymes.

Heterogeneous Catalysis, where the reactants are present in one phase and the catalyst in another. Usually the catalyst is a solid and the reactants are either gases or liquids. Catalytic action occurring at the interface or surface between them.

Heterogeneous catalysis is a mature field that profoundly affects our everyday lives. Indeed, more than 80% of industrial chemical processes in use nowadays rely on one or more catalytic reactions. A number of those, including oil refining, petrochemical processing and the manufacturing of commodity chemicals (e.g. olefins, methanol, ethylene glycol) are already well established [18]. Heterogeneous catalysis is associated with the production of petro- and bulk chemicals whereas fine and specialty chemicals are produced predominantly with non-catalytic organic synthesis [19].

Homogeneous Catalysis, where the reactant molecules and the catalyst are present in a single phase, as in a liquid solution. Acid and base catalyses are the most important types of homogeneous catalysis in liquid solution.

Enzyme Catalysis is a third group. Most of the reactions that occur in living organisms are catalysed by molecules called enzymes. Most enzymes are proteins, which are

formed from amino acid monomers. Enzymes regulate virtually all the reactions in biology [17].

3.3. Catalyst Components

Most catalysts have three types of components: (1) active components, (2) a support or carrier, and (3) promoters. In Figure 3.1. these are represented as three sides of a triangle to emphasise mutual dependence and interaction [20].

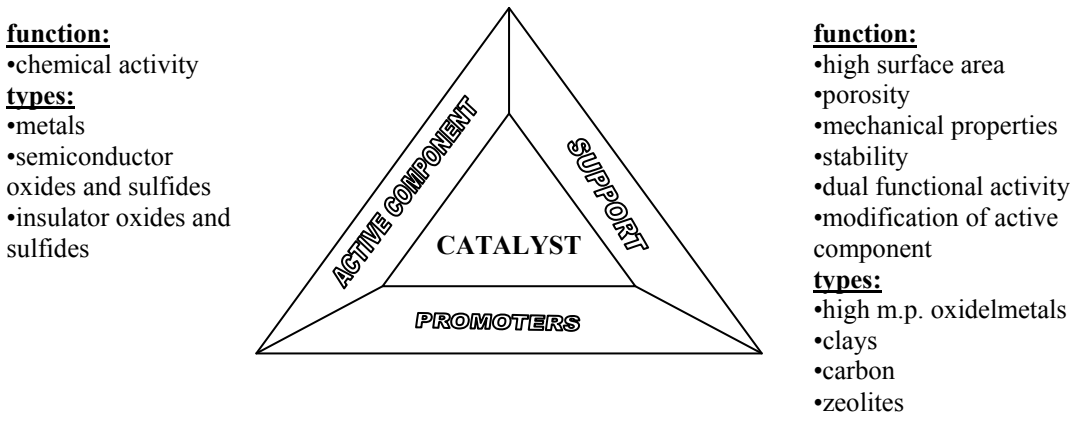

Figure 3.1. Catalyst Components

3.3.1. Active Components

Active components are responsible for the principal chemical reaction. Selection of the active component is the first step in catalyst design. Active components can be classified according to the type of electrical conductivity in Table 3.1. [20].

Table 3.1. Classification of Active Components

Class	Conductivity / Reaction Type	Reactions	Examples
Metals	Conductors Redox	Hydrogenation Hydrogenolysis Oxidation	Fe, Ni, Pt Pd, Cu, Ag
Oxides and Sulfides	Semiconductors Redox	Selective hydrogenation Hydrogenolysis Oxidation	NiO, ZnO, CuO Cr_2O_3, MoS_2
Oxides	Insulators Carbonium ions	Polymerization Isomerization Cracking Dehydration	Al_2O_3, SiO_2, MgO SiO_2 -Al_2O_3 Zeolites

No relationship between conductivity and catalysis should be assumed. However, both depend on atomic electronic configurations. With metals, overlapping electronic energy bands promote electron transfer with adsorbing molecules. Redox or charge transfer reactions such as hydrogenation, hydrogenolysis, and oxidation are found.

Semiconducting oxides and sulfides constitute a large class of catalytic materials. Electron donor and acceptor levels provide redox type activation, but surface configurations are more complicated than with metals. Greater geometric complexity leads to more selective redox reactions, such as partial oxidation, hydrodesulfurization, and denitrogenation. Insulators do not readily promote charge transfer, but surface sites with localised protons are favoured. Acid-like in nature, these sites promote carbonium ion mechanisms, resulting in typically acid-catalysed reactions such as isomerization or cracking [20].

3.3.2. Support

In some cases a catalyst consists of minute particles of an active material dispersed over a less active substance called a support [21].

The selection of a support is based on its having certain desirable characteristics. Principally they are [16]:

1. Inertness to undesired reactions.
2. Desirable mechanical properties, including attrition resistance, hardness and compressive strength.
3. Stability under reaction and regeneration conditions
4. Surface area. High area is usually, but not always, desirable.
5. Porosity, including average pore size and pore size distribution. High area implies fine pores (for example < 5 nm) could become plugged during impregnation, especially if high loading is sought.
6. Low cost.

3.3.3. Promoters

The promoter is a substance that, when added in relatively small amounts in the preparation of a catalyst, imparts better activity, selectivity, or stability [16].

Common promoters and their mode of actions are listed in Table 3.2. [20].

Table 3.2. Examples of Promoters in Major Processes

Catalyst	Promoter	Function
Al_2O_3 Support and catalyst	SiO_2, ZrO_2, P K_2O HCl MgO	Improves thermal stability Poisons coking sites Increases acidity Retards sintering of active component
$SiO_2 – Al_2O_3$ Cracking catalyst and matrix	Pt	Increases CO oxidation
Zeolites Cracking catalyst	Rare earth ions Pd	Increases acidity and thermal stability Increases hydrogenation
Pt / Al_2O_3 Catalytic reforming	Re	Decreases hydrogenolysis and sintering
MoO_3 / Al_2O_3 Hydrotreating	Ni, Co P, B	Increases hydrogenolysis of C-S and C-N Increases carbon removal
Ni / ceramic supports steam reforming	K	Increases carbon removal
$Cu-ZnO-Al_2O_3$ Low temperature shift	ZnO	Decrease Cu sintering

3.4. Catalyst Preparation Methods

Various techniques are available to introduce metals into zeolites, the most widely used being impregnation and ion exchange. When impregnation used, the metal-support integration is weaker, and large metal particles are obtained, which can affect secondary reactions, namely those which are structure-sensitive, an example being hydrogenolysis. On the other hand, the ion exchange technique normally brings about a strong metal-support interaction [22].

3.4.1. Impregnation

Impregnation is the simplest and most direct method. The object is to fill the pores with a solution of metal salt of sufficient concentration to give the correct loading [20].

The impregnation method involves three steps: (1) contacting the support with the impregnating solution for a certain time, (2) drying the support to remove the imbibed liquid and (3) activating the catalyst by calcination, reduction or other appropriate treatment. Two methods of contacting may be distinguished, depending on the total amount of solution.

(1) With excess of solution. The support is placed on a screen and dipped into an excess quantity of solution for the time necessary for total impregnation. The solid is then drained and dried.

(2) With repeated application of solution. A more precise control is achieved by this technique, termed dry impregnation or impregnation to incipient wetness. The support is contacted with a solution of appropriate concentration, corresponding in quantity to the total known pore volume or slightly less. The catalyst is kept in motion in a rotating cylinder or drum, and sprinkled as required with a solution of salt by sprayer.

For both techniques the main operating variable is the temperature which affects both the precurser solubility and the solution viscosity and, as a consequence, the wetting time [23].

3.4.2. Ion Exchange Method

Ion exchange is the reversible interchange of ions between a solid and a liquid in which there is no permanent change in the structure of the solid, that is the ion-exchange material.

Usually, contacting the zeolite with a salt solution of a different cation performs ion exchange. In the exchange reactions, one type of cation is replaced with another.

The ion exchange process may be represented as follows [24]:

$$z_A B^{Z_B}{}_{(z)} + z_B A^{Z_A}{}_{(s)} \Leftrightarrow z_A B^{Z_B}{}_{(s)} + z_B A^{Z_A}{}_{(z)}$$

where ZA, ZB are the charges of the exchange cation A and B, the subscripts z and s refer to the zeolite and solution, respectively.

The ion exchange behaviour of the zeolite depends on upon [24]:

1. The nature of the cation species, the cation size both anhydrous and hydrated, and the cation charge
2. The temperature
3. The concentration of the cation species in solution
4. The anion species associated with the cation in the solution
5. The solvent
6. The structural characteristics of the particular zeolite.

CHAPTER 4

ZEOLITES

4.1. Definition of Zeolites

In 1756, the Swedish mineralogist Cronstedt discovered that a particular type of mineral lost water upon heating. He called this mineral a “zeolite”, from the Greek “zeo” to boil, and “lithos” stone, because many zeolite appear to boil when heated. Zeolites are formed in nature or synthesized.

Zeolites, as synthesized or formed in nature, are porous, crystalline, hydrated aluminosilicates of group IA and group IIA elements such as sodium, potassium, magnesium, calcium, strontium, and barium [25].

The structural formula of a zeolite is best expressed for the crystallographic unit cell as:

$M_{x/n}\,[\,(AlO_2)_x\,(SiO_2)_y\,]\,.\,w\,H_2O$

M is the cation of valance of n, w is the number of water molecules. The ratio y/x (Si/Al ratio) usually has values of 1-5 depending upon the structure. The sum (x+y) is the total number of tetrahedra in the unit cell. The $[(AlO2)_x(SiO2)_y]$ portion represents the framework composition.

Zeolites may be represented by the empirical formula:
$M_{2/n}O\,.\,Al_2O_3\,.\,xSiO_2\,.\,yH_2O$

In this oxide formula, x is generally equal to or greater than 2 since AlO_4 tetrahedra are joined only to SiO_4 tetrahedra, n is the cation valance [24].

4.2. Structure of Zeolites

Zeolites are hydrated aluminasilicates, comprising of hydrogen, oxygen, aluminium and silicon arranged in an interconnecting, open, three-dimensional structure. Structurally the zeolite framework consists of SiO_4 and $[AlO_4]^{1-}$ tetrahedra, linked to each other at the corners by sharing of oxygen ions. This framework structure contains channels or interconnected voids that are occupied by cations and water molecules. The cations are mobile and undergo ion exchange. The water may be removed reversibly, generally by application of the heat. The aluminium and silicon tetrahedra are called primary building units as shown in Figure 4.1. [24].

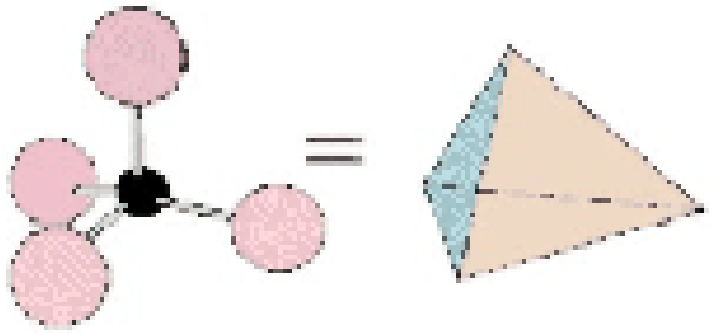

Figure 4.1. An $[SiO_4]^{4-}$ or $[AlO_4]^{5-}$ tetrahedra (primary building unit)

The relatively simple configurations resulting from their linkages are called secondary building units. Some of the more common secondary building units found in zeolite framework is illustrated in Figure 4.2. [24].

There are over 45 known different framework topologies for natural zeolites, and nearly 150 synthetic types have been reported. These natural zeolites can be classified into seven groups based on framework topology as given in Table 4.1. [24].

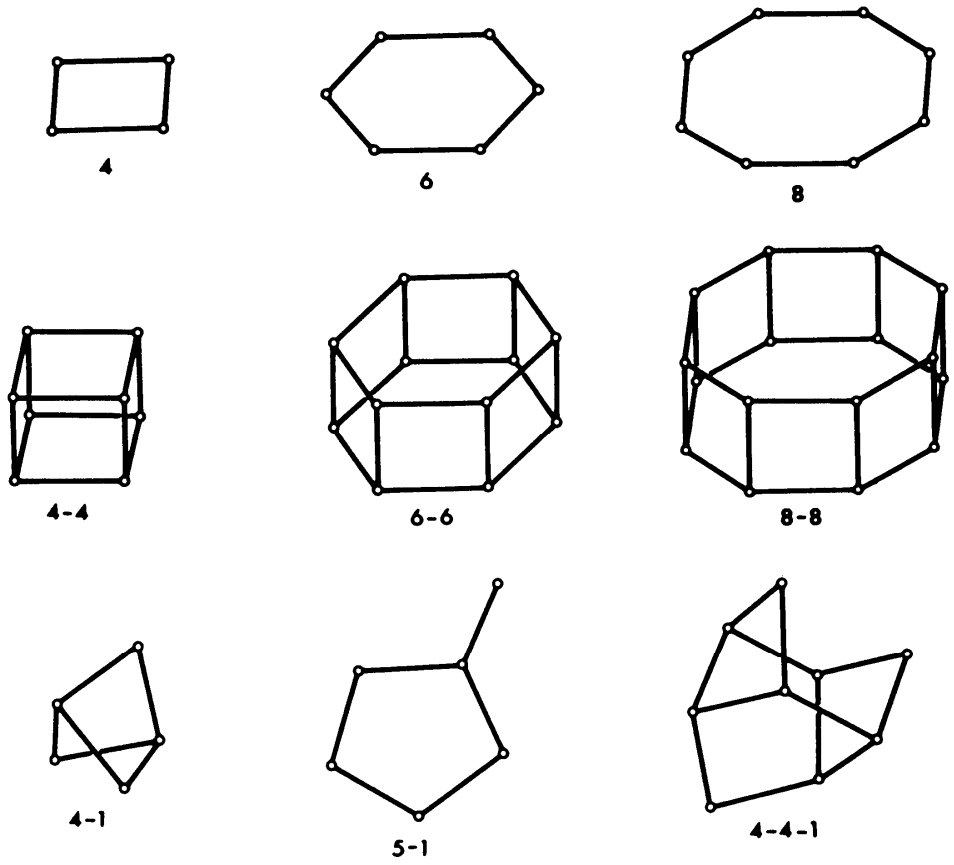

Figure 4.2. Secondary building units of zeolite framework

Table 4.1. Classification of zeolites based on framework topology

Groups	Secondary Buildings Units (SBU)
1	Single, 4-ring, S4R
2	Single, 6-ring, S6R
3	Double, 4-ring, D4R
4	Double, 6-ring, D6R
5	Complex 4-1, T_5O_{10} unit
6	Complex 5-1, T_8O_{16} unit
7	Complex 4-4-1, $T_{10}O_{20}$ unit

4.3. Zeolite Catalysts

Zeolites have been playing an increasing role in heterogeneous catalysis. An impressive number of large-scale industrial processes in petroleum refining, petrochemistry and the manufacture of organic chemicals are nowadays carried out using zeolite catalysts.

The use of zeolites as catalysts for organic reactions began in the early 1960s. Initially, zeolite based catalysts were investigated for applications in the petrochemical industries. In 1968, Venuto and Landis provided the first comprehensive overview of zeolite catalysis for organic reactions within and outside the area of fuels synthesis. In addition to increased use in petrochemicals manufacture, zeolite catalysis is expanding into the areas of speciality and fine chemicals synthesis [9].

Catalytic properties of zeolites depend on several factors including the presence of active sites, e.g. acidic, basic, or cationic sites, the spatial arrangement and size of channels and cavities and presence of extra compounds within the channels. Changing one or several of these factors may affect the catalytic properties [26].

Several varieties of active sites are directly related to the types of framework atoms. For example framework Al^{3+} atoms in zeolites create anionic lattice sites that can be charge balanced by protons or other cations, e.g. transition metal ions [9].

Incorporating metals in order to obtain catalysts for selective hydrocarbon conversions can modify zeolites. They are usually obtained from transition metal zeolites. The zeolite catalysts loaded with finely dispersed noble metals have been used in hydrogenation, hydro-cracking, hydroisomerization, and the oxidation of hydrocarbons [27].

4.3.1. Aluminium Content and Acidity

Zeolites are classified according to their chemical composition on the basis of their silica to aluminium ratio as shown in Table 4.2. Since the ion exchange capacity is equal to the concentration of Al^{3+} ions in the zeolite, the structures with low Si/Al ratios can have higher concentrations of catalytic sites than the others.

Table 4.2. Acid Form Zeolites Classified by Their Si/Al Ratios [17]

Si/Al Ratio	Zeolites	Properties
Low (1-1.5)	A, X	Relatively low stability of framework; low stability in acid; high stability in base; high concentration of acid groups with moderate acid strength
Intermediate (2-5)	Erionite Chabazite Clinoptilolite Mordenite Y	
High (≈10 to ∞)	ZSM-5 Erionite Mordenite Y	Relatively high stability of framework; high stability in acid; low stability in base; low concentration of acid groups with high acid strength

The general changes that occur in the physical and chemical properties of the zeolites as the framework silica to alumina ratio is increased from one to infinity are shown in Table 4.3. [28].

Table 4.3. The physical and Chemical Properties of Zeolites as the Framework Si/Al ratio is increased.

SiO_2/Al_2O_3	From 0.5 to infinity
Stability	From 700°C to 1300°C
Surface selectivity	From hydrophilic to hydrophobic
Acid site density	Decreasing
Acid strength per site	Increasing
Cation concentration	Decreasing
Structure	From 4-, 6- and 8-membered rings to 5-membered ring

The reactivity and the selectivity of molecular sieve zeolites as catalysts are determined by active sites. The active sites are provided by an imbalance in charge between the silicon and the aluminium ions in the framework. Each aluminium atom contained within the framework structure induces a potential active acid site. The replacement of SiO_4 tetrahedra by the $[AlO_4]^{-1}$ tetrahedra in the zeolite framework causes excess

negative charges and protons are needed to neutralize them. Compensation of the negative charge by an associated cations, e.g. H^+, Na^+, K^+, Ca^{2+}, NH_4 generates the acid sites.

If the charge compensating cation associated with the thetrahedral aluminium is hydrogen, the zeolite surface obtains the capacity to act as a proton donor and therefore can serve as a Bronsted acid that is proton-donor acidity;

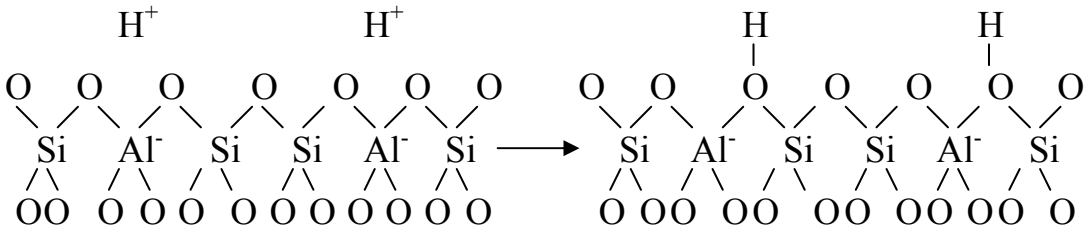

When a hydrogen form zeolite is heated to a temperature higher than 550°C, Lewis acid site and water occur. Lewis acidity is electron acceptor acidity. One Lewis acid site is formed from two Bronsted acid sites. Formation of Lewis acid site is shown schematically as follows:

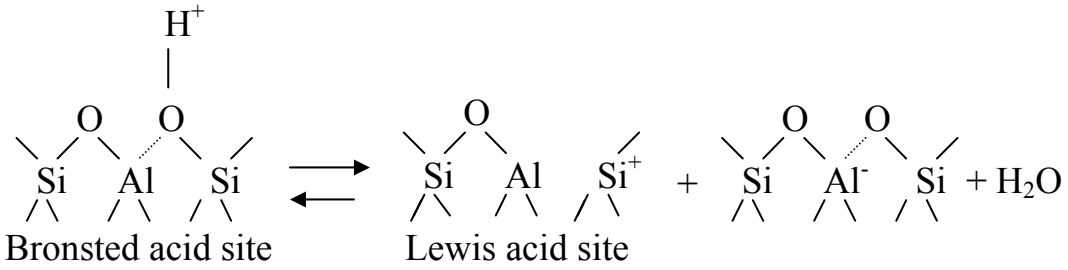

If transition metals are introduced into the zeolite by conventional ion exchange techniques, a third type of active site can be generated [17].

4.3.2. Pore Size and Molecular Sieving

All zeolites that are significant for catalytic and adsorbent applications can be classified according to the pore opening. There are three pore openings that are referred to as the 8, 10, 12 ring openings. Zeolites containing these pore openings may also be referred to as small (8-member ring), medium (10-member ring) and large (12-member ring) pore zeolites.

Table 4.4. includes the number of oxygen atoms in the aperture of each zeolite (8, 10 or 12) and the aperture dimension that the smallest being about 0.4 nm for Zeolite A and the largest being 0.74 nm for fujasite [17].

Table 4.4. Zeolites and their pore (aperture) dimensions

Zeolite	**Number of Oxygens in the Ring**	**10 x Aperture Dimensions, nm**
Chabazite	8	3.6 x 3.7
Erionite	8	3.6 x 5.2
Zeolite A	8	4.1
ZSM-5 (or silicate)	10	5.1 x 5.5; 5.4 x 5.6
ZSM-11	10	5.1 x 5.5
Heulandite	10	4.4 x 7.2
Ferrierite	10	4.3 x 5.5
Fujasite	12	7.4
Zeolite L	12 12	7.1 7.0
Mordenite	12	6.7 x 7.0
Offretite	12	6.4

Shape selectivity is one of the most important properties of zeolites in their application in the field of catalysis. For a given zeolite, this property is related to the pore size. There different types of selectivity are observed over zeolites as shown in Figure 4.3. [28].

1. Reactant selectivity occurs when some of the molecules are too large to diffuse through the catalyst pores.
2. Product selectivity occurs when some of the products formed within the pores are too bulky to diffuse out as observed products. The bulky molecules are either converted to less bulky molecules or to coke that eventually deactivates the catalyst.
3. Restricted transition state selectivity occurs when certain reactions are prevented because the corresponding transition state would require more space than available in the cavities or pores. Neither reactant nor product molecules are prevented from diffusing through the pores. Reactions requiring smaller transition states proceed unhindered.

REACTANT SELECTIVITY

PRODUCT SELECTIVITY

RESTRICTED TRANSITION STATE SELECTIVITY

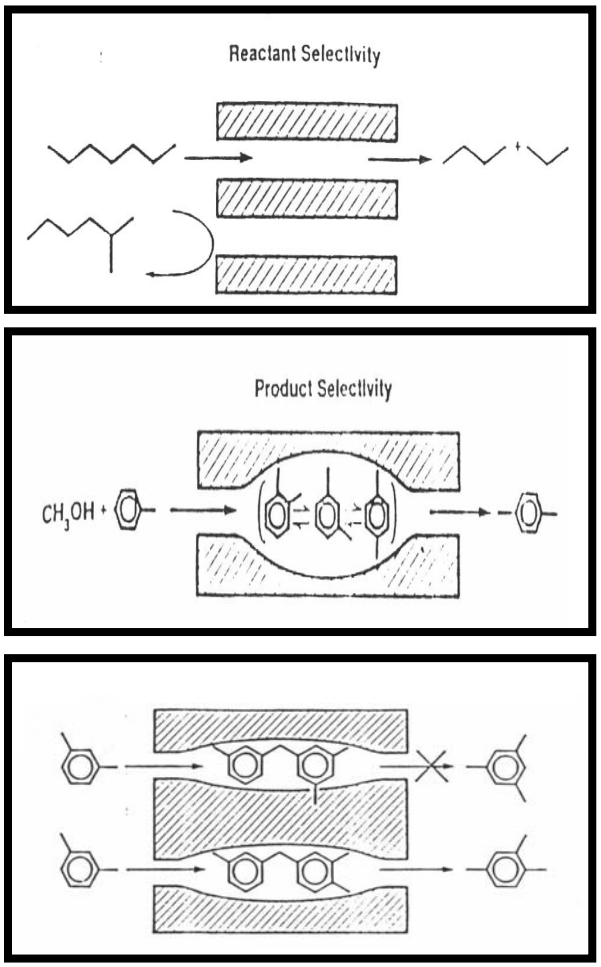

Figure 4.3. Shape selectivity of zeolites

4.4. Clinoptilolite

Clinoptilolite is one of the natural zeolites found in abundance in many locations [29]. It is a member of the heulandite group of natural zeolites, being isostructural with the heulandite zeolite, which it differs in having higher Si/Al [30]. Clinoptilolite has a Si/Al ratio greater than 4. Heulandite contains a Si/Al ratio below 4. The key difference between natural heulandite and clinoptilolite is thermal stability. Clinoptilolite is thermally stable to temperatures in excess of 500°C, while heulandite undergoes structural collapse by 350°C [31]. Clinoptilolite can also be distinguished from heulandite on the basis of cation content, having alkali cations dominant [(Na+K) > Ca], whereas heulandite has [(Ca > (Na+K)] [31].

Clinoptilolite can be represented by typical oxide formula as:

$(Na_2, K_2)\ O\ .\ Al_2O_3\ .\ 10\ SiO_2\ .\ 8\ H_2O$

Unit cell contents of clinoptilolite can be represented as:

$(Na, K)_6\ (Al_6Si_{30}O_{72})\ .\ 24\ H_2O$

The unit cell of clinoptilolite is monoclinic and is usually characterized on the basis of 72 oxygen atoms (n=36) and m=24 water molecules, with Na^+, K^+, Ca^{2+}, and Mg^{2+} as the most common charge-balancing cations. Representative unit cell parameters are a=1.762 nm, b=1.791 nm, c=0,739 nm, β= 2.029 rad. [32]. Some of the structural properties of clinoptilolite are given in Table 4.5. [24].

Table 4.5. Structural Properties of Clinoptilolite

SBU	Unit 4-4-1
Void Volume	0.34 cc/cm^3
Framework Density	1.71 g/ cm^3
Dehydrated-Effect of Dehydration	Very stable in air up to 700°C
Largest Molecule Adsorbed	O_2
Kinetic Diameter, σ, A	3.5
Unit Cell Volume	2100 A^3
Density	2.16 g/cm^3
Si/Al	4.25-5.25

Clinoptilolite is assigned to the same framework HEU in which 4-4-1 secondary building units. These units are linked together to form a two dimensional channel structure with elliptical pore openings [33]. Channel A (10-membered ring) and B (8-membered ring) are parallel to each other and the c axis of the unit cell, while the C channel (8-membered ring) lies along a axis, intersecting both the A and B channels as shown in Figure 4.4. [30, 34, 35]. Small hydrated cations (Na^+, K^+, Ca^{2+}, and Mg^{2+}) can easily enter the channels of clinoptilolite and compete for the major exchangeable

cation sites, designated as M(1), M(2), M(3), and M(4) [36]. Channel characteristics and cation sites of clinoptilolite are summarized in Table 4.6.

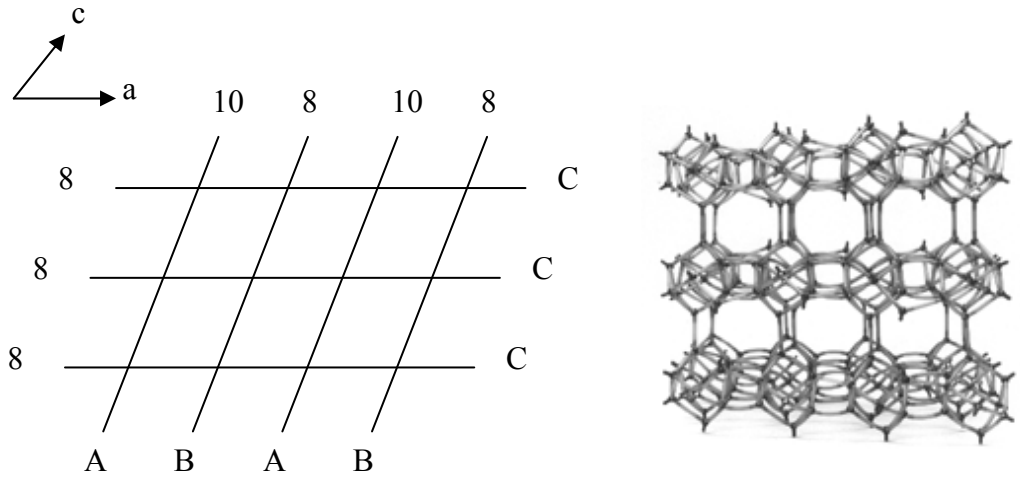

(a) (b)

Figure 4.4. (a) Orientation of clinoptilolite channel axes (b) Model framework for the structure of clinoptilolite

Table 4.6. Channel Characteristics and Cation Sites in Clinoptilolite

Channel	Tetrahedral Ring Size/ Channel axis	Cation Site	Major Cations	Approximate Channel Dimensions (nm x nm)
A	10 / c	M (1)	Na, Ca	0.72 x 0.44
B	8 / c	M (2)	Ca, Na	0.47 x 0.41
C	8 / a	M (3)	K	0.55 x 0.40
A	10 / c	M (4)	Mg	0.72 x 0.44

The major cations are located and distributed in Figure 4.5. [37] as follows: M(1) is located in channel A, coordinated with two framework oxygen and five water molecules. This site is occupied by Ca^{2+} and preferably by Na^{+}. M(2) is located in channel B, coordinated with three framework oxygen and five water molecules. M(2) is occupied by Na^{+} preferably by Ca^{2+}. M(3) is located in channel C, coordinated six framework oxygen and three water molecules. This site is occupied by K^{+} and preferably by Ba^{2+}. Because this position is very close to M(1) a simultaneous occupancy of both sites is not possible. M(4) is located in the center of channel A

different from M(1). It is coordinated by six water molecules forming an octahedral system and occupied by Mg^{2+}.

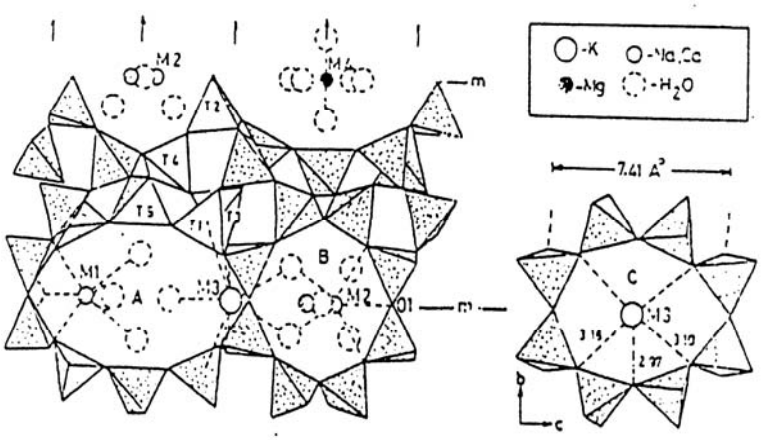

Figure 4.5. The c-axis projection of the structure of clinoptilolite, showing the cation

Clinoptilolite has been applied to gas cleaning, waste water cleaning, agriculture and aquaculture, fertilizers, animal health and nourishment, gas separation, deodorization, construction materials and cleaning of radioactive wastes. These applications rely on the adsorption and ion exchange ability of clinoptilolite. Clinoptilolite may be useful as a catalyst [11].

CHAPTER 5

PREVIOUS STUDIES ON CITRAL HYDROGENATION

The selective hydrogenation of α,β-unsaturated aldehydes has been the subject of numerous investigations. The development of catalysts for selective hydrogenation of α,β-unsaturated aldehydes is reviewed in this chapter. Many factors have been reported to the influence the selectivity of the reaction, among them are the nature and particle size of the metal [4, 5, 12, 38], the presence of promoters [6, 39, 40, 41, 42] and the catalyst support [8, 12, 39, 40, 41, 42].

5.1. Particle Size Effects

Galvagno et al. [6] studied a Ru catalyst prepared by impregnation of activated carbon with aqueous solutions of $RuCl_3$ and reducing at 573 K for 1 h. That the selectivity to geraniol + nerol is about 36 % on all catalysts investigated, regardless of metal particle size, is shown in Figure 5.1.

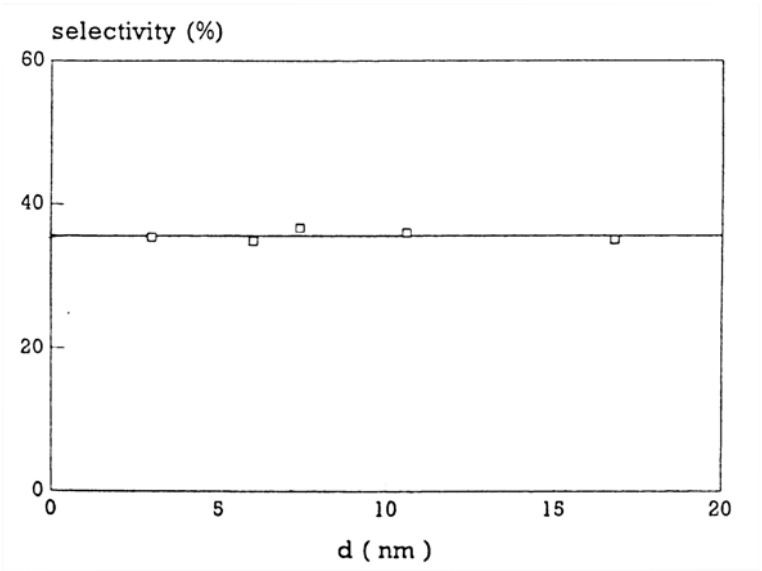

Figure 5.1. Influence of Ru particle size (*d*) on the selectivity to geraniol + nerol

In the case of citral, where no aromatic ring is present, the steric effect can not play an important role and therefore no difference in the product distribution is observed with a change of the metal particle size.

Mercadante et al. [43] studied the hydrogenation of citral on a Ru/Al_2O_3 catalysts having a different metal dispersion and obtained from different metal precursors such as ruthenium acetylacetonate ($Ru(acac)_3$) or ruthenium nitrosyl nitrate ($Ru(NO)(NO_3)_3$).

The effect of Ru dispersion (measured by the H/Ru ratio) on the initial rate of hydrogenation of citral is reported in Figure 5.2. The initial turnover rate was found almost constant in all range of dispersion investigated. Samples prepared from ($Ru(acac)_3$) and ($Ru(NO)(NO_3)_3$) gave similar results.

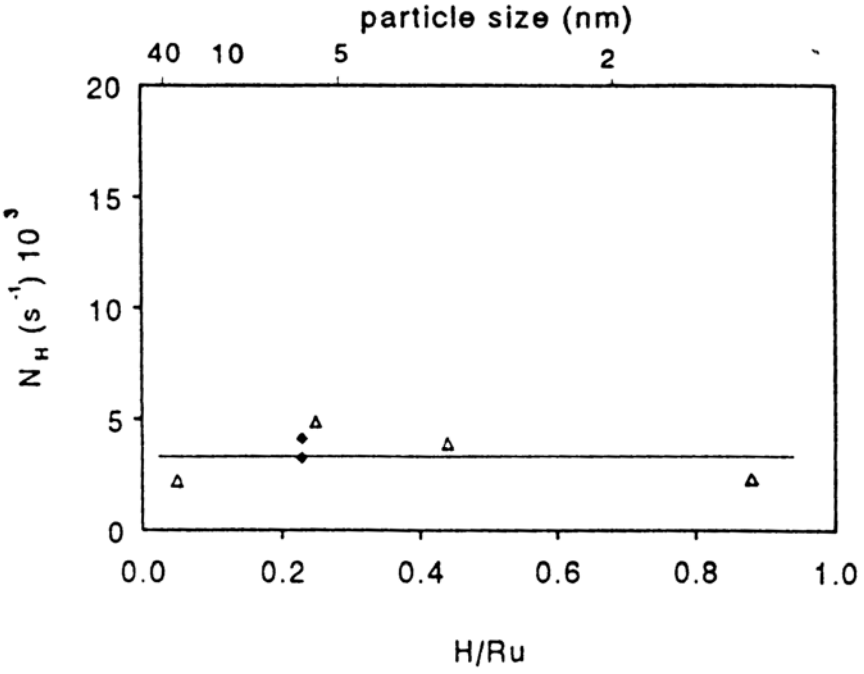

Figure 5.2. Influence of Ru dispersion (H/Ru) on the rate of hydrogenation of citral. N_H, (Δ) RuEC series, (♦) RuNI series

Figure 5.3. shows the influence of the Ru dispersion on the selectivity geraniol + nerol, S_{GN}. For comparison the results previously obtained on Ru/C (taken from ref. [38]) have also been reported. In all ranges of Ru dispersion, investigated S_{GN} remains constant (about 15 % on Ru/Al_2O_3 and about 35 % on Ru/C).

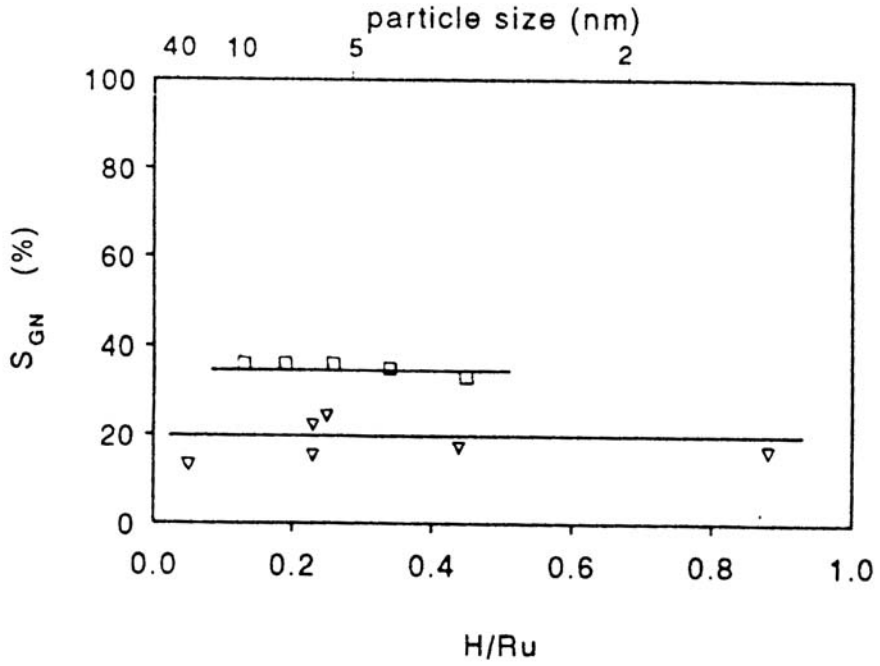

Figure 5.3. Hydrogenation of citral: Influence of Ru dispersion (H/Ru) on the selectivity to unsaturated alcohols, $S_{GN,}$ (□) Ru/C, (▽) Ru/Al_2O_3

Results on the influence of the conversion levels on the product selectivity are reported in Figure 5.4. The selectivity to citronellal was instead found to decrease with increasing conversion, with a corresponding increase in the selectivity to citronellol.

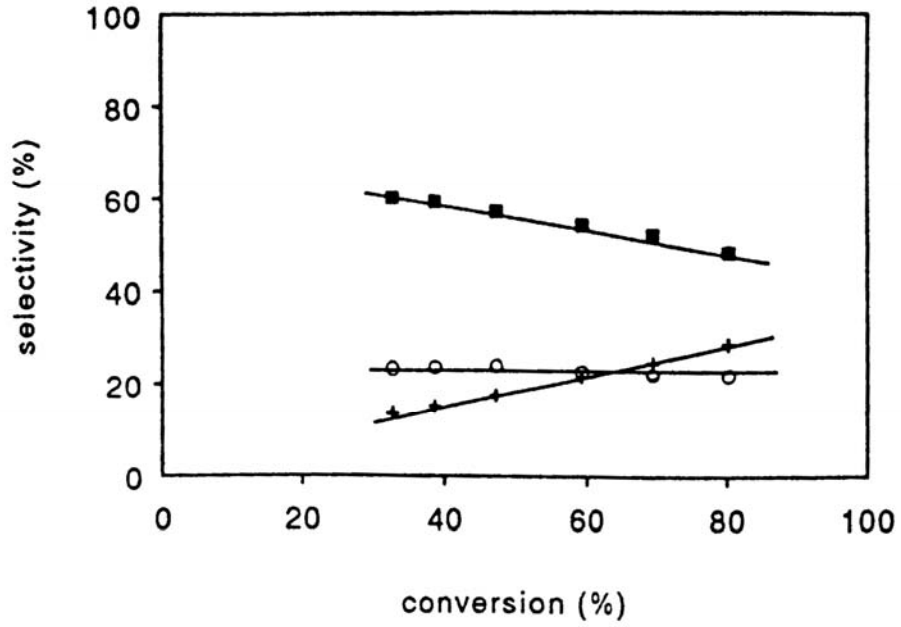

Figure 5.4. Hydrogenation of citral: Selectivity to reaction products as a function of conversion. Catalyst: RuNI. (□) citronellal, (O) geraniol + nerol, (+) citronellol

5.2. Promoter Effects

Galvagno et al. [38] studied the hydrogenation of citral on a Ru-Sn catalyst; prepared by incipient wetness impregnation of activated carbon with aqueous solutions of $RuCl_3$ and $SnCl_2$ and reducing at 573 K. In all catalysts the amount of Ru was kept constant at 2 wt %, whereas the Sn content was varied between 0 and 2 wt %. In this study, the effect of tin addition to Ru/C has been studied. Figure 5.5. shows the effect of tin on the reaction selectivity. Selectivity values shown in Figure 5.5. have been measured at a conversion level of 30 %.

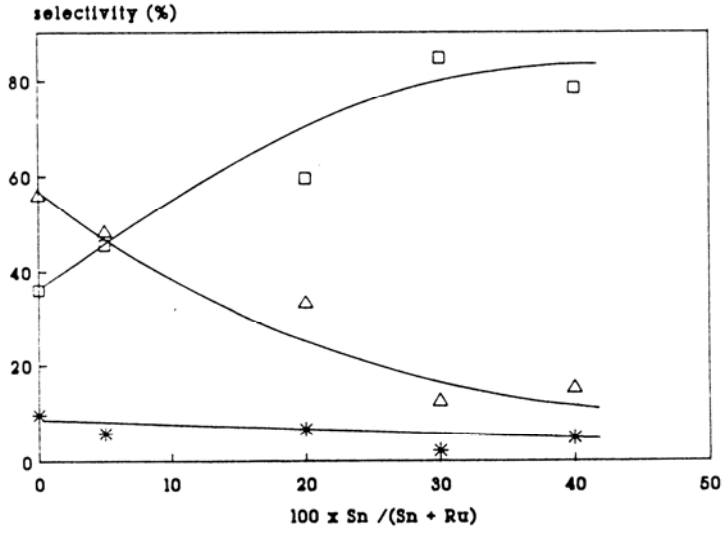

Figure 5.5. Hydrogenation of citral. Influence of the Sn/Ru ratio on the products selectivity. (□) Geraniol + nerol, (Δ) citronellal + isopulegol, (*) citronellol

Addition of Sn to Ru/C (Figure 5.5.) increased the selectivity to the unsaturated alcohols (geraniol + nerol) from a value of about 35 up to 80 % with a corresponding decrease in the selectivity to products obtained by hydrogenation of the conjugated C=C double bond (citronellal and isopulegol). A small decrease of the selectivity to citronellol with addition of Sn was also observed. It is interesting to note that products formed by hydrogenation of the isolated C=C double bond were never detected.

Neri et al. [40] have studied the hydrogenation of citral on a Pt-Sn catalyst prepared by incipient wetness impregnation of activated carbon with aqueous solution of H_2PtCl_6 and $SnCl_2$ and reducing under H_2 at 573 K. As the percentage of tin increased from 0%

to 20% in the bimetallic catalysts, the activity passed through a maximum corresponding to a fivefold increase of activity. The selectivity to unsaturated alcohols (geraniol and nerol, E and Z forms of 3,7-dimethyl-2,6-octadienol, respectively) increased from 65% to 90%. Pt/C sample, the isomers geraniol and nerol were obtained with a selectivity of about 65%, which is significantly higher than that (35%) previously obtained on Ru dispersed on the same carbon support.

Addition of tin modifies the reaction selectivity, shifting the distribution of the products towards the formation of higher amounts of unsaturated alcohols. On all catalysts investigated selectivity unsaturated alcohols remains constant within the range of conversion 10-80 % (Figure 5.6.). This confirms a reaction scheme where the unsaturated alcohols are obtained by a parallel pathway. Selectivity to citronellal decreases slightly with conversion whereas a parallel increase in the selectivity to citronellol is observed. This suggests that, in the first stage of reaction, citronellol is formed mainly through the reduction of citronellal.

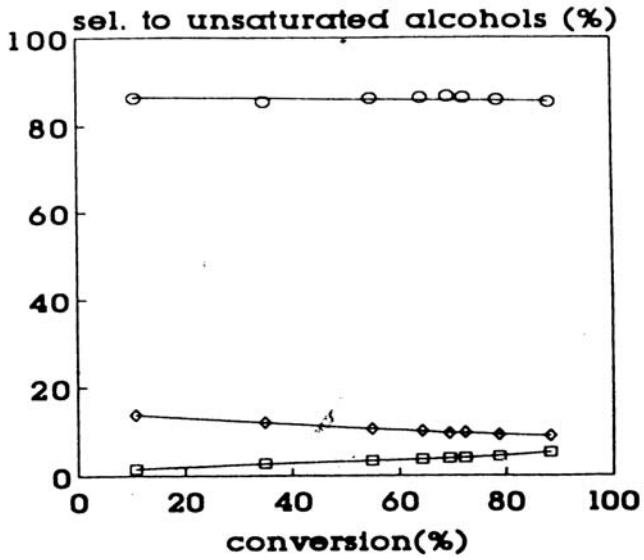

Figure 5.6. Influence of citral conversion on the products selectivity. (O) Geraniol + nerol, (□) citronellal, (□) citronellol

Figure 5.7. shows the selectivity to unsaturated alcohols (measured at a citral conversion of 50 %) as a function of Sn/Pt ratio. Selectivity increases with the Sn content reaching a value of about 90 % over the Pt/C sample

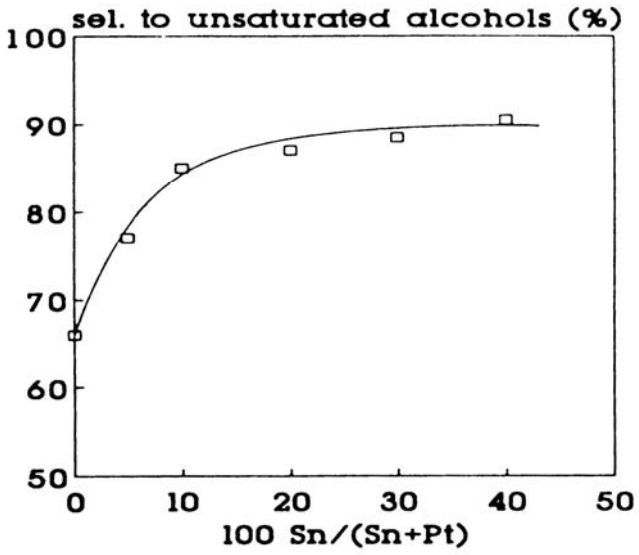

Figure 5.7. Influence of the Sn/Pt ratio on the selectivity to unsaturated alcohols (geraniol + nerol)

The mechanism they postulated was that, the substrate was adsorbed through the carbonyl group on active sites and it was activated by interaction with Sn^{n+} ions, whereas metallic platinum provided the active hydrogen, as shown below.

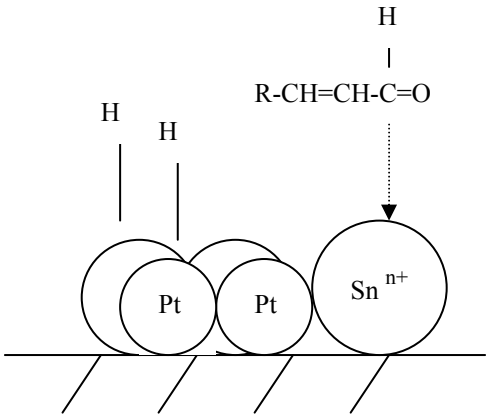

Hydrogen chemisorbed on noble metal could be considered nucleophilic in nature. Therefore it reacted more easily with the activated carbonyl group to give unsaturated alcohol.

Sordelli et al. [42] found that the monometallic Rh/SiO_2 catalyst shows a high activity but a very low selectivity to unsaturated alcohols, with citronellal and citronellol as the main products. As shown in Table 5.1. the effect of the addition of tin was to

significantly decrease the catalytic activity with a corresponding increase in the selectivity to unsaturated alcohols.

Table 5.1. Catalytic Activity towards Citral Hydrogenation (308 K, 1 atm)

Catalyst [a]	**Conversion** [b] **(%)**	**Selectivity to Unsaturated Alcohols (%)**
Rh/SiO_2	100	5.2
$Rh\text{-}Sn/SiO_2$	57	70
$Rh\text{-}Sn/SiO_2$ [c]	95	11
Rh/MgO	100	0
Rh-Sn/MgO	45	10

[a] Rh metal loading = 4 wt%, Sn/Rh molar ratio = 0.5.

[b] Conversion is reported after 24 h from the beginning of the reaction.

[c] Fresh catalyst has been pretreated in H_2 flow at 773 K. All the other samples have been exposed to a calcination-reduction cycle at 773 K.

A $Rh\text{-}Sn/SiO_2$ catalyst was prepared whose catalytic behavior was almost the same as that of the monometallic sample. The use of MgO as support did not increase the selectivity to unsaturated alcohols. The monometallic catalyst showed the same catalytic properties as the silica-supported one. Tin addition to the Rh/MgO catalyst decreased the conversion rate, but this was not compensated by any increase in the selectivity to unsaturated alcohols.

5.3. Support Effects

Promoted and unpromoted metals, metal oxides, carbon based supports have been used as catalysts in the citral hydrogenation.

Activated carbon has been used as catalysts [6, 38, 40]. Galvagno et al. [38] have studied over Ru catalysts supported on activated carbon. Figure 5.8. shows a typical time course of the hydrogenation of citral over Ru/C which has been recorded up to a citral conversion of about 90%.

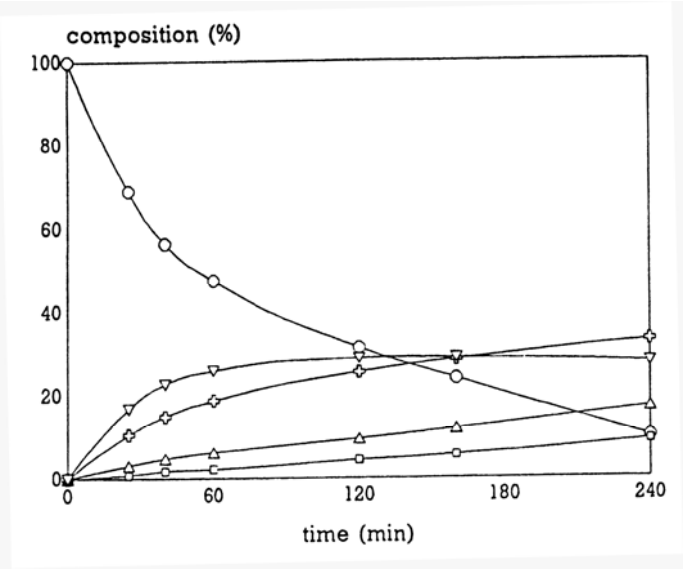

Figure 5.8. Hydrogenation of citral over 2% Ru/C catalyst. *T* = 333 K; (O) citral, (+) geraniol + nerol, (∇) citronellal, (□) isopulegol, (Δ) citronellol

Figure 5.9. shows typical results of the change in the selectivities towards the main reaction products as a function of the level of citral conversion. It can be noted that the selectivity to α,β-unsaturated alcohols (geraniol + nerol) is nearly constant in all ranges of conversion investigated. The increase observed in the selectivity to cironellol and isopulegol is accompanied by a decrease in the selectivity to citronellal. Hydrogenation of geraniol and nerol had been observed only after citral had almost disappeared from the reaction vessel. This indicates that hydrogenation of the C=C double bond of the unsaturated alcohols was inhibited by the strong adsorption on the catalyst surface of the molecules containing a carbonyl group. The strong adsorption of the carbonyl group can also well explain the inactivity of the isolated C=C double bond.

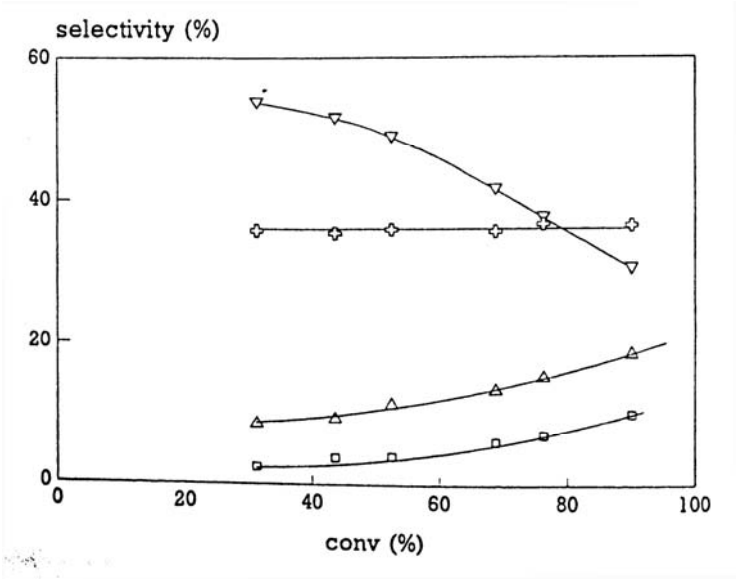

Figure 5.9. Influence of citral conversion on the products selectivity. Catalyst 2% Ru/C; (+) geraniol + nerol, (□) isopulegol, (∇) citronellal, (Δ) citronellol

Neri et al. [40] have studied over Pt and Pt-Sn catalysts supported an activated carbon. Figure 5.10. shows typical results obtained on a Pt-Sn/C catalyst. On the Pt/C sample the results were qualitatively similar but with a lower selectivity to geraniol and nerol.

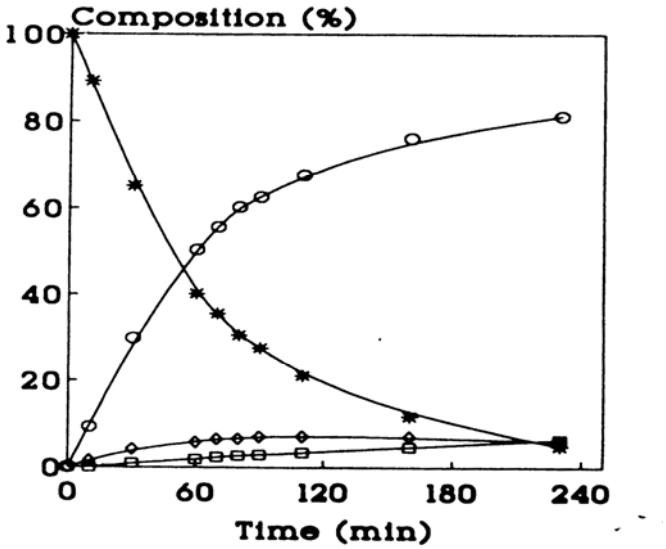

Figure 5.10. Hydrogenation of citral over Pt80/C catalyst. (*) Citral, (O) geraniol + nerol, (□) citronellal, (□) citronellol

The carbon used in this work as support contains about 1000 ppm of Fe together with Ca, K and other minor components. Iron is well known to improve selectivity to unsaturated alcohols when added to platinum.

Mercadante et al. [43] found the lower selectivity obtained on Ru/Al_2O_3 compared to the values previously reported on Ru/C is likely due to the presence of impurities (mainly Fe) on the surface of the carbon support. Fe is known to act as promoter for selective hydrogenation of unsaturated aldehydes. Moreover it has been suggested that an electron transfer from the support to metal can decrease the probability of the activation of the C=C bond.

Aramendia et al. [44] studied the hydrogenation of citral, by palladium catalysts supported on a mixed 80:20 $SiO_2/AlPO_4$ system and sepilolite from Vellecas. The addition of a small amount of $FeCl_2$ to the reaction medium was found to alter the sequence and increase the selectivity with which the C=O group was reduced.

The selectivity change introduced by $FeCl_2$ arises from the presence of positively charged ferrous ions on the surface of Pd particles. These species may originate from unreduced Fe^{2+} ions or electron-deficient Fe^0 atoms resulting from electronegativity differences between iron and palladium (Figure 5.11.).

Figure 5.11. Model for the selective adsorption-reduction of citral on a Pd catalyst doped with $FeCl_2$

Only a few of initial ferrous ions appear either as Fe^0 atoms over palladium or unreduced Fe^{2+} ion associated with palladium particles. The rest of ferrous ions stay in solution, far from the palladium, and they do not take part in the reaction. The interaction of positively charged iron with the carbonyl group causes an electron to be transferred from the oxygen atom in the C=O group of citral, which is thus made electron-deficient. Next, an electron rearrangement takes place by which one of the electrons in the pair that forms the double bond is transferred to the oxygen atom while the other is used to form a C-H bond between the carbonyl carbon and a proton bonded

to the more electronegative metal (Pd). Finally, the formation of a bond between the second proton and the oxygen causes the alcohol to be released.

Salmi et al. [12] used nickel-impregnated silica fibres in the hydrogenation of citral in a tubular glass reactor. The fibre catalyst favoured the formation of citronellal as a primary and secondary product. The most active catalyst was 5 wt. % Ni on Silica fibre calcined at 700°C. The catalyst activity decreased with increasing nickel contents as shown in Table 5.2.

Table 5.2. The initial hydrogen uptake rates and selectivity to citronellol in citral hydrogenation with different Ni-silica fibre catalysts and the mean Ni particle size determined by XRD[a]

Ni/SiO_2 catalyst (wt. & Ni)	**Initial H_2 uptake rate (mmol min^{-1} g_{Ni}^{-1})**	**Selectivity to citronellol (%)**	**Mean Ni particle size (nm)**
5	22	92[b]	1.3
10	14	84	3.6
15	11	74	5.6
20	6	69	10.3

[a] The catalyst support was calcined at 700°C.

[b] At maximum yield of citronellol.

When the support material was calcined at three different temperatures (700, 800 and 900°C), the specific surface area decreased in the same order as shown in Table 5.3.

Table 5.3. The BET specific surface area of the support materials calcined at three different temperatures

Calcination temperature (°C)	**BET-area (m^2 g_{cat}^{-1})**	**Specific pore volume (cm^3 g^{-1})**
700	184	0.4
800	138	0.3
900	81	0.2

Coupe et al. [5] investigated the hydrogenation of citral on bimetallic silica supported Rh-Sn catalysts using different preparation methods, namely coimpregnation, successive impregnation and an orgonometallic route. All preparation methods create active sites suitable for the formation of unsaturated alcohols. The results obtained from the orgonometallic catalyst (RhSn-OM), successive impregnation (RhSn-SI) and coimpregnation catalysts (RhSn-CI) are shown in Figure 5.12., Figure 5.13. and Figure 5.14., respectively.

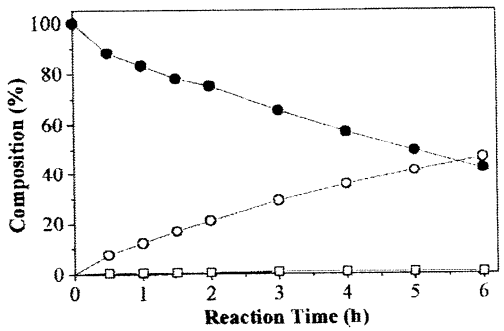

Figure 5.12. Hydrogenation of citral over RhSn-OM: (•) citral, (O) geraniol+nerol, (□) citronellal

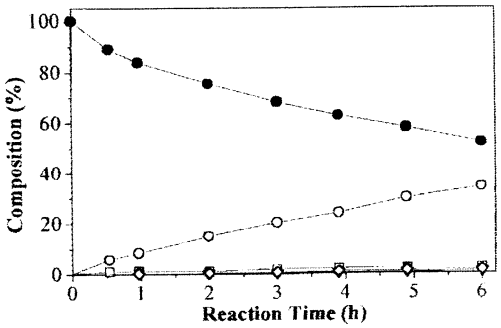

Figure 5.13. Hydrogenation of citral over RhSn-SI: (•) citral, (O) geraniol+nerol, (□) citronellal, (∇) citronellol (♦) other by-products

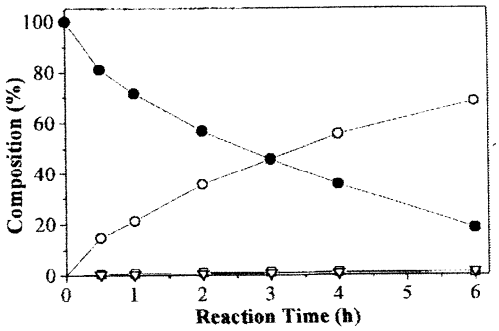

Figure 5.14. Hydrogenation of citral over RhSn-CI: (•) citral, (O) geraniol+nerol, (□) citronellal, (∇) citronellol

Singh et al. [2, 45, 46] studied on Pt/SiO_2 and Pt/TiO_2 catalyst which were studied between 298 – 423 K and 7 - 21 atm. H_2. The effects are shown in Table 5.4.

Table 5.4. Effect of metal-support interactions on the product distribution, extrapolated to zero conversion, during reaction at 373 K, 20 atm H_2, and 2 M citral in hexane

Catalyst	**Geraniol + nerol**	**Citronellal**	**Citronellol**	**Isopulegol**	**3,7-Dimethyloctanol**
1.44% Pt/SiO_2	40	40	7	7	5
1.78% Pt/TiO_2-LTR	88	7	0	5	0
1.78% Pt/TiO_2–HTR	88	7	0	5	0

Malathi et al. [8] investigated supported platinum catalysts for selective hydrogenation of citral to the unsaturated alcohol. The titania (commercial and gel), the mixed oxide (titania-alumina) and ceria (commercial) supported platinum catalysts were prepared and reduced at 573 K (low temperature of reduction, LTR) and 773 K (high temperature of reduction, HTR). The results of the hydrogenation on various supported platinum catalysts are shown in Table 5.5.

Table 5.5. Percentage conversions of hydrogenation of citral (in mol%)

Time (min)	**5% Pt/TiO_2 (C)**		**5% Pt/TiO_2 (G)**		**5% Pt/T-A(22-78)**		**5% Pt/CeO_2**	
	573 K	**773 K**	**573 K**	**773 K**	**573 K**	**773 K**	**573 K**	**773 K**
30	-	11	-	-	17	5	2	-
60	-	13	-	5	27	4	7	1
90	-	14	-	7	-	-	-	2
120	-	16	2	18	25	23	7	6
180	-	16	3	22	26	-	5	12
210	-	17	7	27	25	28	-	-
240	12	17	10	30	26	30	7	25
300	13	17	8	29	29	27	20	22

From Table 5.5. it can be observed that, in all cases the reduction produces only the unsaturated alcohol, geraniol, in 100% selectivity in both LTR and HTR catalysts.

The C=O bond is hydrogenated rather than the thermodynamically favourable C=C bond on supported platinum systems. This is attributed to the influence of the SMSI (strong metal-support interaction) state in these supported platinum catalysts thus selectively producing the unsaturated alcohols rather than the saturated aldehydes.

The titania gel and mixed oxide supported platinum catalysts gave the maximum conversion and a higher activity. In all the supported catalyst systems, the formation of geraniol (E isomer) was observed as the sole product of the hydrogenation of citral.

Baeza et al. [39] used Ce and Mg as promoters in two series of Ru based catalysts supported on alumina (Al_2O_3) and activated carbon (AC).

Table 5.6. compiles the initial catalytic activities obtained with the two series of catalysts and Figure 5.15. shows composition versus time plot for citral hydrogenation over the Ru/Al_2O_3 and Ru/AC samples. The products initially formed are the saturated aldehyde, citronellal and the unsaturated alcohols, geraniol and nerol, coming from the two isomers, Z and E, of the citral.

Table 5.6. Catalytic properties of the catalyst for the hydrogenation of citral in liquid phase at 333 K.

Catalyst	**Activity (μmol g_{RuS}^{-1})**	**S_{G+N}[a] (%)**
Ru/Al_2O_3	11.62	54
$Ru\text{-}Ce/Al_2O_3$	4.83	68
Ru/AC	37.40	38
Ru-Ce/AC	78.42	82
Ce/AC	9.77[b]	100

[a] Selectivity to geraniol + nerol at 70% of conversion.

[b] μmol g_{CeS}^{-1}

Comparison of the selectivity patterns for Ru/AC and Ru/Al_2O_3 catalysts revealed differences in the formation and evolution of products. For the Ru/AC catalyst, in the first stages of the reaction, apart from the formation of the primary products, citronellal, geraniol and nerol, large amounts of acetal of citronellal and secondary products that could not be identified completely, were formed.

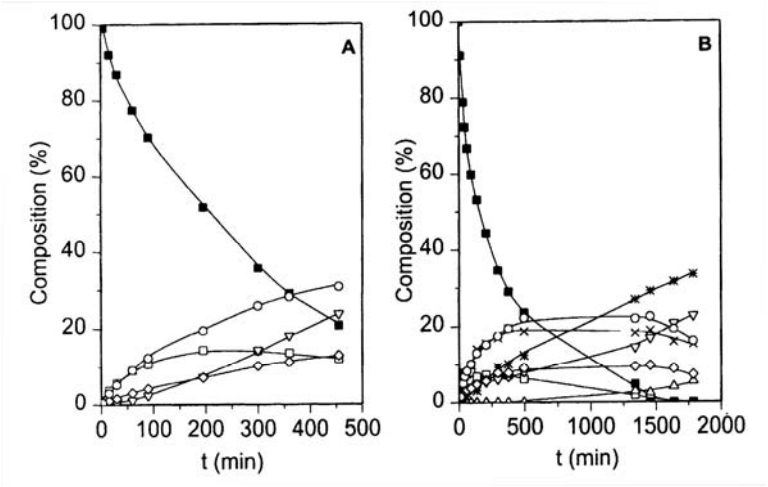

Figure 5.15. Hydrogenation of citral at 333 K over Ru/Al_2O_3 (A) and Ru/AC (B).
□ Citral; □ citronellal, O geraniol, ≀ nerol, ∇ citronellol, Δ 3,7-dimethyloctanol, * non-identified, x acetals of citronellal

5.4. Influence of Reaction Conditions

The effects of reaction conditions on the selectivity were rarely studied systematically for a given catalyst and reaction, particularly for reactions conducted in liquid phase. Therefore, only fragmentary information is available on the influence of reaction parameters such as prereduction of the catalyst, nature of the solvent, temperature, pressure, and concentration of reactant.

Tianen et al. [4] studied the hydrogenation of citral in ethanol over an Ni/Al_2O_3 catalyst in a slurry reactor operating at atmospheric pressure and at a temperature range of 60-77°C.

The roles of external and internal mass transfer resistances were investigated with three different kinds of experiments: hydrogenation with different flow rates, hydrogenation with different particle sizes and, finally, hydrogenation with different amounts of catalyst.

Citral was hydrogenated at 70°C with two different hydrogen flows: 75 and 100 ml/min. With these hydrogen flows, no considerable differences in the yields of different products could be detected.

Two different particle sizes were tested in hydrogenation: <45 and 65-90 μm. No significant differences were found in the hydrogenation velocities.

With the larger amount of the catalyst (the citral-to-nickel ratio 25), the yield of citronellol was lower than with a smaller amount of the catalyst (the citral-to-nickel ratio 51). The same trend was obtained with a used catalyst with three different citral-to-nickel ratios, the yield of citronellol decreased in the order 100>51>25.

Neri et al. [40] found both a marked effect of solvent and the presence of chloride on the support in the hydrogenation of citral on ruthenium catalysts. Table 5.7. gives the selectivities in ethanol and cyclohexane of silica supported ruthenium catalysts prepared by dry impregnation with $RuCl_3$ or $Ru(NO)(NO_3)_3$ aqueous solutions and reduction under hydrogen at 623 K. Large amounts of citronellal acetal and of 3,7-dimethyl-octanal acetal were formed by reaction of ethanol with citronellal on the catalyst prepared from a $RuCl_3$ precursor. Formation of acetals is favored by the presence of chloride ions from precursor on catalyst support, whereas negligible amounts of acetals were formed on the catalyst issued from the $Ru(NO)(NO_3)_3$ precursor. In the presence of cyclohexane, no acetal was detected and isopulegol was formed with high yields by isomerization of citronellal; this could not occur in ethanol, because acetal formation prevents the isomerization of citronellal.

Table 5.7. Effect of solvent in the hydrogenation of citral over silica-supported ruthenium catalysts

		Maximum yield (mol%)				
Catalyst	**Solvent**	**Citronellal**	**Geraniol + nerol**	**Acetals**	**Isopu legol**	**Citronellol**
RuC_2/Sa	Ethanol	<3	12	50	<1	15
$RuNI_2$/Sb	Ethanol	58	4	<1	<1	55
RuC_2/S	Cyclohexane	5	<1	0	55	<5
$RuNI_2$/S	Cyclohexane	40	8	0	23	19

Aramendia et al. [44] investigated the type of solvent which were adjusted in order to optimize the reduction process. Table 5.8. shows the influence of solvent, temperature and hydrogen pressure on $S_{citronelal}$ and $S_{E/Z}$. Selectivities were determined at 10 and 25% of conversion. The standard reaction conditions were 0.5 *M* citronelal in dioxane, 303 K, 50 mg. of catalyst Pd_3/PM2, and 60 psi (initial H_2 pressure). From the results it follows that low pressures and temperatures, in combination with methanol as the solvent, are the best in order to ensure high values of both types of selectivity.

Table 5.8. Influence of the Temperature, Hydrogen Pressure, Solvent, and Metal Support on the Initial Rate (r_g), Turnover Frequency (TON), and Selectivities ($S_{citronelal}$ and $S_{E/Z}$) of the Process

		r_g $Nmol.s^{-1}.g_{Pd}^{-1}$	TON s^{-1}	$S_{citronelal}$/%		$S_{E/Z}$/%	
				a	b	a	b
Temperature	293	13.4	7.87	94	84	79	74
°C	303	14.6	8.57	88	81	77	69
	313	16.3	9.57	80	73	73	60
	323	17.8	10.45	76	69	68	60
$P_{hydrogen}$	20	11.3	6.63	97	86	83	78
psi	40	12.9	7.57	94	83	81	76
	60	14.6	8.57	88	81	77	69
	80	15.7	9.22	82	75	76	61
Solvent	MeOH	1.3	0.76	99	96	78	74
	THF	5.1	2.99	97	91	85	73
	CHA	11.7	6.87	92	87	81	69
	DIO	14.6	8.57	88	81	77	69
Catalyst	Pd_3/PM2	14.6	8.57	88	81	77	69
	Pd_3/PS_{400}	8.7	11.82	82	73	75	67

Conversion: a = 10%; b = 25%.

CHAPTER 6

EXPERIMENTAL STUDY

A clinoptilolite rich natural zeolite was loaded by Pd and Ni through impregnation and ion exchange methods using $Pd(NO_3)_2.2H_2O$ and $Ni(NO_3)_2.6H_2O$ compounds. Modified zeolites were characterized and tested for liquid phase hydrogenation of citral in a semi-batch reactor.

6.1. Materials

The chemical types and their origins used in the experiments are given in Table 6.1.

Table 6.1. Chemicals used in the experiments

Chemicals	**Properties of Chemicals**
Clinoptilolite	From Gördes Doğu, 15-30 mm
$Pd(NO_3)_2.2H_2O$	Sigma
$Ni(NO_3)_2.6H_2O$	Aldrich
Citral	Fluka, 97%
Ethanol	Carlo Erba, 99.8%
	J.B. Baker, 99.5 %
Cyclohexanone	Sigma, 99%
Methanol	Merck, 99.5 %

6.2. Methods

The experimental study can be explained in three main headings:

1. Preparation of catalysts
2. Characterization of catalysts
3. Catalysts testing

6.2.1. Preparation of Catalysts

Clinoptilolite rich zeolite tuffs from Gördes were crushed using a hammer and sieved to a desired particle size range of 38-150 μm using stainless steel sieves. The ground samples were put into the deionized water and the mixture was boiled on a hot plate for 2 hours and then washed with water twice. This procedure was repeated twice to purify the zeolite samples. Then, the washed zeolite particles were dried at 110°C overnight and used as catalyst and a catalyst support.

6.2.1.1. Impregnation Method

$Pd(NO_3)_2.2H_2O$ and $Ni(NO_3)_2.6H_2O$ metal salts were used for impregnation and ion exchange methods. The impregnated catalysts were prepared by contacting a methanol solution of the Pd salt and zeolite in a rotary evaporator. Three different amounts of Pd loaded clinoptilolite (0.72, 2.42 and 5.63 % Pd) were prepared. 2.42 % Pd supported on clinoptilolite catalysts were prepared as follows:

4.85 g of clinoptilolite, 0.35 g $Pd(NO_3)_2.2H_2O$ and 141 ml methanol were mixed and the solvent was evaporated slowly at 60°C in a rotary evaporator. After that, the impregnated catalyst was dried overnight at 120°C and calcined under O_2 (200ml/min) flow at 345, 430 and 515°C for 2.5 h in a tubular quartz reactor.

The same method was also applied for preparation of Ni loaded sample.

6.2.1.2. Ion Exchange Method

The ion exchange experiments were carried out in a waterbath at a constant temperature of 60°C. The clinoptilolite was added to 0.01 M $Pd(NO_3)_2.2H_2O$ aqueous solution. The solid to solution ratio was 4/100. The mixture was agitated at 60°C for 24h. Pd exchanged samples were filtered, washed several times with deionized water and dried overnight at 120°C and calcined under O_2 (200ml/min) flow at 430°C for 2.5 h in a tubular quartz reactor.

6.2.2. Characterization of Catalysts

Characterization studies were carried out by different instrumental techniques.

Particle size distribution of the clinoptilolite was determined using Micromeritics Sedigraph 5100.

Pd, Ni contents and SiO_2/AlO_3 ratios of clinoptilolite were determined using Varian model Liberty II ICP-AES.

Fusion method was applied to dissolve zeolite samples. In this method: 0.1 g sample of zeolite was mixed with 1 g of lithium tetraborate and mixed in the platina crucible. The mixture was then kept at 1000°C for 1h. After cooling, it was dissolved in a hot aqueous solution of 1.6 M HNO_3.

The morphology of the samples were investigated by Philips SFEG 30S scanning electron microscopy (SEM).

The infrared spectra of the samples were taken by Shimadzu FTIR-8601PC Fourier Infrared Spectrophotometer using KBr pellet technique. A typical pellet containing 2 wt. % of sample was prepared by mixing 4 mg sample with 200 mg KBr. Infrared spectra were taken in the wavelength range of 400 - 4000 cm^{1-}.

The crystalline structure of the samples were determined by Philips X'Pert diffractometer with CuKα radiation.

The thermal properties of the samples were analyzed by the Thermogravimetric Analyzer (TGA–51, Shimadzu) and the Differential Thermal Analyzer (DTA–50, Shimadzu). Thermogravimetric (TGA) and Differential Thermal Analyses (DTA) give information about the dehydration and thermal stability properties of zeolites. TGA measures weight loss of the sample as it is heated to elevated temperatures. It gives information about the water content and types of water within the zeolite structure. DTA determines the temperatures at which thermal reactions take place in zeolite

structure. 10 mg sample was heated at 10°C/min under 40 ml/min nitrogen stream, up to 1000°C in TGA and DTA analyses.

Surface areas of the samples were determined by using the nitrogen adsorption technique at 77 K over on ASAP 2010 Micromeritics.

6.2.3. Catalysts Testing

Citral hydrogenation experiments were carried out in a stirred, semi batch reactor (500 ml, 4575 model, Parr Instrument Co.). The reactor system illustrated in Figure 6.1. was constructed and equipped with a magnetic stirring bar and an electrical heater with a temperature controller (4842 model, Parr Instrument Co.). The reaction temperature was controlled with a thermocouple probe placed inside the reactor. The system was equipped also with a high-pressure Oxytrap (Altech) and a bubbling unit, by which the oxygen is removed. Swagelock valves (needle, three-way and shut off valves), fittings and connectors were used.

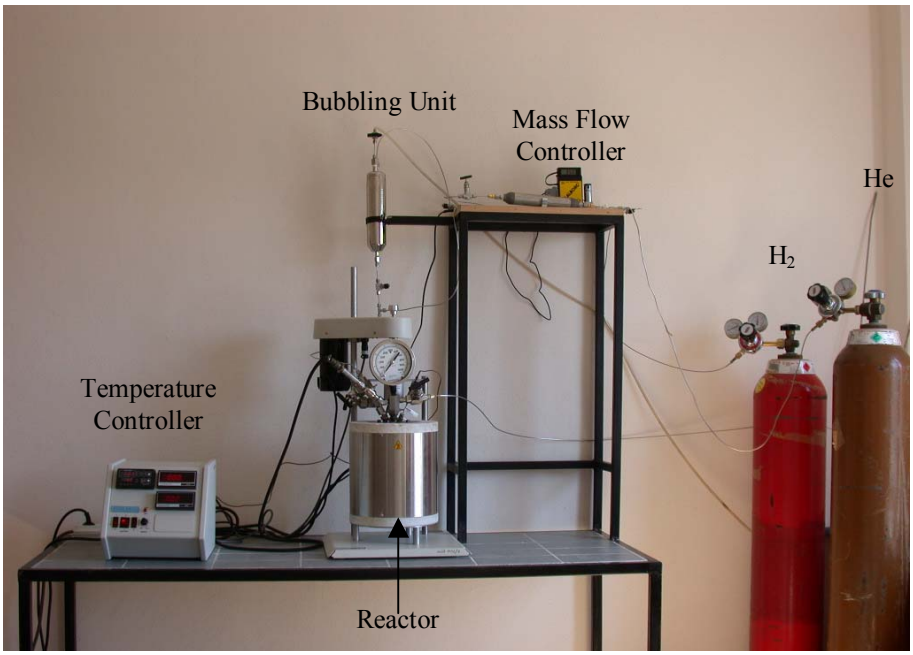

Figure 6.1. The experimental Set-Up

A typical run was carried out as follows. The reactor was loaded with the desired amount of catalyst, sealed and leak tested at 4 bar with Helium to ensure a tight seal. After that, vacuum was applied for 10 min. At the same time, temperature was set to 200°C. The reactor was filled up to 4 bar and released. This was repeated three times.

Helium was fed to the reactor at a flow rate of 60-80 ml/min for 1h while the reactor temperature was 200°C and inside pressure was 4 bar to purge air content from the reactor. The flow was then switched to H_2. Temperature was set to 400°C. The reactor was filled up to 4 bar with H_2 and released for three times. The catalyst was activated at 400°C for 2h by flowing hydrogen and then the reactor was cooled to reaction temperature and stored overnight under 2 bar H_2.

A mixture of substrate 0.1 M citral, 0.025 M cyclohexanone as internal standard in ethanol with a total reaction volume of 100 ml was injected to the bubbling unit, in which the reactants were saturated with hydrogen to remove oxygen, for 20 min. After that, the reactants were injected to the reactor with hydrogen, and citral was hydrogenated at 80°C and 6 bar while stirring the reaction mixture at 400 rpm. The liquid samples were taken from the reactor at the 0, 10 min, 30 min, 60 min, 180 min and 300 min reaction durations.

The reaction products were analysed with a Shimadzu GC-17A gas chromatograph equipped with a flame ionization detector and a capillary column DB-225 (J&W, 30 m, 0.53 mm i.d.). The temperature program used comprised of the following steps: (1) heating from 80°C to 100°C at 2°C/min. (2) heating from 100°C to 180°C at 3°C/min and (3) holding at 180°C for 1 min. The injector and detector temperatures were 220°C and 250°C, respectively. The velocity of the carrier gas helium in the column was 22 cm/s.

The peak identification was based on the retention times obtained from a standard solution containing the following commercially available hydrogenation products of citral: citronellal (≥80 %, Fluka 27470), citronellol (90-95 %, Fluka 27480), nerol (90%, Fluka 72170), geraniol (99.5 %, Fluka 48798), isopulegol (99 %, Fluka 59765). The analyses were carried out as follows:

Approximately 150 mg of the standard solution, 0.1 M citral, 0.025 M cyclohexanone and 20 ml ethanol were mixed in a flask. Then 0.25 ml of the mixture was injected into another flask, which contained 1 ml ethanol.

The peak identification was confirmed with GC-MS technique.

CHAPTER 7

RESULTS AND DISCUSSIONS

7.1. Catalyst Characterization

7.1.1. Particle Size Distribution Measurements

Particle size distribution of the clinoptilolite is given in Figure 7.1.

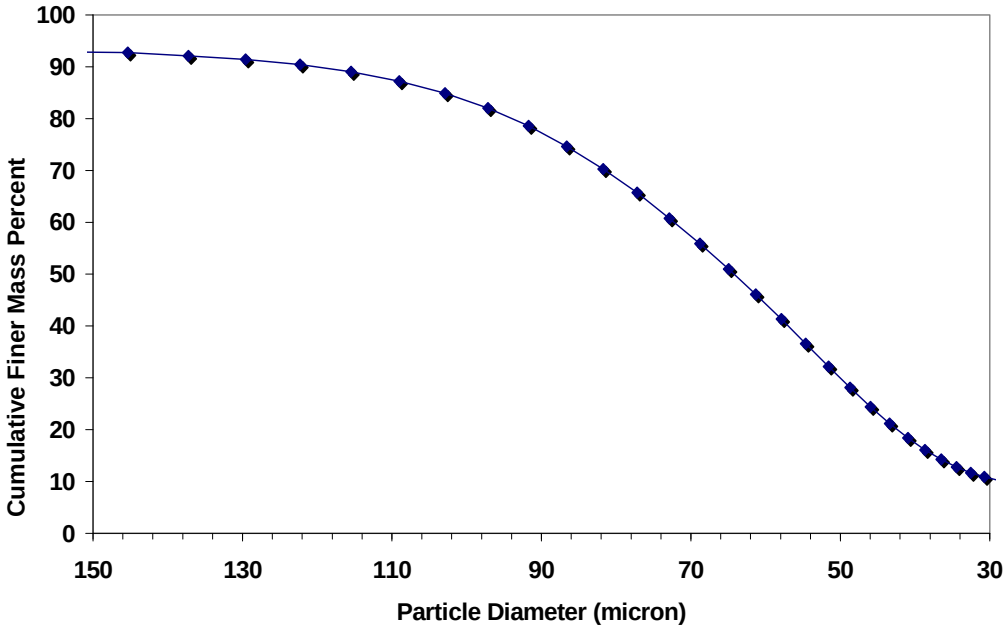

Figure 7.1. Particle size distribution of the clinoptilolite

As shown in Figure 7.1, 93 % (mass) of particles have sizes lower than 150 μm while 15 % (mass) of the particles have diameters lower than 38 μm. The mean diameter calculated from the size distribution was 66.95 μm.

7.1.2. Elemental Analysis by Inductively Coupled Plasma

Si/Al ratio of the clinoptilolite and catalysts Pd, Ni contents were determined using inductively coupled plasma (ICP). The chemical composition of the clinoptilolite samples in oxide form is given in Table 7.1.

Table 7.1. Chemical composition of the clinoptilolite rich natural zeolite

Element	**Element % Weight**
Al_2O_3	11.81
CaO	1.61
Fe_2O_3	0.71
K_2O	9.81
MgO	0.8
Na_2O	0.98
SiO_2	63.07
H_2O	10.81

Si/Al ratio for the clinoptilolite sample was found as 5.34. This ratio was reported to be in the range of 4.25-5.25 by Breck [24] and in the 4.5-5.5 range by Tsitsishvili et al. [47]. Thermal stability of clinoptilolite depends on the Si/Al ratio. Thermal behaviour of zeolites increases as Si/Al ratio increases.

Catalysts prepared by impregnation were found to have 0.72 wt % Pd, 2.42 wt % Pd, 5.63 wt % Pd and 3.12 wt % Ni. These catalysts were denoted as 0.72Pd/CLI-430-IM, 2.42Pd/CLI-430-IM, 5.63Pd/CLI-430-IM and 3.12Ni/CLI-430-IM. Catalyst prepared by ion exchange method contained 5.66 wt % Pd and it was named as 5.66Pd/CLI-430-IE.

7.1.3. Scanning Electron Microscopy Analysis

SEM micrographs of the clinoptilolite samples taken from different regions of the same sample are given in Figure 7.2.

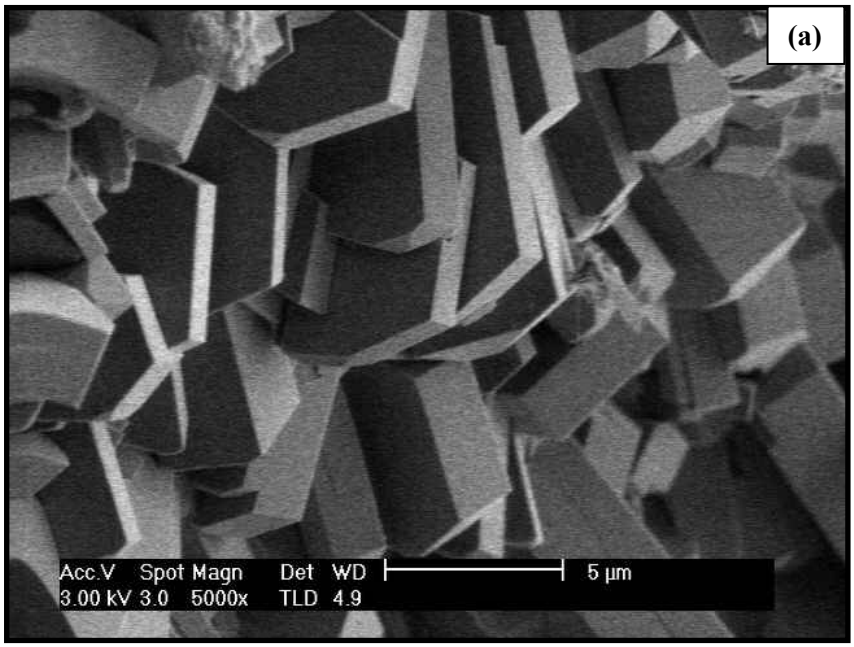

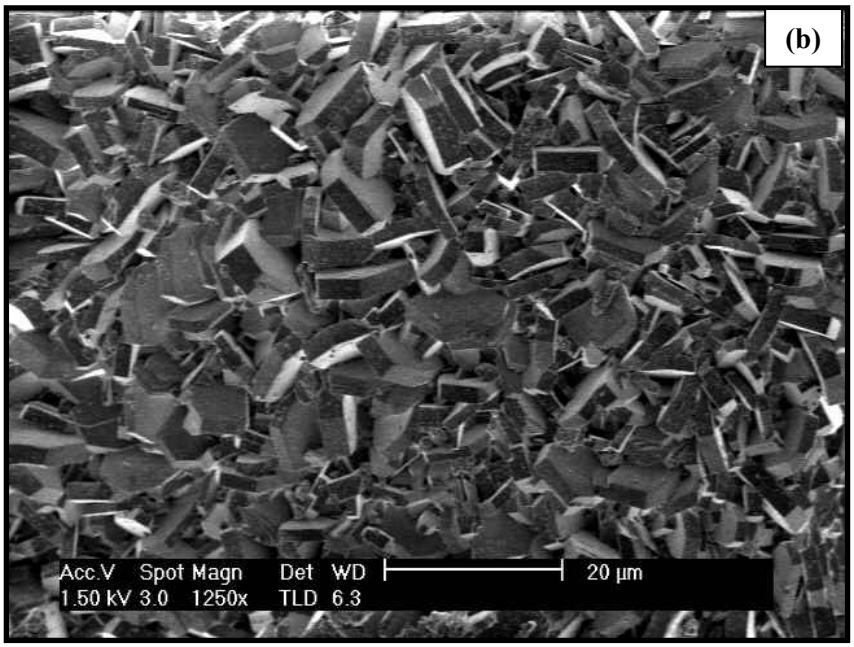

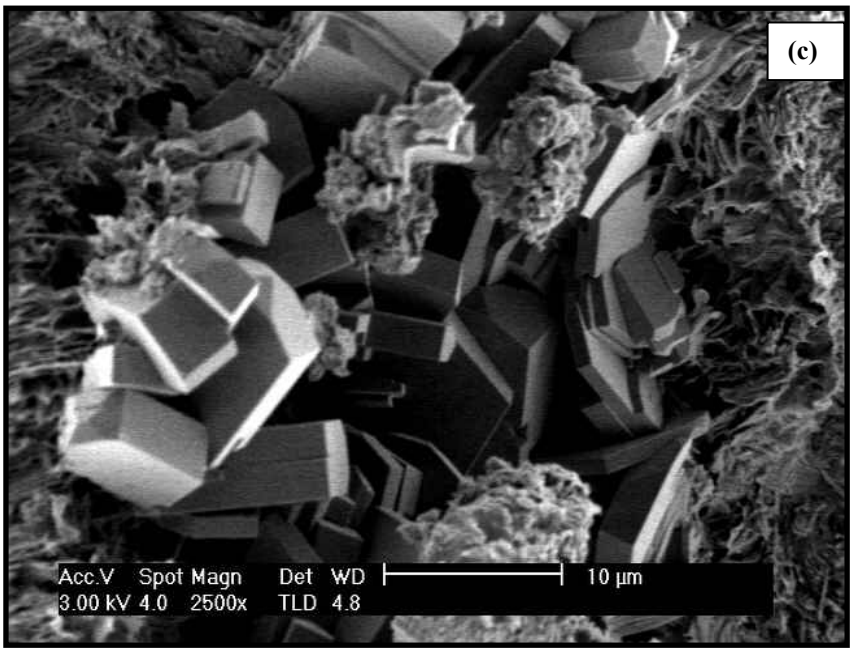

Figure 7.2. SEM micrographs of the clinoptilolite rich natural zeolite

Figure 7.2 (a) shows the classic clinoptilolite crystalline morphology, it had regular platelike crystals. The clinoptilolite crystals were observed very neatly which indicated that this SEM picture was taken from a region where clinoptilolite did not contain much impurities. In Figure 7.2 (b), the irregular arrangement of the clinoptilolite crystals can be seen clearly. Figure 7.2 (c) showed the SEM picture of the clinoptilolite, which contains impurities. Since the zeolite being studied is natural, it is obvious that it contains different impurities as discussed in section 7.1.4.

SEM picture and examples of the EDX spectrum of Pd loaded clinoptilolite are given in Figure 7.3. and Figure 7.4., respectively. The surface of the clinoptilolite is different when compared with the original clinoptilolite. Agglomerates of particles are observed. Beside this, EDX analyses showed peaks for the element obtained in the chemical analysis. SEM pictures and examples of the EDX spectrum of Ni loaded clinoptilolite are given in Figure 7.5. and Figure 7.6. respectively.

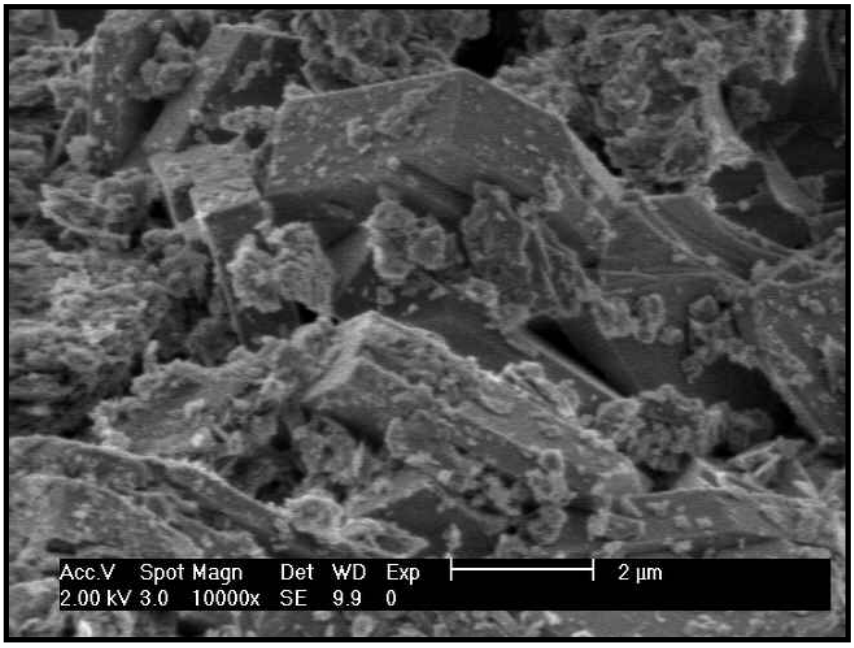

Figure 7.3. SEM picture of 5.63Pd-CLI-430-IM catalyst

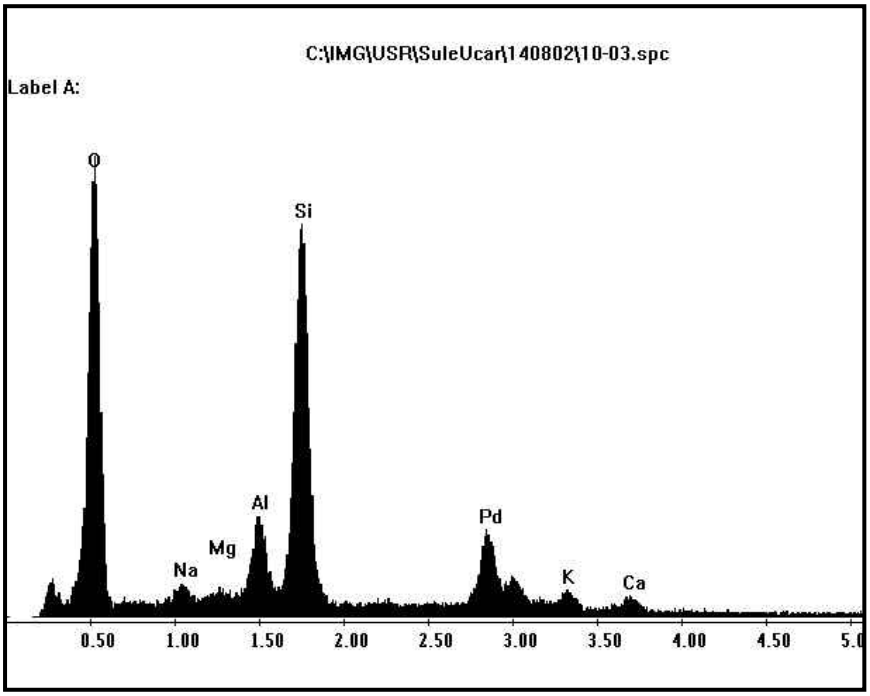

Figure 7.4. EDX spectrum of 5.63Pd-CLI-430-IM catalyst

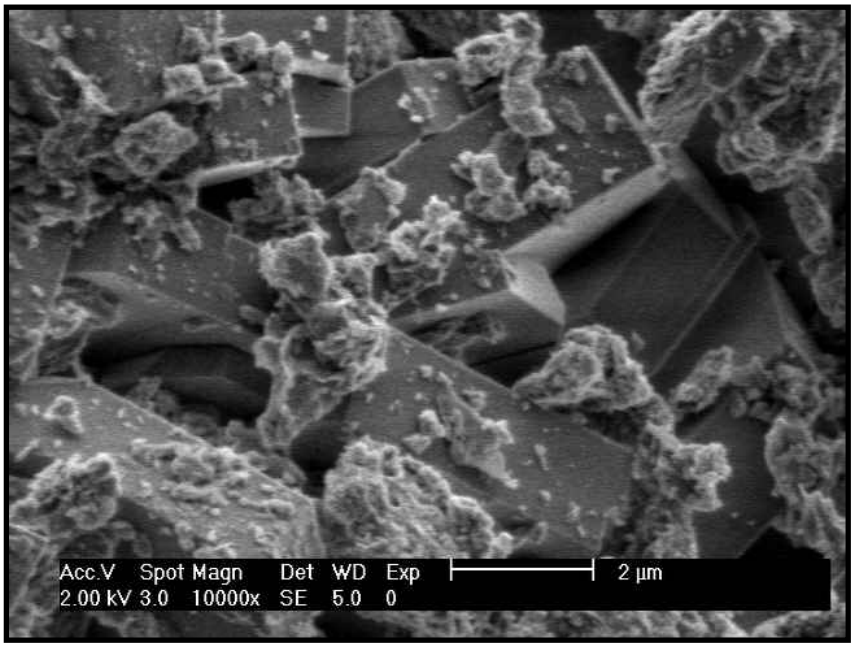

Figure 7.5. SEM picture of 3.12Ni-CLI-430-IM catalyst

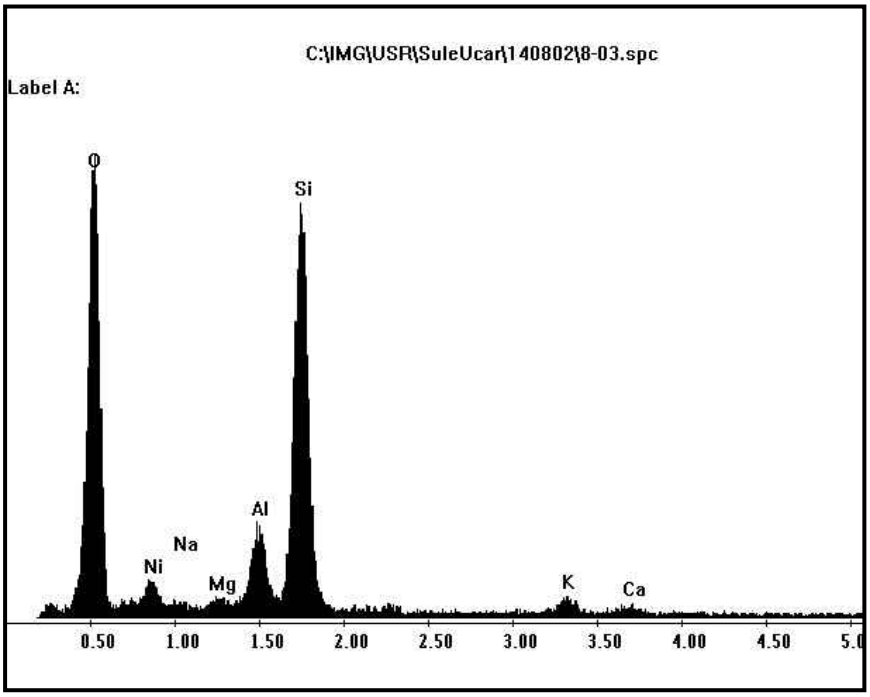

Figure 7.6. EDX spectrum of 3.12Ni-CLI-430-IM catalyst

A similar picture to Pd loaded catalyst was obtained for Ni loaded catalyst. Again EDX analyses of the sample showed peaks for the element obtained in the chemical analysis.

7.1.4. X-Ray Diffraction Analysis

The results of the X-Ray diffraction analysis are given in Figure 7.7. and Figure 7.8. The characteristic peaks of clinoptilolite were observed at 2θ = 9.93°, 22.48° and 30.18°. These results showed that clinoptilolite was the main mineral phase in the natural zeolite material.

No significant change has been observed either in the position of the most intense peaks of the clinoptilolite nor in its crystallinity with different treatments. There were slight changes in the peak intensities, which could be attributed to cation migration and elimination of the water molecules from the channels of the framework due to heating.

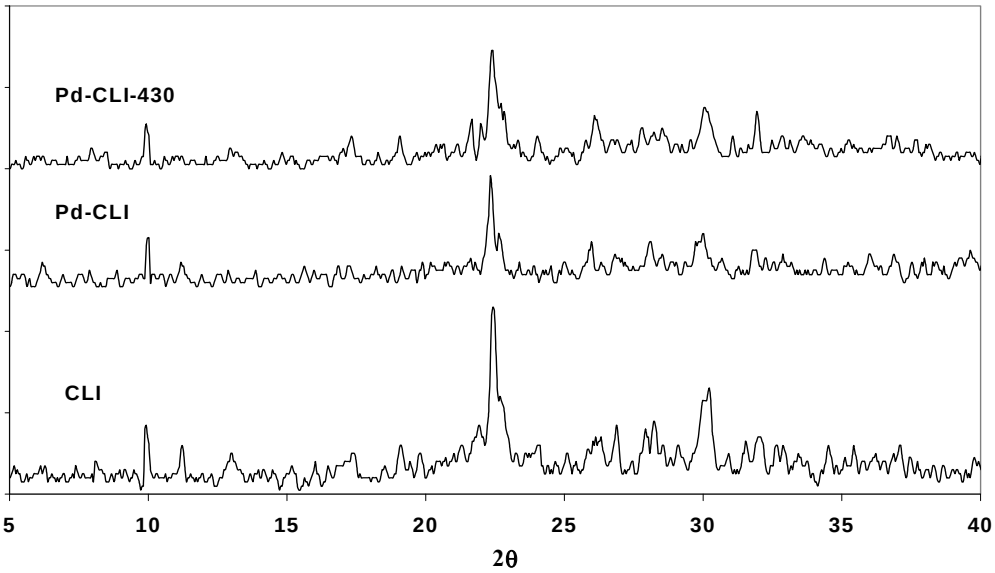

Figure 7.7. X-Ray diffraction of CLI, 2.42 Pd/CLI and 2.42 Pd/CLI-430-IM

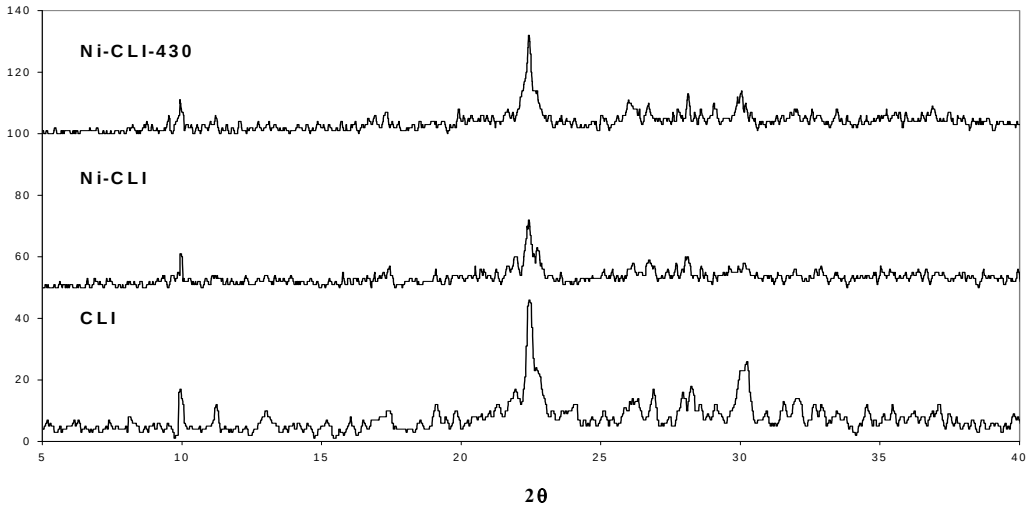

Figure 7.8. X-Ray diffraction of CLI, 3.12Ni/CLI and 3.12Ni/CLI-430-IM

The natural zeolite contained about 90 % clinoptilolite, 5-10 % opal-CT (opal-crystobollite-tridimite), 1-2 % felspat and 1-2 % quartz. The XRD analysis results showed good agreement with the previously reported composition data for the natural zeolitic material from the same region [57].

7.1.5. Fourier Transform Infrared Spectroscopy Analysis

Infrared spectroscopy has been widely used for studying the structure and properties of materials. According to Breck [24], the fundamental vibrations can be observed in the range 200-1300 cm^{-1} and IR spectra can be divided into two classes (Table 7.2.). In addition, there are three typical bands due to the presence of zeolite water: Characteristic of hydrogen-bonded OH about 3400 cm^{-1}, isolated OH at 3700 cm^{-1} and the usual bending vibration of water at 1645 cm^{-1}.

Table 7.2. Zeolite IR Assignments (in cm^{-1}) [24]

1. Internal tetrahedra	- Asym. Stretch - Sym. Stretch - T-O bend	1250 – 950 720 – 650 500 – 420
2. **External tetrahedra**	- Double ring - Pore opening - Sym. Stretch - Asym. Stretch	650 – 500 420 – 300 750 – 820 1150 – 1050

IR spectra of the clinoptilolite, impregnated and ion exchanged forms of the clinoptilolite were investigated between the 400 and 4000 cm^{-1} region. The IR spectra of clinoptilolite, 0.72Pd/CLI-430-IM, 2.42Pd/CLI-430-IM, 5.63Pd/CLI-430-IM and 5.66Pd/CLI-430-IE samples are given in Figure 7.9. The vibration bands of samples are shown in Table 7.3.

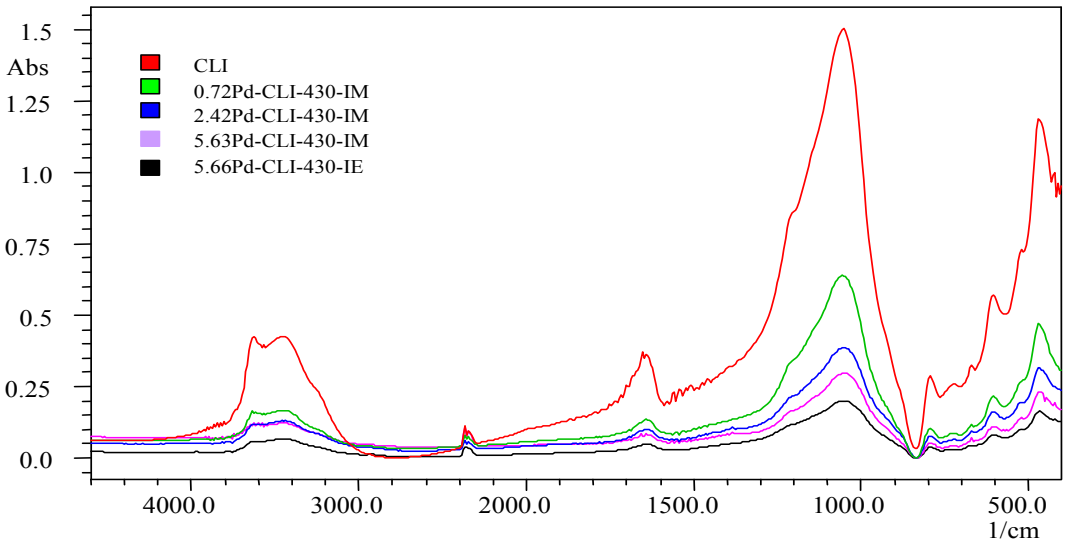

Figure 7.9. IR spectra of clinoptilolite, 0.72Pd/CLI-430-IM, 2.42Pd/CLI-430-IM, 5.63Pd/CLI-430-IM and 5.66Pd/CLI-430-IE

Table 7.3. Assignment of vibration bands for the clinoptilolite, 0.72Pd/CLI-430-IM, 2.42Pd/CLI-430-IM, 5.63Pd/CLI-430-IM and 5.66Pd/CLI-430-IE

Vibration Bands	**CLI**	**0.72Pd/ CLI-430-IM**	**2.42Pd/ CLI-430-IM**	**5.63Pd/ CLI-430-IM**	**5.66Pd/ CLI-430-IE**
Internal T-O bending	467.7	468.7	468.7	468.7	468.7
External double bonding	606.6	603.7	603.7	603.7	603.7
Internal symmetric stretch	720.4	721.3	721.3	721.3	721.3
External asymmetric stretch	792.7	794.6	788.8	794.6	788.8
External symmetric stretch	1050.2	1047.3	1047.3	1047.3	1047.3
Internal asymmetric stretch	1210.3	1209.3	1209.3	1209.3	1209.3
OH bending	1653.9	1633.6	1643.2	1637.5	1643.2
H-bonded OH stretching	3460	3435	3454.3	3465.8	3435
Isolated OH stretching	3625.9	3620.1	3620.1	3629.8	3606.6

The IR spectra of clinoptilolite and 3.12Ni/CLI-430-IM samples are given in Figure 7.10. The vibration bands of samples are shown in Table 7.4.

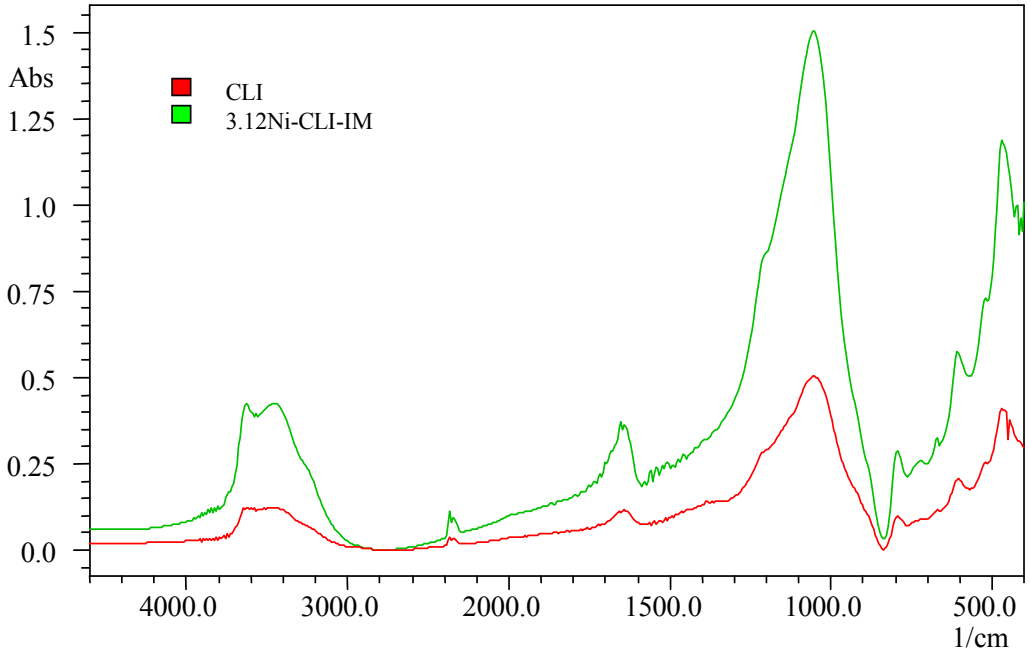

Figure 7.10. IR spectra of clinoptilolite and 3.12Ni/CLI-430-IM

Table 7.4. Assignment of vibration bands for the clinoptilolite, 3.12Ni/CLI-430-IM

Vibration Bands	**CLI**	**3.12Ni/CLI-430-IM**
Internal T-O bending	467.7	468.7
External double bonding	606.6	603.7
Internal symmetric stretch	720.4	721.3
External asymmetric stretch	792.7	788.8
External symmetric stretch	1050	1047.3
Internal asymmetric stretch	1210.3	1209.3
OH bending	1653.9	1637.5
H-bonded OH stretching	3460	3465.8
Isolated OH stretching	3625.9	3629.8

As shown in Figure 7.9. and Figure 7.10. all of the samples showed similar structural properties. The strongest band was observed around 1050 cm^{-1}, which was assigned to the asymmetry-stretching mode. The second strongest band was found around 467 cm^{-1}, which was assigned to the internal T-O bending mode. The clinoptilolite characteristic

band, which was related to the presence of the double rings in the framework structure, was observed at 606 cm^{-1}. After metal loaded and calcined at 430°C, no significant changes were recorded in absorbance values of these peaks. The other common bands were observed at about 3400-3700 cm^{-1} and 1645 cm^{-1}.

A shift was observed for the 1050 cm^{-1} band to 1047 cm^{-1} with metal loading, thereby indicating the interactions between cations and zeolite framework. The band at 1653 cm^{-1}, which represents the usual bending vibration of the water shifted to 1633-1643 cm^{-1}. The bands at 3625 cm^{-1} shifted to 3606-3620 cm^{-1}. These bands are attributed to interaction of water hydroxyl with the cation. Similar frequency shifts were observed for the 3460 cm^{-1} band, which are formed due to the interactions of water molecules with the framework via hydrogen bands. A strong H-bond, tends to lower the wave number. Therefore, the shifts of the vibration band at 3460 cm^{-1} indicated how strong extra framework cations affect the interactions between water molecules and the framework.

Adsorbed H_2O gives rise to a typical deformation band around 1645 cm^{-1}. The IR spectra showed several adsorbtion bands around 1600 cm^{-1}, caused by deformation of water molecules and the spectra contained adsorbtion bands due to the hydrogen bonded OH about 3400 cm^{-1} and isolated OH at 3700 cm^{-1} [47].

7.1.6. Thermal Analysis

TGA curves of clinoptilolite, Pd forms of clinoptilolite and Ni forms of clinoptilolite are shown in Figure 7.11. and Figure 7.12. respectively.

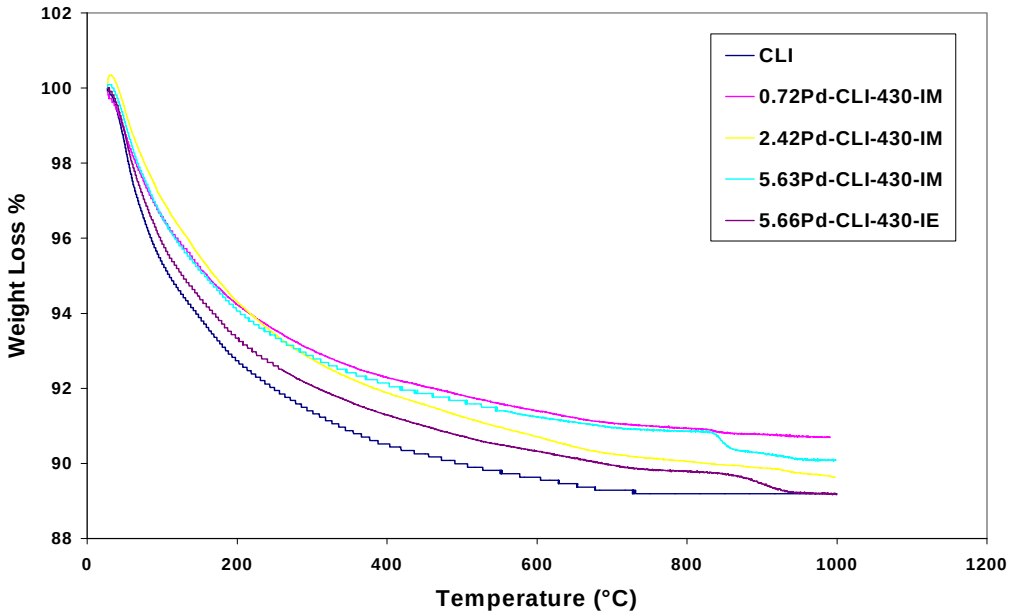

Figure 7.11. TGA curves of original clinoptilolite and Pd forms of clinoptilolite

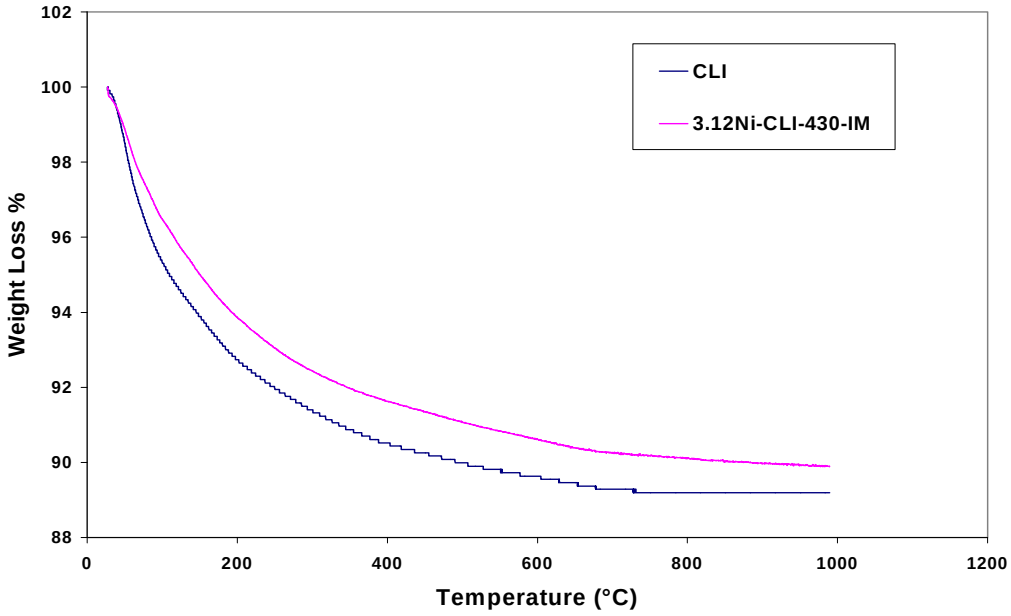

Figure 7.12. TGA curves of the original clinoptilolite and Ni forms of the clinoptilolite

TGA curves showed that the water contents of the samples were different. The average percent weight losses up to 800°C were calculated as 10.81 % for clinoptilolite, 9.06 % for 0.72Pd/CLI-430-IM, 9.95 % for 2.42Pd/CLI-430-IM, 9.14 % for 5.63Pd/CLI-430-IM, 10.22 % for 5.66Pd/CLI-430-IE and 9.88 % for 3.12Ni/CLI-430-IM. The water in clinoptilolite was classified in three groups as external, loosely bound water and tightly bound water [48]. Based on their study external water released up to 85°C, loosely

bound water is lost rapidly up to 285°C. After 285°C the clinoptilolite started to loose its tightly bound water. After 700°C there is noticeable weight loss that takes place in the structure [48]. The percent loss of external, loosely and tightly bound zeolites for Pd forms and Ni forms of clinoptilolite are given in Table 7.5. and Table 7.6. respectively. These differences in percent weight loss could be resulted from the differences in water contents and depend on the amount and type of the extra-framework cations [24, 47].

Table 7.5. The percent Weight Loss of External, Loosely Bound and Tightly Bound Water for Pd Forms of Clinoptilolite

Sample	External Water (< 85°C)	Loosely Bound Water (85°C-285°C)	Tightly Bound Water (285°-500°C)	(>500°)	Total
Org-CLI	3.99	4.42	1.60	0.8	10.81
0.72Pd/CLI-430-IM	2.47	4.27	1.40	0.92	9.06
2.42Pd/CLI-430-IM	2.35	4.67	1.74	1.19	9.95
5.63Pd/CLI-430-IM	2.74	4.30	1.28	0.82	9.14
5.66Pd/CLI-430-IE	3.42	4.37	1.49	0.94	10.22

Table 7.6. The percent Weight Loss of External, Loosely Bound and Tightly Bound Water for Ni Forms of Clinoptilolite

Sample	External Water (< 85°C)	Loosely Bound Water (85°C-285°C)	Tightly Bound Water (285°-500°C)	(>500°)	Total
Org-CLI	3.99	4.42	1.60	0.8	10.81
3.12Ni/CLI-430-IM	2.52	4.77	1.60	0.99	9.88

DTA curves of clinoptilolite, Pd loaded clinoptilolites and Ni loaded clinoptilolite are shown in Figure 7.13. and Figure 7.14. Mainly, one endotherm and one exotherm were obtained in all samples. The dehydration behaviour of the samples is given in Table 7.7.

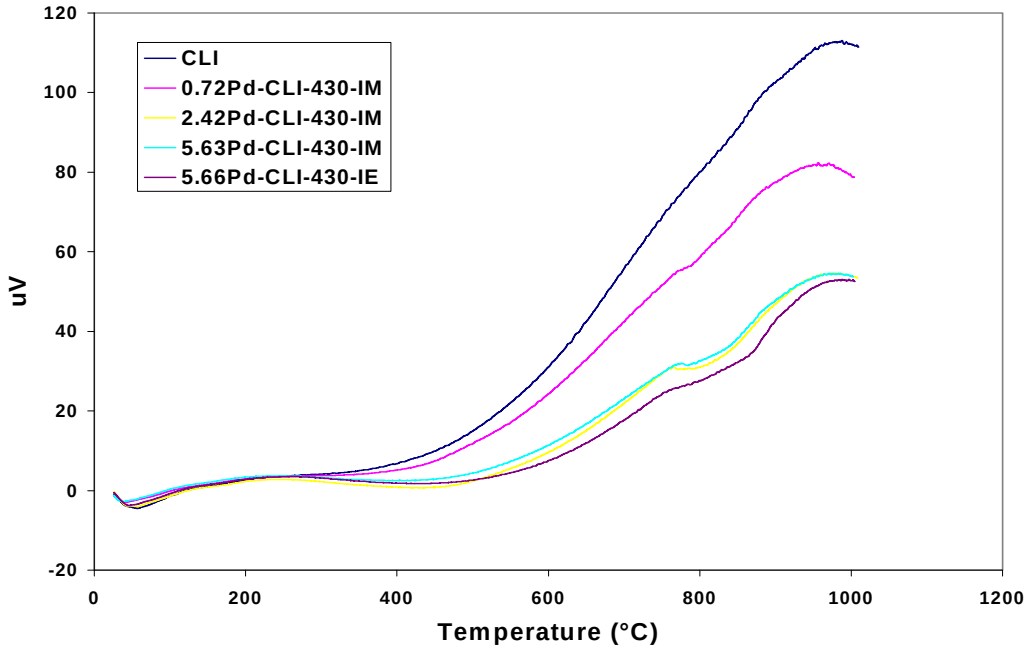

Figure 7.13. DTA curves of the CLI, 0.72Pd/CLI-430-IM, 2.42Pd/CLI-430-IM, 5.63Pd/CLI-430-IM and 5.66Pd/CLI-430-IE

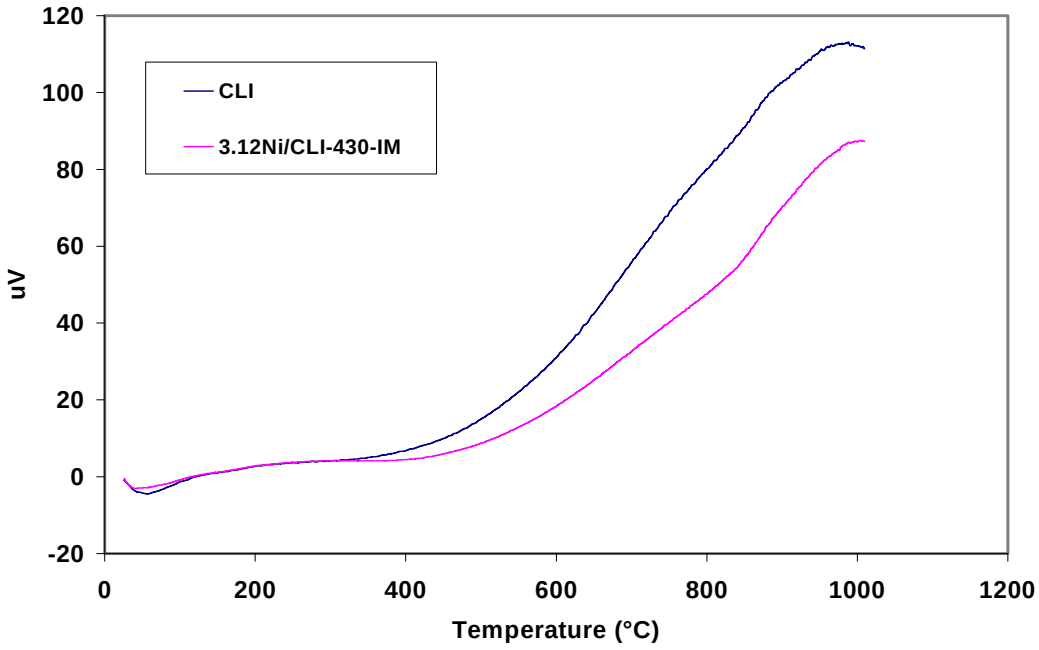

Figure 7.14. DTA curves of CLI and 3.12Ni/CLI-430-IM

Table 7.7. The dehydration behaviour of CLI, Pd loaded CLI and Ni loaded CLI

Sample	**Endotherm (°C)**	**Peak Max. (°C)**
CLI	57.28	988.2
0.72Pd/CLI-430-IM	49.23	959.8
2.42Pd/CLI-430-IM	57.78	970.7
5.63Pd/CLI-430-IM	43.89	978.8
5.66Pd/CLI-430-IE	50.16	987.4
3.12Ni/CLI-430-IM	40.83	1002

A schematic DTA curve for a zeolite is given in Figure 7.15. The low temperature endotherm represents the loss of water while the higher temperature exotherm represents conversion of the zeolite to another amorphous or crystalline phase [24].

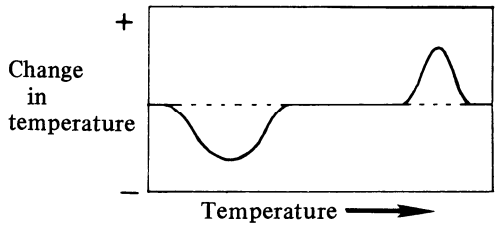

Figure 7.15. Schematic DTA curve for a zeolite

For all samples, the shape of the first endotherms, which is the characteristic of the natural zeolites, was the same. These first endotherm temperatures correspond to presence of zeolite water in the structure. Shifts in the peak minimum temperatures observed in the clinoptilolite samples may be indicative of the dependence of bond strength of water to the composition. According to the DTA curves, no thermal reaction took place for the 0.72Pd/CLI-430-IM catalyst up to 440°C, while other Pd catalysts were stable up to 500°C. 3.12Ni/CLI-430-IM catalyst was found to be stable up to 450°C. These results were also confirmed with XRD studies.

Clinoptilolite and catalyst samples collapsed between 959-1000°C.

7.1.7. Pore Volume and Surface Area Measurements

The results of pore volume, pore size and surface area measurements for clinoptilolite and Pd and Ni loaded clinoptilolite are given in Table 7.8. It was observed that pore size and surface areas change with metal loading, with preparation method and catalyst calcination temperature. The catalyst surface area increased by increase of the catalyst loading from 0.72 % to 2.42 %. However, it decreases when the metal content is 5.63 %. Highest surface area was obtained with 2.42Pd/CLI-430-IM catalyst (38.96 m^2/g). This implied that at high loading probably some of the pores were blocked.

Higher surface areas were obtained for catalysts prepared by ion exchange compared to impregnation method. This indicated that ion exchange did not block the pores in comparison to impregnation. Also ion exchange was performed in an aqueous solution which might have removed some of the impurities in the clinoptilolite.

The highest surface area (38.96 m^2/g) was obtained for the sample calcined at the temperature of 430°C, among the temperatures studied. The surface area was lower at the higher temperature of 515°C. This was probably due to partial collapse of the crystals as discussed in sections 7.1.4 and 7.1.6. The surface area was also lower at the calcination temperature of 345°C. This temperature might not be high enough to remove all the volatiles and rearranges the surface properties of the catalyst.

Table 7.8. Summary of adsorption and desorption measurements for clinoptilolite, Pd loaded clinoptilolite and Ni loaded clinoptilolite

Area	**CLI**	**0.72 Pd/CLI-430-IM**	**2.42 Pd/CLI-345-IM**	**2.42 Pd/CLI-430-IM**	**2.42 Pd/CLI-515-IM**	**5.63 Pd/CLI-430-IM**	**5.66 Pd/CLI-430-IE**	**3.12 Ni/CLI-430-IM**
BET Surface Area (m^2/g)	28.8649	36.7096	36.6106	38.9633	36.0287	35.4584	49.4643	43.6581
Langmuir Surface Area (m^2/g)	42.1362	53.5879	52.1321	54.7162	51.0986	51.3393	69.1347	61.7816
Micropore Area (m^2/g)	20.2729	29.8718	24.5539	18.1069	21.9190	25.9954	14.5173	23.3794
Volume								
Micropore Volume (cm^3/g)	0.010622	0.015531	0.012601	0.009235	0.011191	0.013472	0.007552	0.012034
Pore Size								
Average Pore Diameter (4V/A by BET) (A)	56.8546	50.9571	51.2068	53.2216	51.5833	49.2809	50.3181	42.4286
H-K Method								
Median Pore Diameter (A)	7.6087	7.3023	7.7209	7.8990	7.7177	7.5274	8.3377	7.2360

7.2. Catalyst Testing

Citral hydrogenation reactions were performed over 0.72Pd/CLI-430-IM, 2.42Pd/CLI-430-IM, 5.63Pd/CLI-430-IM, 5.66Pd/CLI-430-IE and 3.12Ni/CLI-430-IM catalysts.

Hydrogenation experiments were carried out under different conditions and with the catalyst samples calcined at different temperatures (345, 430 and 515°C). Reaction variables employed in this study were pressure (6 and 10 bar), stirring rate (400 and 800 rpm), temperature (80, 100 and 120°C), amount of the catalysts (150, 250, 400 mg), ethanol source (Carlo Erba and J.B. Baker), catalyst metal loading (0.72, 2.42 and 5.63 % Pd) and catalyst preparation method (impregnation and ion exchange). Catalyst deactivation was also investigated.

The conversion of citral was defined as the mass percent of reactant consumed. In addition, the selectivity to citronellal is defined as the mass percent fraction of citronellal to the consumed reactant and the yield of citronellal is defined as the mass percent fraction of citronellal to the reactant. Calculations were done as follows:

$$\text{Conversion (mass \%)} = \frac{(\text{citral})_{in} - (\text{citral})_{out}}{(\text{citral})_{in}} \times 100$$

$$\text{Selectivity to citronellal (mass \%)} = \frac{(\text{citronellal})_{out}}{(\text{citral})_{in} - (\text{citral})_{out}} \times 100$$

$$\text{Yield of citronellal (mass \%)} = \frac{(\text{citronellal})_{out}}{(\text{citral})_{in}} \times 100$$

The following relationship exists between conversion, yield and selectivity.

Yield of citronellal = conversion x selectivity to citronellal

7.2.1. Effect of the Calcination Temperature

The influence of calcination temperature on the citral hydrogenation was studied at three different calcinations temperatures: 345°C, 430°C and 515°C. Figure 7.16. shows the product distribution of citral, up to the reaction time of 300 min for the different calcination temperatures.

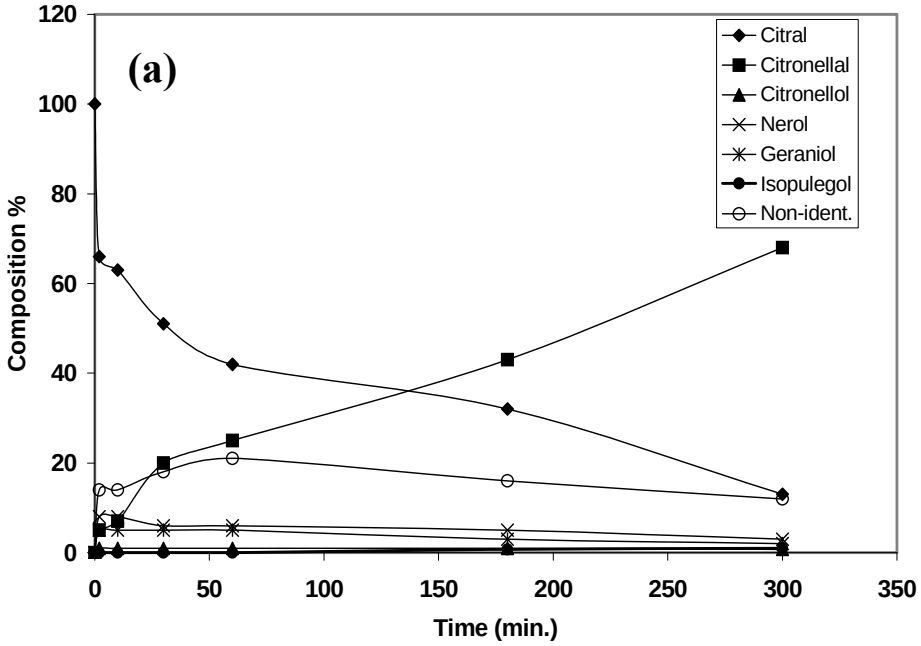

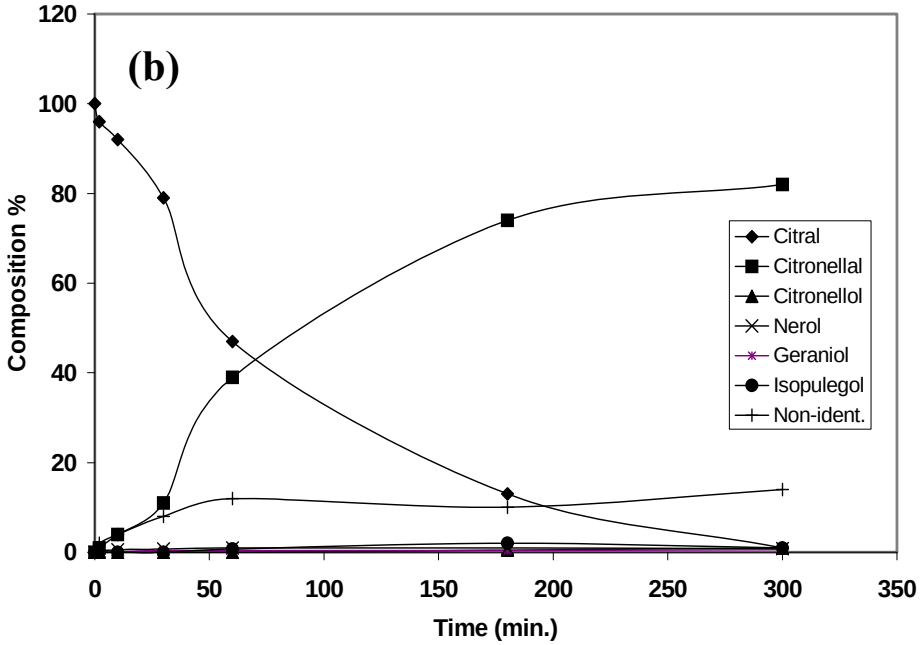

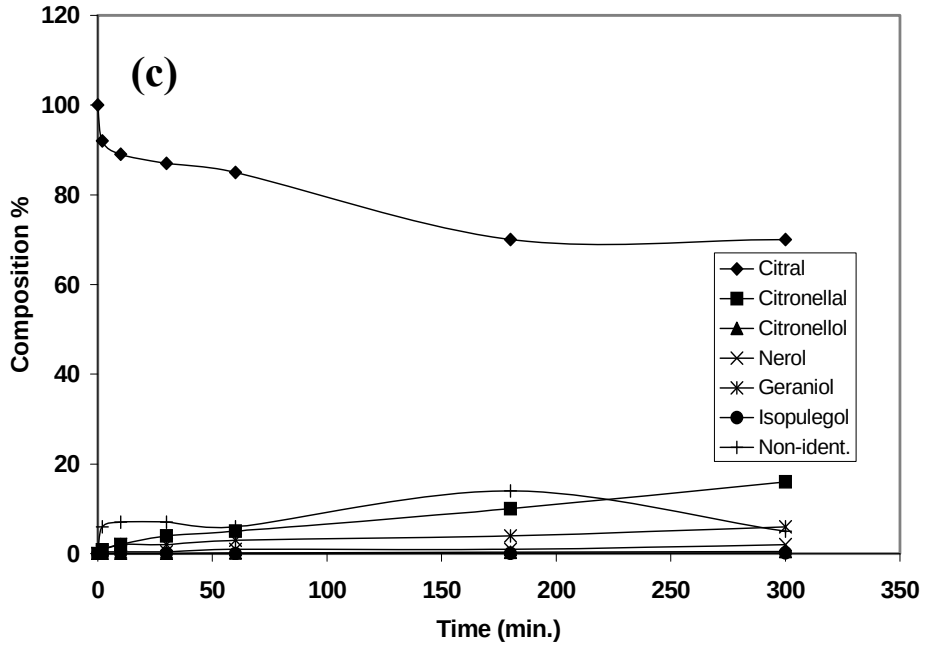

Figure 7.16. Hydrogenation of citral at 80°C, 6 bar, 400 rpm and m= 250 mg over 2.42Pd/CLI-345-IM (a), 2.42Pd/CLI-430-IM (b) and 2.42Pd/CLI-515-IM (c)

The hydrogenation of citral leaded to a variety of products; citronellal, citronellol, nerol, geraniol, isopulegol and non-identified products were observed for the different calcination temperatures as shown in Figure 7.16. For 2.42Pd/CLI-345-IM catalyst, large amount of citronellal (68 %) and only small quantities of nerol (3 %), geraniol (2 %), citronellol (1 %) and non-identified products (<12 %) were obtained at 300 min. Similar trend was observed for 2.42Pd/CLI-430-IM catalyst. But the formation of citronellal increased to 82 %. However, the small amount of citronellal (16 %) was obtained at reaction time of 300 min for 2.42Pd/CLI-515-IM catalyst.

The plot of conversion, selectivity to citronellal and yield of citronellal for the hydrogenation of citral for various calcination temperatures are given in Figure 7.17.

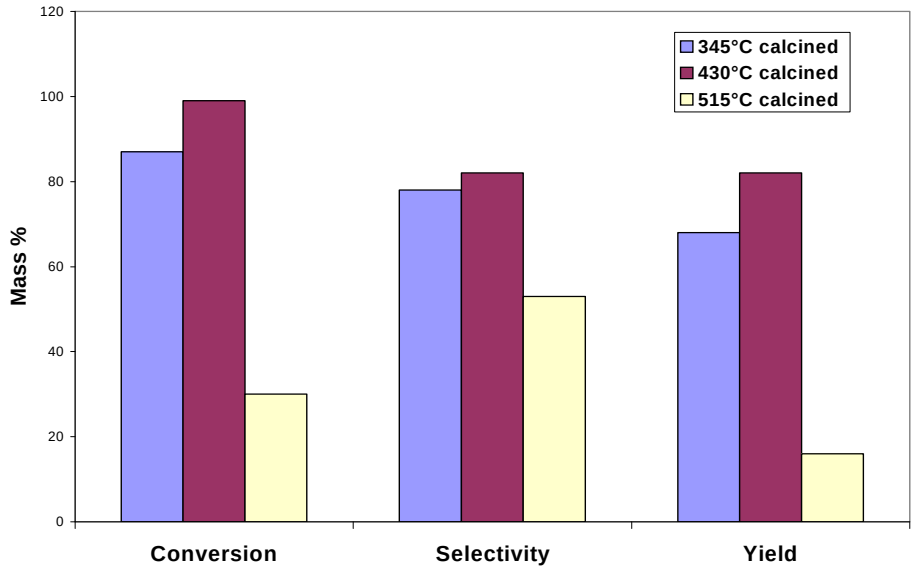

Figure 7.17. Conversion, selectivity to citronellal and yield of citronellal as a function of calcination temperature at reaction time of 300 min over 2.42Pd/CLI-430-IM catalyst at 80°C, 6 bar, 400 rpm, and m= 250 mg

The highest conversion (99 %), selectivity (82 %) and yield (82 %) were obtained with the catalyst which was calcined at 430°C. This could be attributed the change in catalyst surface area, in crystal structure and rearrangement of active metals with calcination temperature. Characterization results showed that surface area was maximum for 430°C. Salmi et. al. [4] also reported that surface area changes with calcination temperature, thereby effects the reaction rate.

7.2.2. Effect of Pressure

The influence of hydrogen pressure on the citral hydrogenation was studied at two different hydrogen pressures: 6 bar and 10 bar. Figure 7.16 (b) and Figure 7.18 show the product distribution of citral up to the reaction time of 300 min at different pressures.

No significant pressure effect on product distribution was detected during citral hydrogenation over 2.42Pd/CLI-430-IM catalyst because the product distribution at 80°C between 6 bar and 10 bar H_2 at reaction time of 300 min were the same. This implied that the reaction orders in H_2 for the formation of citronellal and other products were similar.

Singh et. al. [2] did not find significant pressure effect on the product distribution during citral hydrogenation over Pt/SiO_2 catalyst.

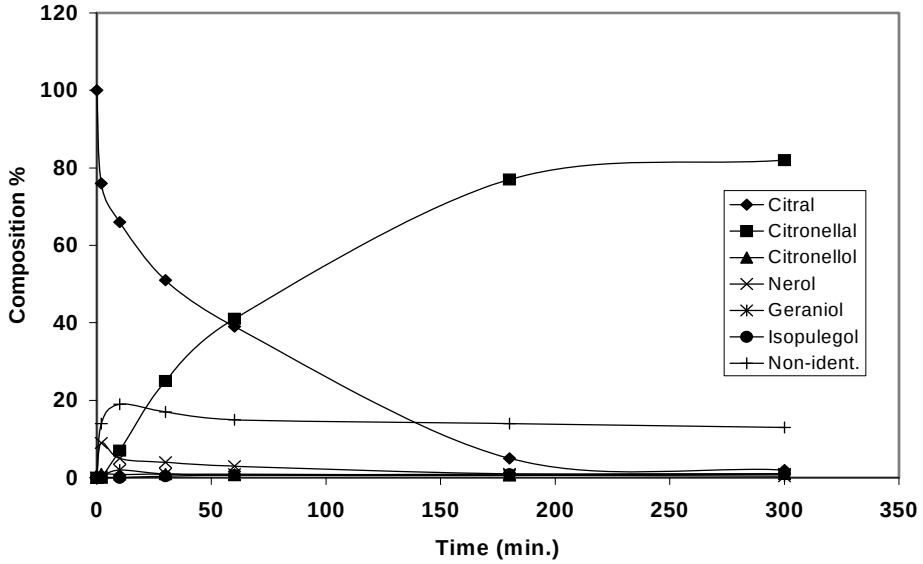

Figure 7.18. Hydrogenation of citral over 2.42Pd/CLI-430-IM at 80°C, 10 bar, 400 rpm and m= 250 mg

The plot of the yield of citronellal versus time for different pressures is given in Figure 7.19. The yield of citronellal increased with time. No significant differences were found in citronellal formation with increasing the pressure. At different pressures, the same citronellal yields (% 82) were observed at 300 min.

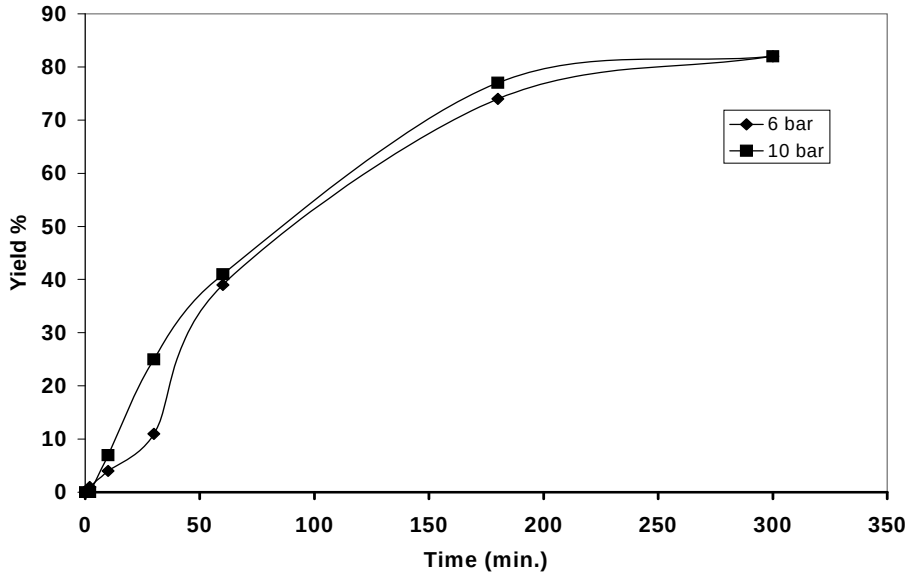

Figure 7.19. The yield of citronellal with different pressures over 2.42Pd-CLI-430-IM catalyst at 80°C, 400 rpm and m= 250 mg

Figure 7.20 compares the conversion, the selectivity to citronellal and the yield of the citronellal for two different pressures for the reaction time of 300 min. Increasing the pressure did not effect the conversion, selectivity and yield of citronellal. These results showed that hydrogen mass transfer in the gas phase was not a limiting step for the hydrogenation of citral.

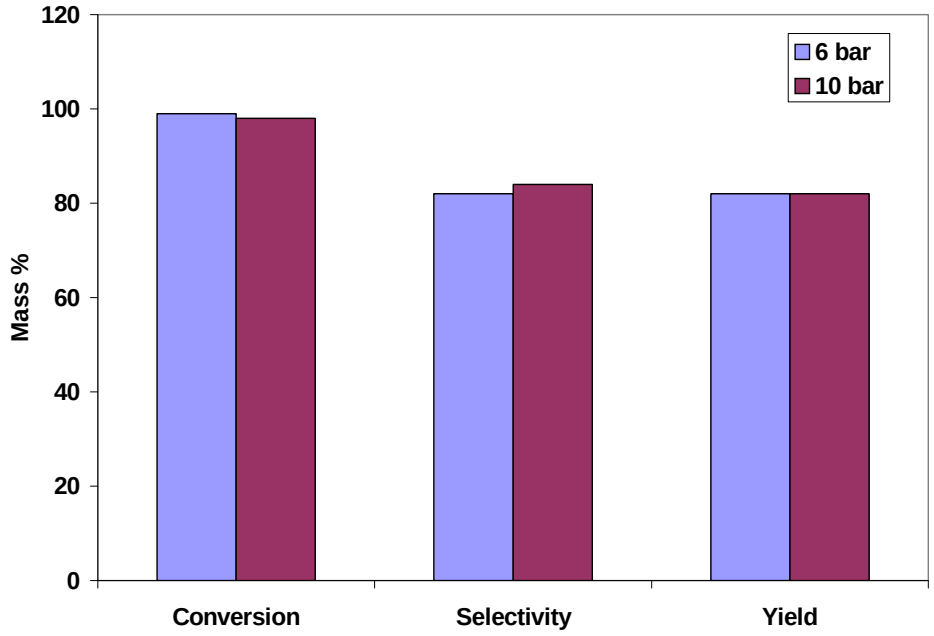

Figure 7.20. Conversion, selectivity to citronellal and yield of citronellal as a function of pressure over 2.42Pd/CLI-430-IM catalyst at 80°C, 400 rpm and m= 250 mg

7.2.3. Effect of the Stirring Rate

The influence of stirring rate on the citral hydrogenation was studied at two different stirring rates: 400 rpm and 800 rpm. Figure 7.16 (b) and Figure 7.21 show the product distribution of citral up to the reaction time of 300 min with various stirring rates. Similar product distributions were obtained.

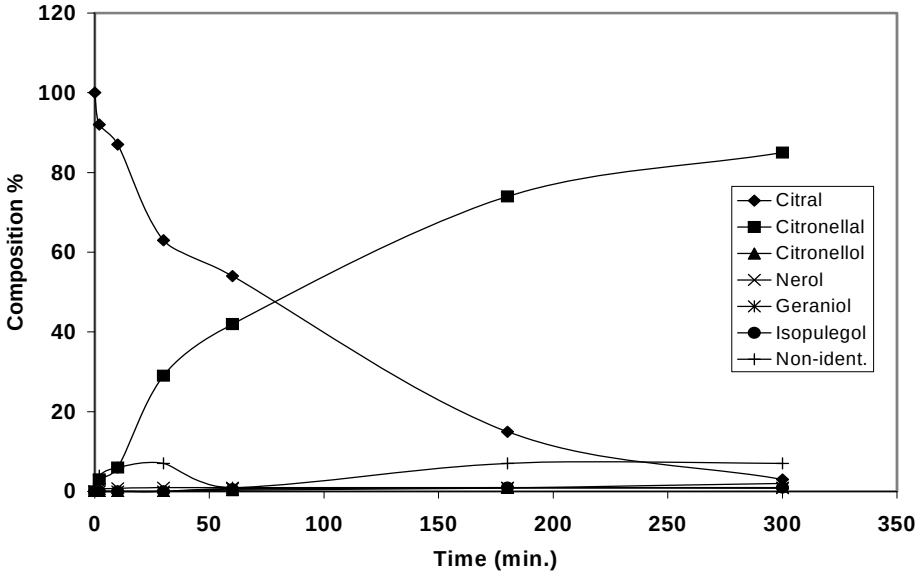

Figure 7.21. Hydrogenation of citral over 2.42Pd/CLI-430-IM at 80°C, 10 bar, 800 rpm and m= 250 mg

The plot of the yield of citronellal versus time is given in Figure 7.22. and the conversion, the selectivity to citronellal and the yield of citronellal for the hydrogenation of citral for various stirring rates is given in Figure 7.23.

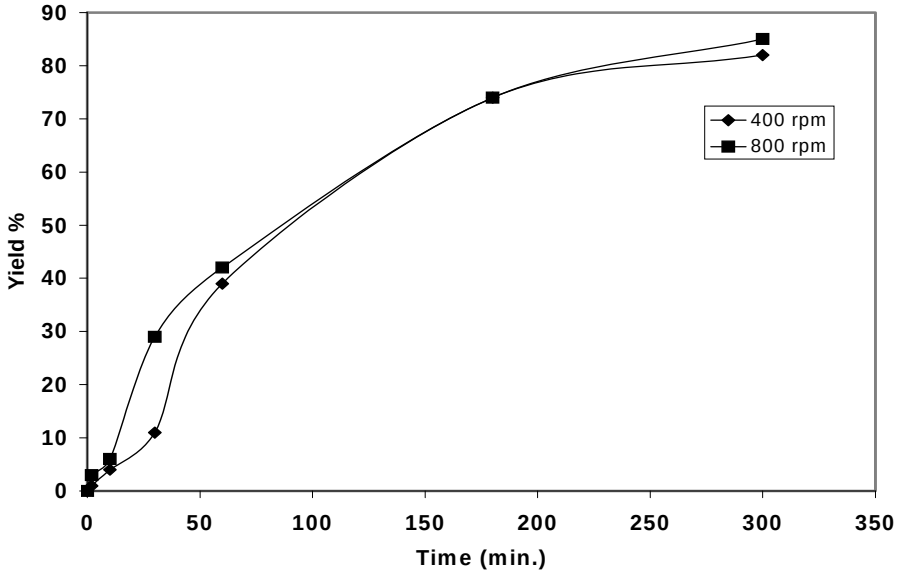

Figure 7.22. The yield of citronellal with different stirring rate over 2.42Pd/CLI-430-IM catalyst at 80°C, 6 bar and m= 250 mg

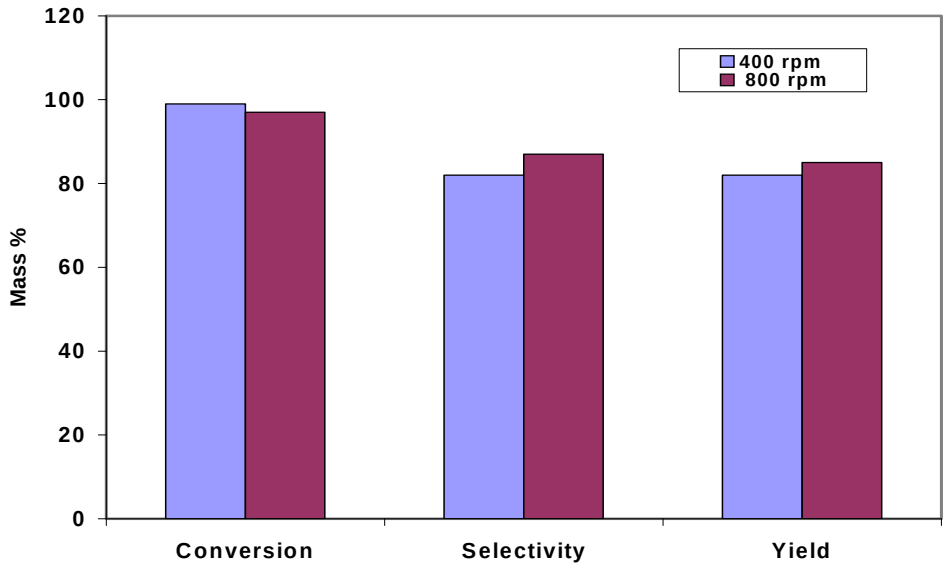

Figure 7.23. Conversion, selectivity to citronellal and yield of citronellal as a function of stirring rate over 2.42Pd/CLI-430-IM catalyst at 80°C, 6 bar and m= 250 mg

These results indicated that the stirring rate did not affect the reaction rate. This showed that the reaction was performed in the absence of gas phase and liquid phase diffusional limitations. Galvagno et. al. [3] reported that the stirring speed of 200 – 800 rpm was found to be sufficient to eliminate gas and liquid phase diffusion resistances.

7.2.4. Effect of the Reaction Temperature

The influence of the reaction temperature on the citral hydrogenation was studied at three different temperatures: 80°C, 100°C and 120°C. Figure 7.16 (b) and Figure 7.24 show the product distribution of citral up to the reaction time of 300 min for various temperatures. It can be seen that temperature has a significant effect on the product distribution. At 80°C, the formation of citronellal increased to 82 % for a reaction time of 300 min. At 100°C, the formation of citronellal increased rapidly to 75 % in 60 min, then increased to 86 % for the reaction time of 180 min. At higher reaction time, the concentration of citronellal began to decrease when the concentration of non-identified products increased during the citral hydrogenation. At 120°C, the formation of citronellal increased rapidly to 76 % for the reaction time of 30 min, then a small increase (to 87 %) was observed until the reaction time was 60 min. At the higher

reaction time, citronellal seems to be transformed to the non-identified product. The non-identified product here could be citronellal acetal [3,7].

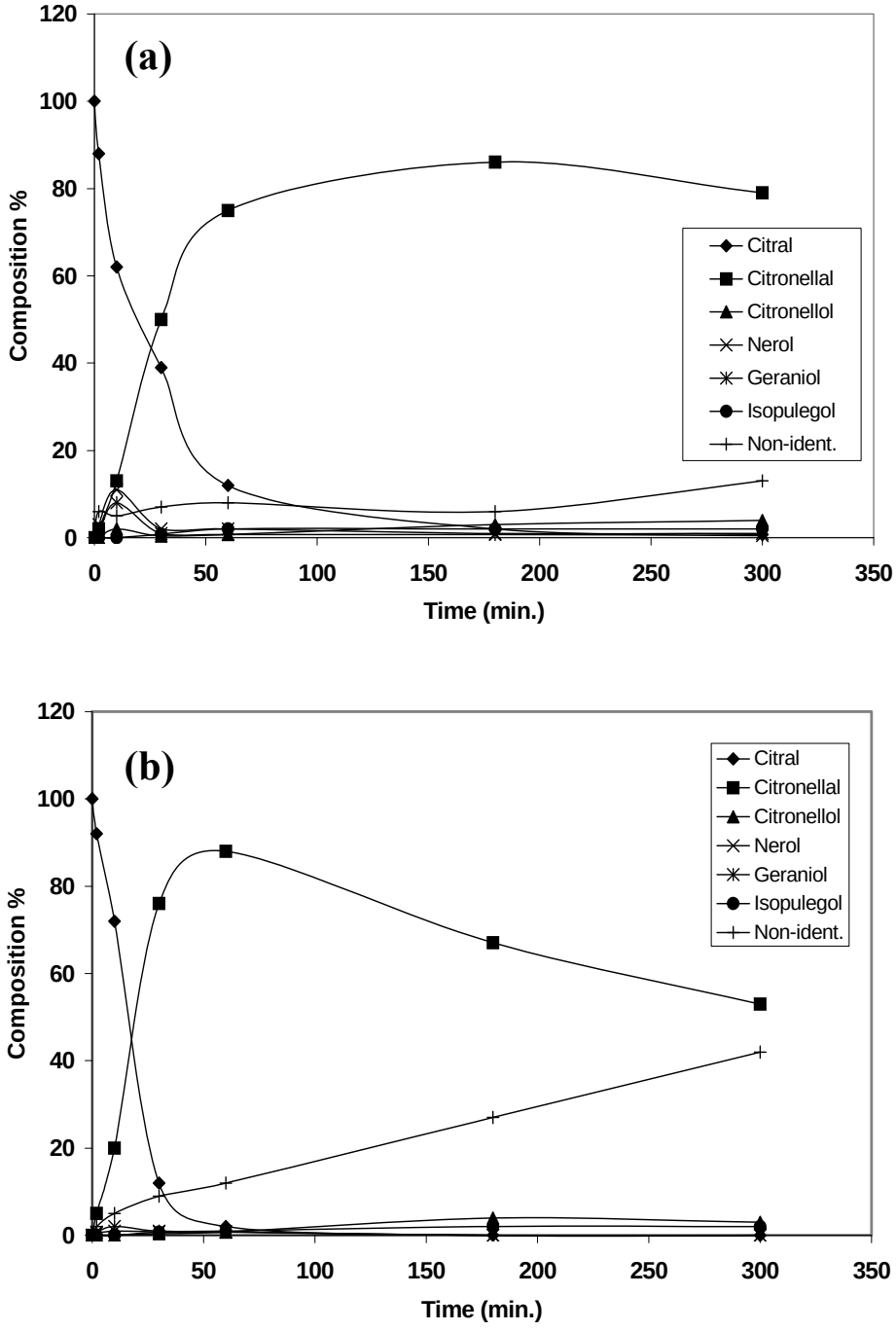

Figure 7.24. Hydrogenation of citral over 2.42Pd/CLI-430-IM at 6 bar, 400 rpm and m= 250 mg, 100°C (a) and 120°C (b)

The plots of conversion, selectivity to citronellal and yield of citronellal versus time for various temperatures are given in Figure 7.25. As shown in the figure, the citronellal

formation rates increased with the temperature. The yield of citronellal attained its maximum fastest at 120°C in 60 min. At 120°C, citronellal yield attained its maximum value of 87 % in 60 min. The maximum yield of citronellal was obtained after 180 min at 100°C and after 300 min at 80°C. This was attributed to the temperature dependence of the rate constant. The reaction rate constant increased by increasing the temperature. As a result, the reaction rate also increased. The temperature did not affect the total conversion, but the selectivity to citronellal and the yield of citronellal increased slightly.

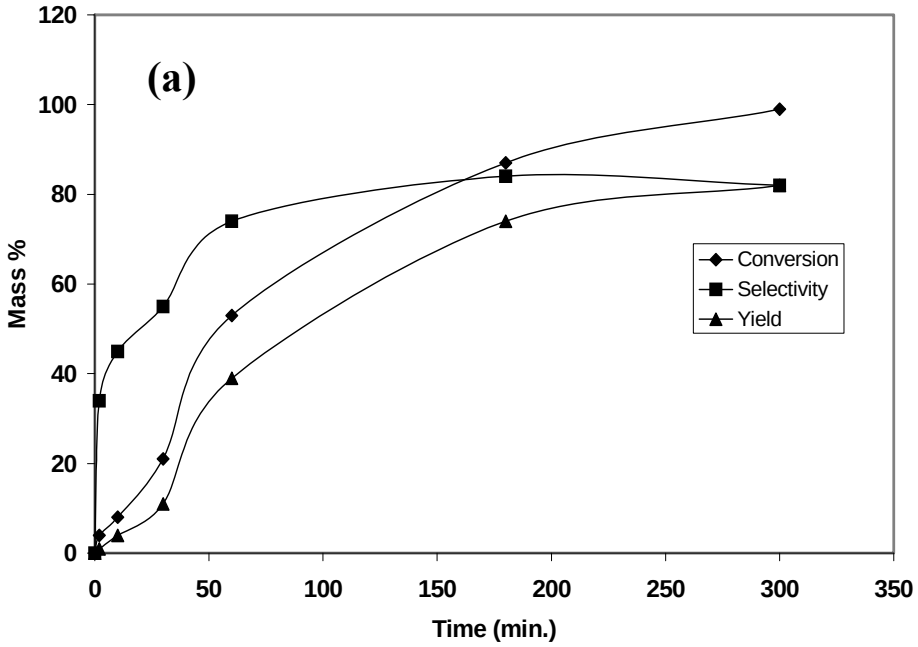

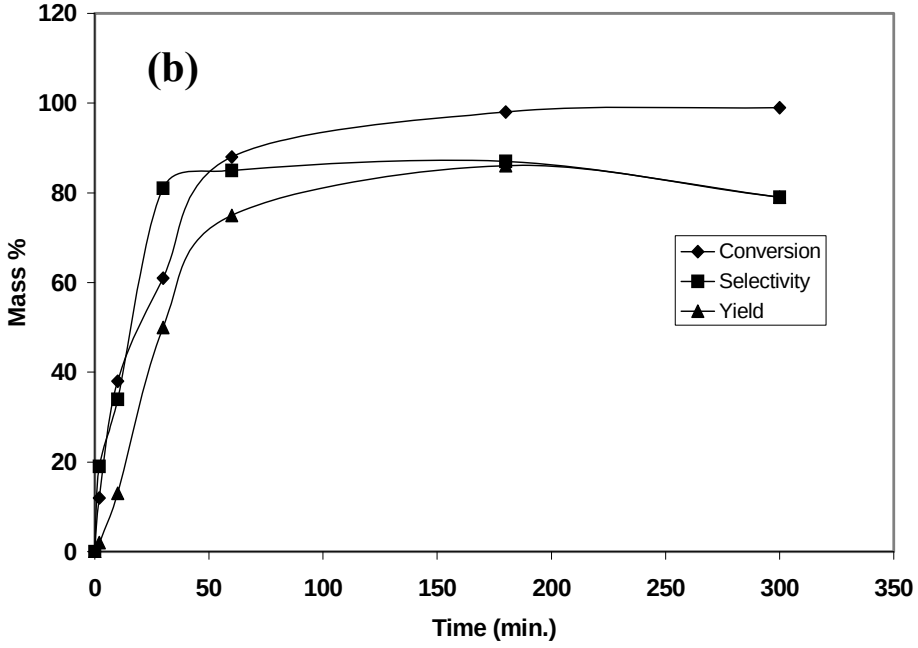

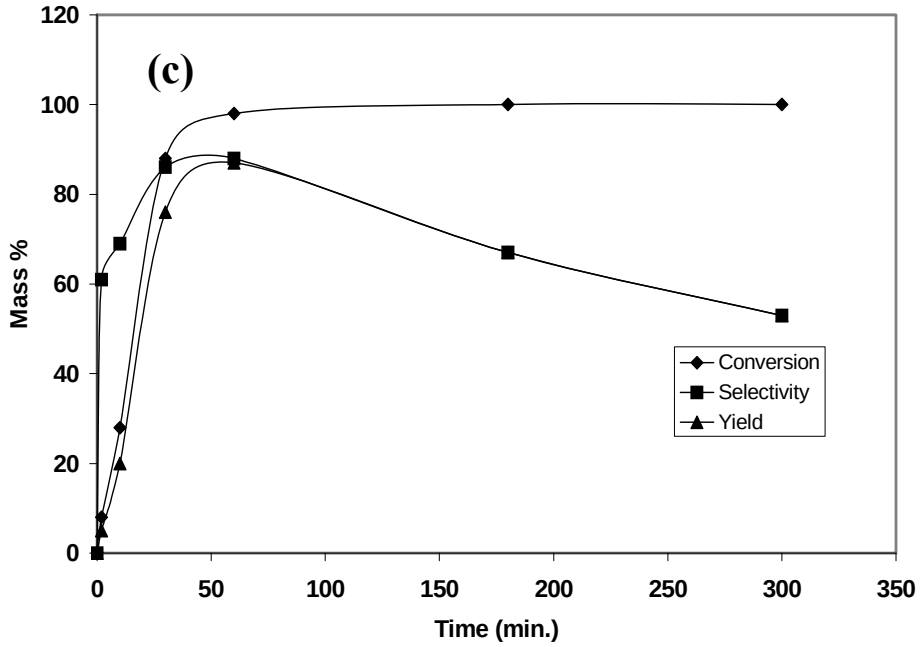

Figure 7.25. Conversion selectivity to citronellal, yield of citronellal as a function of temperature of 80°C (a), 100°C (b) and 120°C (c) over 2.42Pd/CLI-430-IM catalyst at 6 bar, 400 rpm and m= 250 mg

7.2.5. Effect of the Amount of the Catalyst

The amount of the catalyst effect was examined for 150 mg, 250 mg and 400 mg by using the initial citral concentration of 0.1 M in ethanol with a total volume of 100 ml. Figure 7.16 (b) and Figure 7.26 show the product distribution up to the reaction time of 300 min with various amounts of catalysts.

As shown in these figures, the same trend was observed during citral hydrogenation for 150 mg and 250 mg catalyst. The formation of citronellal increased with time. For 250 mg catalyst higher concentration of citronellal (82 %) than 150 mg catalyst (citronellal, 72 %) at 300 min were obtained. For 400 mg catalyst, the formation of citronellal increased rapidly to 89 % for reaction duration of 60 min. Then, at reaction time up to 180 min it remained nearly constant. At higher reaction time, citronellal transformed to the non-identified products. The number of active sites increased with increasing the

amount of the catalyst, as a result the reaction rate increased. Therefore, it can be concluded that the rate of a reaction is proportional to the number of active sites.

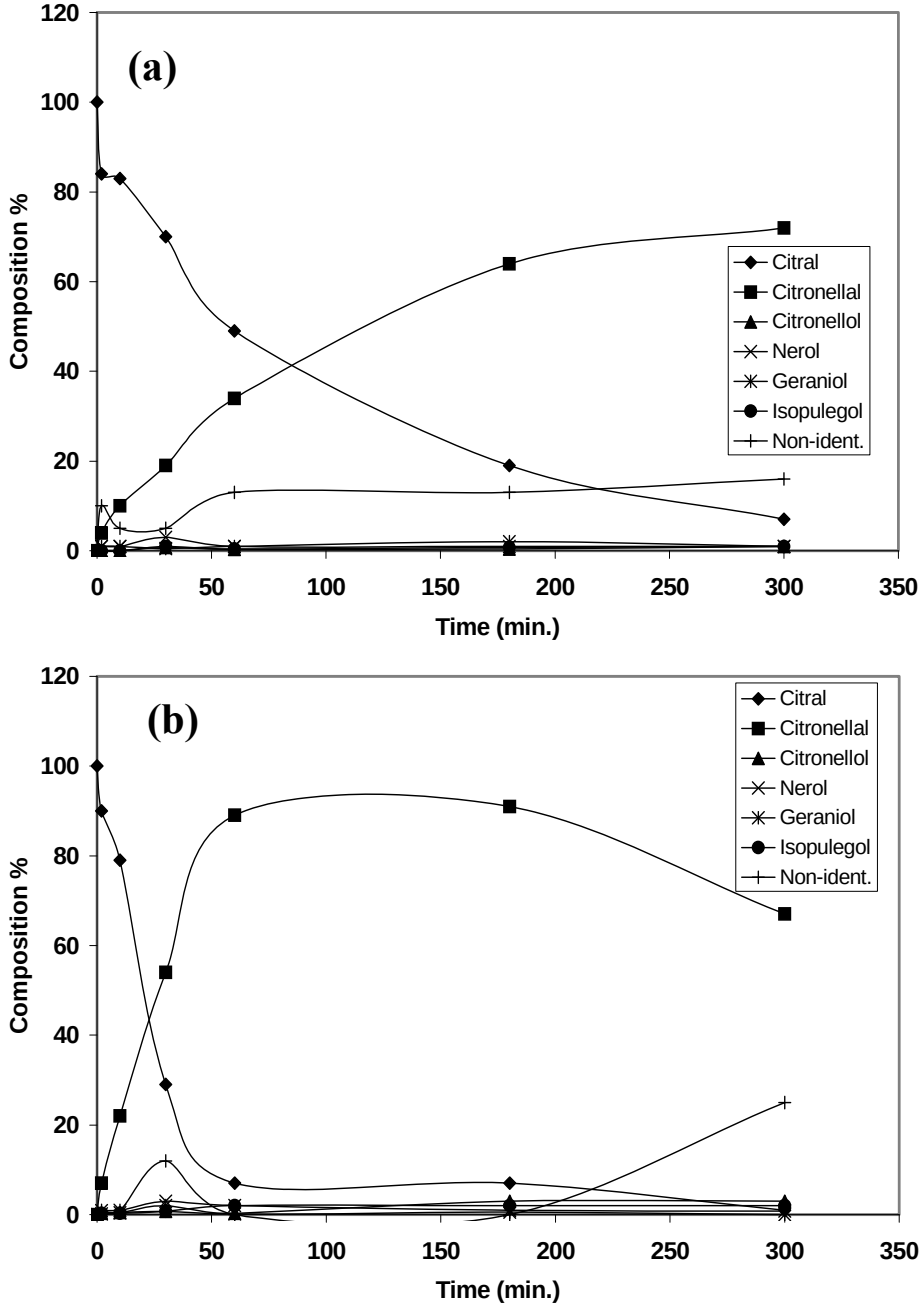

Figure 7.26. Hydrogenation of citral over 2.42Pd/CLI-430-IM catalyst at 80°C, 6 bar, 400 rpm, m= 150 mg (a), m= 400 mg (b)

The plot of conversion, the selectivity to citronellal and the yield of citronellal versus time for various reaction temperatures are given in Figure 7.27.

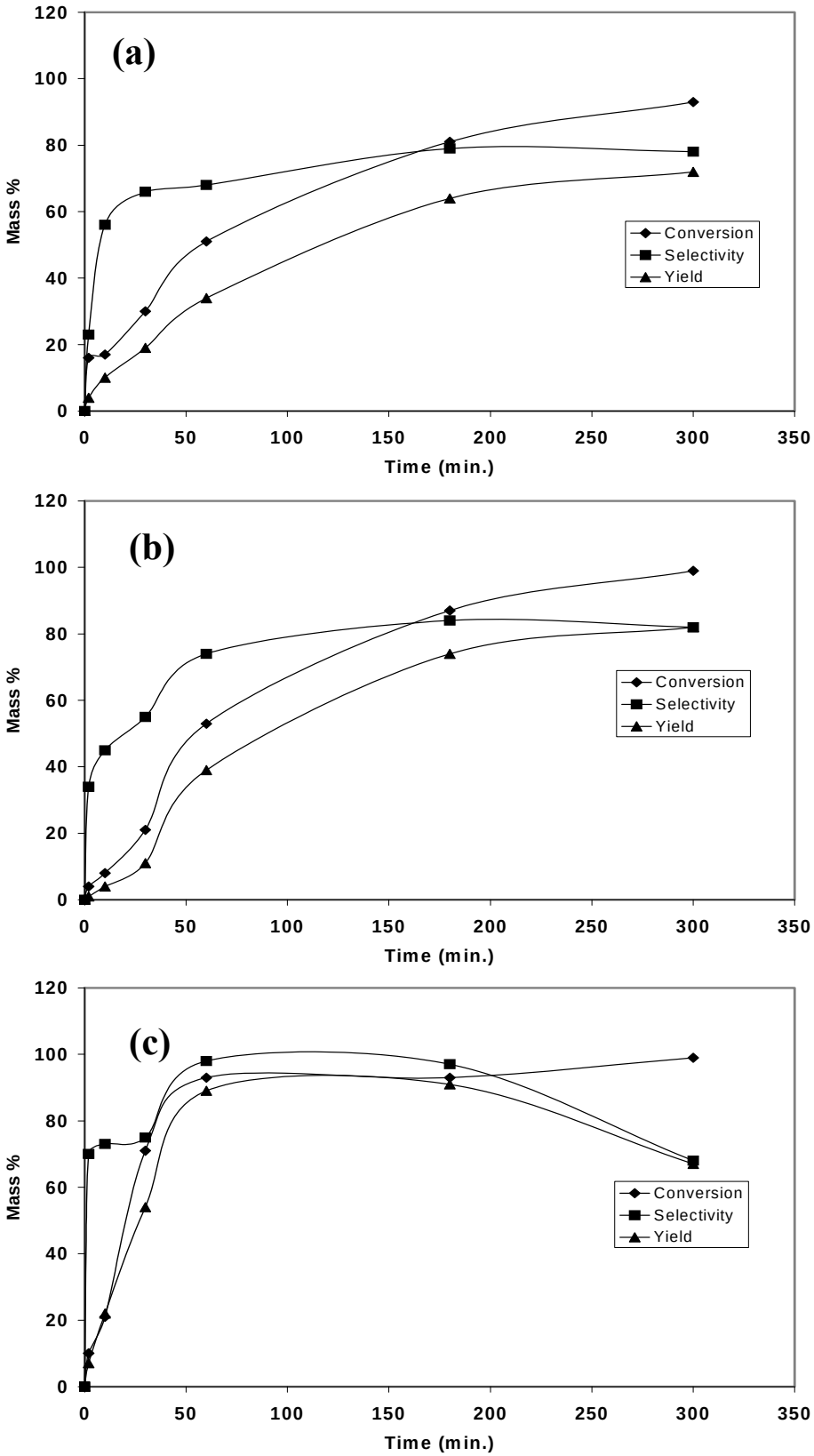

Figure 7.27. Conversion, selectivity to citronellal, yield of citronellal as a function of amount of catalyst of 150 mg (a), 250 mg (b) and 400 mg (c) over 2.42Pd/CLI-430-IM catalyst at 6 bar, 400 rpm

Figure 7.27 shows that the total conversion did not change with increasing the amount of the catalyst, while the selectivity and the yield of citronellal increased. The yield of citronellal attained its maximum value (91 %) with highest amount of the catalyst, after 180 minutes, at 400 mg catalyst. These results indicate that the reaction is performed in the absence of diffusional limitations. This is also supported by the results obtained for different pressures, stirring speeds and temperatures.

7.2.6. Effect of the Ethanol Source

Two different ethanol sources (from Carlo Erba and J.B. Baker) were used as solvents in the experiments. Figure 7.28 shows the product distribution of citral hydrogenation up to the reaction time of 300 min for various ethanol sources.

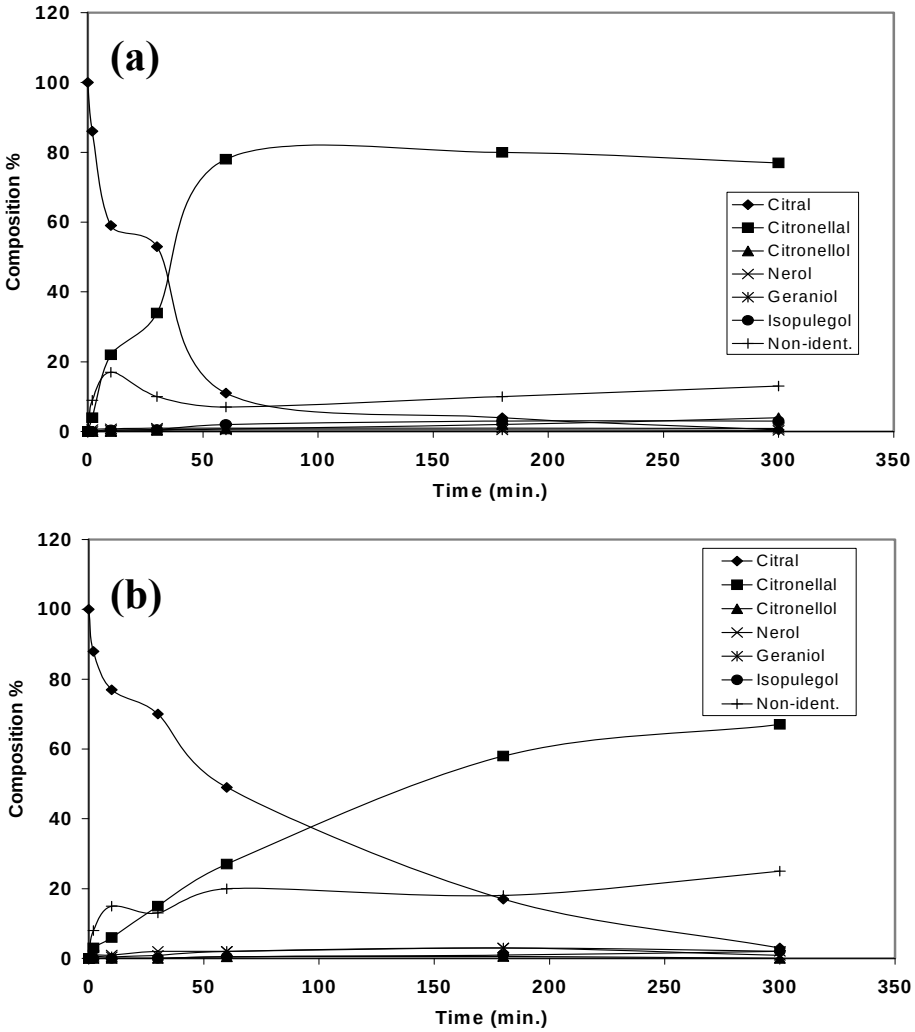

Figure 7.28. Hydrogenation of citral over 2.42Pd/CLI-430-IM catalyst at 100°C, 6 bar, 400 rpm and m= 250 mg in Carlo Erba Ethanol (a), J.B. Baker Ethanol (b)

Product distributions obtained with different ethanol sources were different. As shown in Figure 7.28(a), the formation of citronellal increased rapidly to 78 % in 60 min, then it remained nearly constant up to the reaction time of 180 min. At higher reaction time, the amount of citronellal began to decrease while the amount of non-identified products increased by using Carlo Erba Ethanol. As shown in Figure 7.28(b), when J.B. Baker Ethanol was used the formation of citronellal increased up to 67 % up to reaction time of 300 min. Also non-identified product increased steadily to 22 %.

Figure 7.29. compares the conversion, the selectivity to citronellal and the yield of citronellal for two different ethanols. Although the total conversion did not change with different ethanol sources, selectivity to citronellal decreased from 78 % to 69 % and citronellal yield decreased from 78 % to 67 % when J.B. Baker Ethanol was used instead of Carlo Erba Ethanol. The chemical composition of different ethanol sources is given in Table 7.9. Ethanol having high amount of impurities, gave low selectivity and yield.

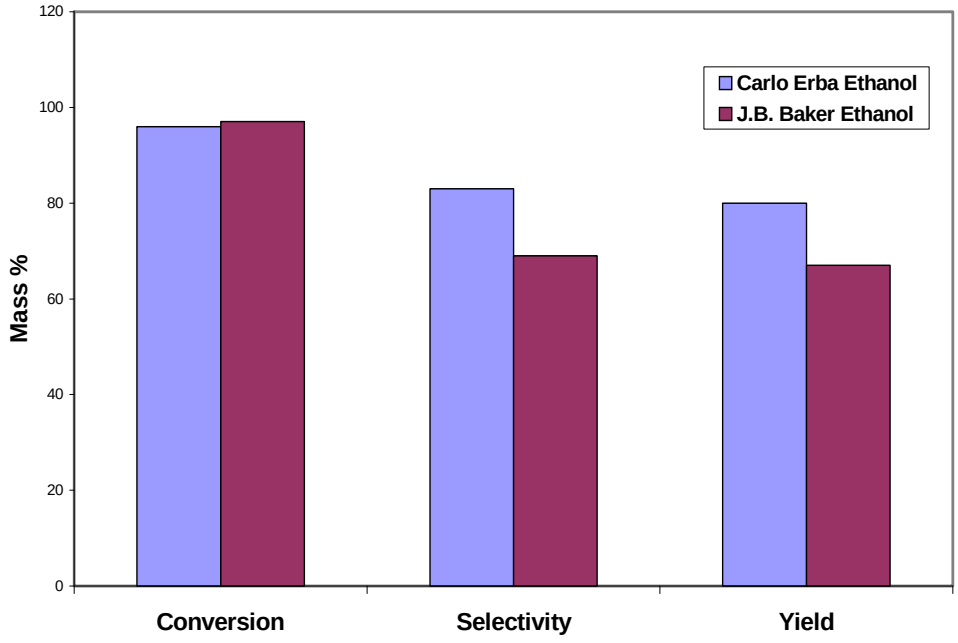

Figure 7.29. Conversion, selectivity to citronellal and yield of citronellal for different ethanol sources t= 300 min over 2.42Pd/CLI-430-IM catalyst at 100°C, 6 bar, 400 rpm and m= 250 mg

Table 7.9. The chemical composition of the different ethanols

Properties	Carlo Erba Ethanol	J.B. Baker
Purity	99.8 %	99.5 %
Impurities		
Acidity	≤ 0.0005 meq/g	Max. 0.001
Alkalinity	≤ 0.0002 meq/q	
Residue on evaporation	≤ 0.0005 %	Max. 0.001
Water (H_2O)	≤ 0.1 %	Max. 0.2

7.2.7. Effect of Catalyst Metal Loading

The metal loading effect was also investigated. Three Pd catalysts (0.72 % Pd, 2.42 % Pd and 5.63 % Pd) prepared with the impregnation method were used. Figure 7.28 (b) and Figure 7.30 show the product distribution up to the reaction time of 300 min with these catalysts.

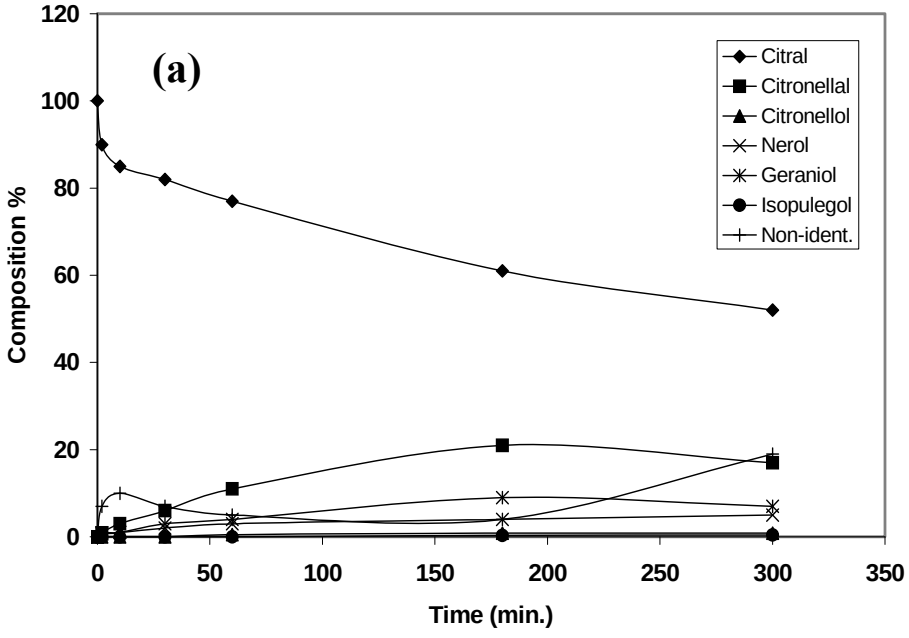

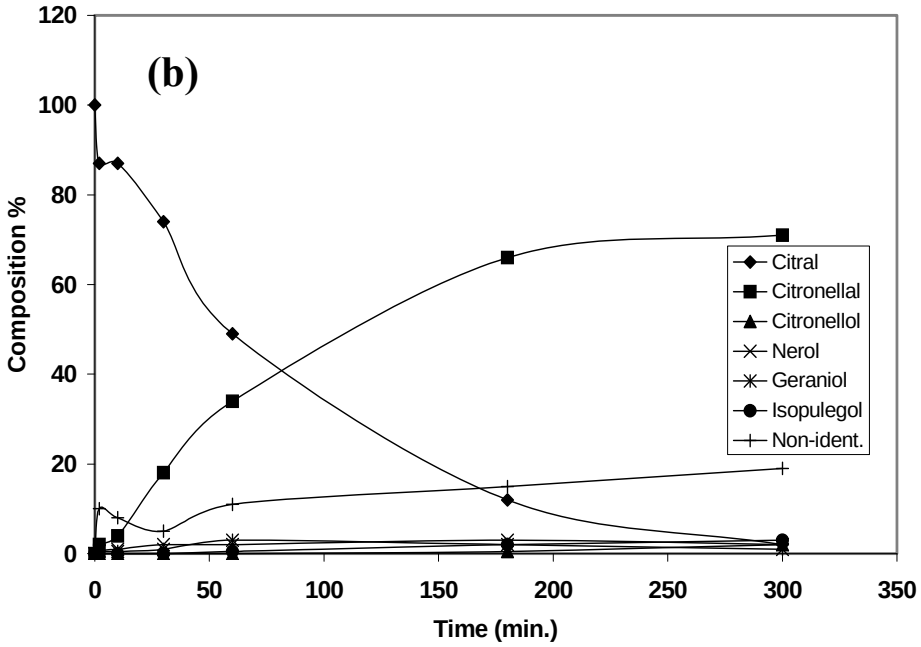

Figure 7.30. Hydrogenation of citral at 100°C, 6 bar, 400 rpm and m= 250 mg over 0.72Pd/CLI-430-IM catalyst (a) and over 5.63Pd/CLI-430-IM catalyst (b)

Citronellal was formed much more slowly for the lower metal loading (0.72Pd/CLI-430-IM). The formation of citronellal (21 %) reached its maximum after 180 min, then it transformed to the non-identified products. Small amount of nerol, geraniol, citronellol and isopulegol were detected. For 2.42Pd/CLI-430-IM and 5.63Pd/CLI-430-IM catalysts, the same trend was observed. The formation of citronellal increased with time. The amount of citronellal increased from 67 % to 71 % with increasing the catalyst metal loading from 2.42 to 5.63 % Pd. Catalytic test results are given in Figure 7.31.

There is a significant change in the yield as metal loading content changed from 0.72 to 2.42 % Pd. However, the change in yield by increasing metal loading from 2.42 to 5.63 % Pd was small.

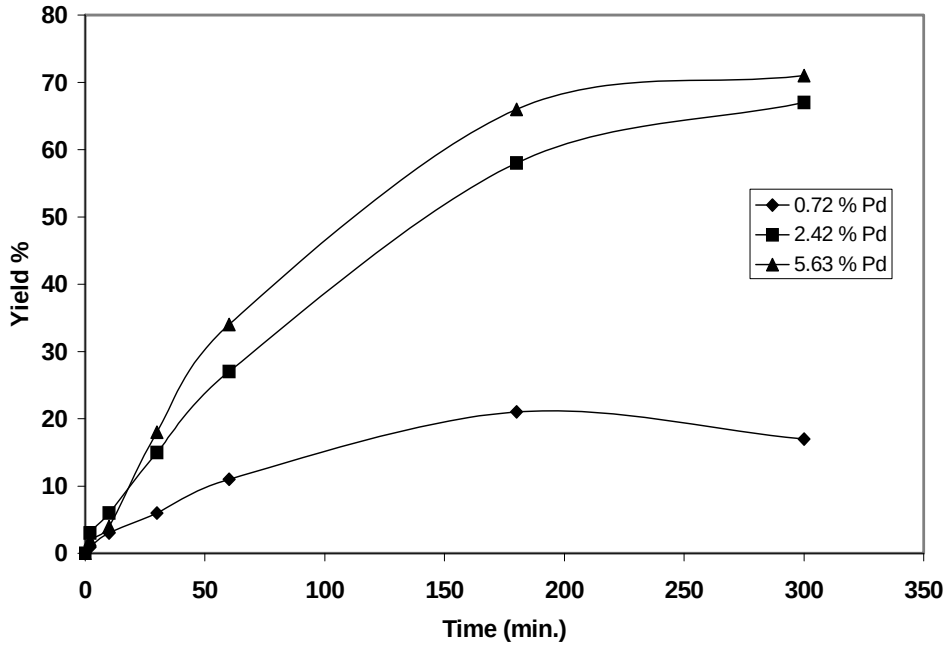

Figure 7.31. The yield of citronellal with different metal loading at 100°C, 6 bar, 400 rpm and m= 250 mg

Figure 7.32. compares conversion, selectivity to citronellal and yield of the citronellal for three different metal loading at 300 min.

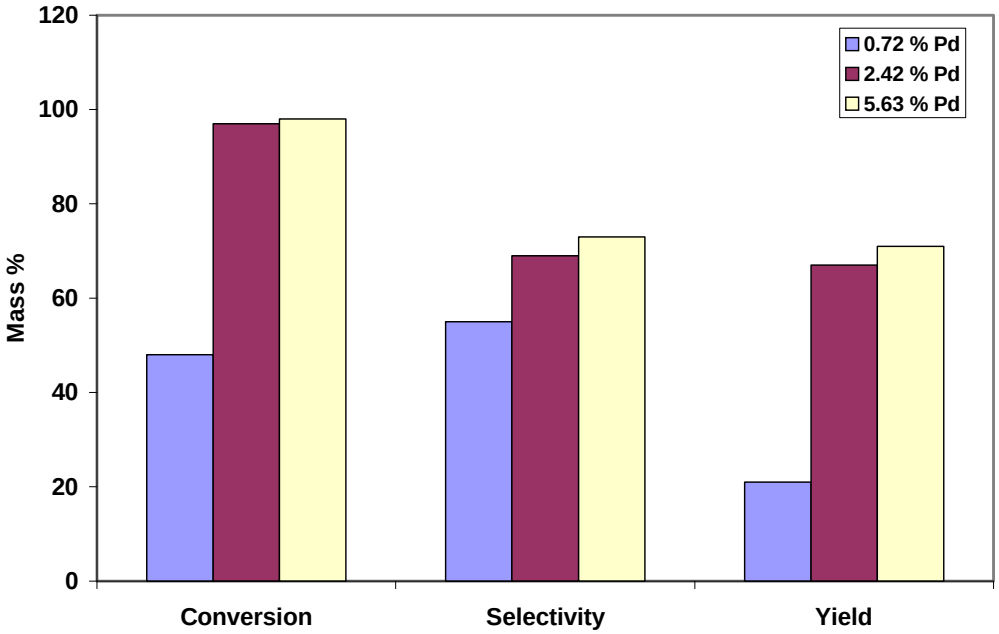

Figure 7.32. Conversion, selectivity to citronellal and yield of citronellal as a function of metal loading at 100°C, 6 bar, 400 rpm and m= 250 mg

It can be seen that an important increase was observed for conversion, selectivity and yield of the citronellal between 0.72Pd/CLI-430-IM and 2.42Pd/CLI-430-IM catalysts.

Higher Pd contents increased the conversion, selectivity and yield of citronellal in small amounts.

Probably, the change in the product distribution was caused by active metal surface area and its dispersion on the catalyst surface, as discussed by Canizares et. al. [22]. They reported that large particles located outside the zeolites are formed when Pd was loaded by impregnation.

7.2.8. Effect of the Catalyst Preparation Method

The performance of the catalysts prepared using different preparation methods namely impregnation and ion exchange were investigated under exactly the same conditions. Figure 7.30 (b) and Figure 7.33 show a product distributions up to the reaction time of 300 min with various preparation methods.

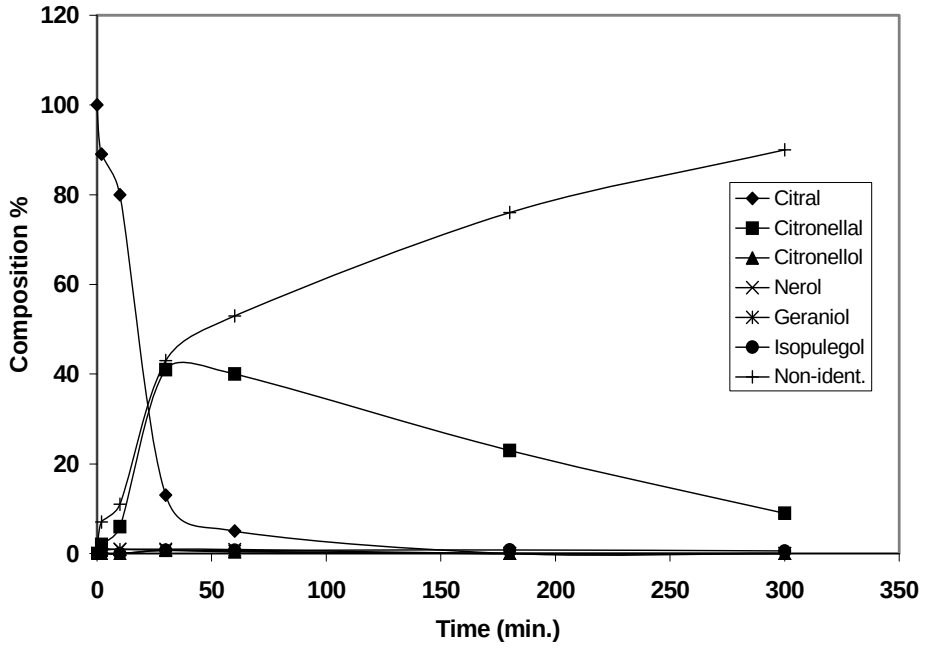

Figure 7.33. Hydrogenation of citral over 5.66Pd/CLI-430-IE catalyst at 100°C, 6 bar, 400 rpm and m= 250 mg

For 5.63Pd/CLI-430-IM catalyst, the formation of citronellal increased steadily to 71 % at reaction time of 300 min. For 5.66Pd/CLI-430-IE catalyst, the hydrogenation of citral nearly completed in the first 40 min. A large amount of non-identified product (43 %),

some citronellal (41 %) and small amount of nerol, geraniol, citronellol (less than 2 %) were formed. At longer reaction duration citronellal is converted to acetals.

The plot of conversion, selectivity to citronellal and yield of citronellal versus time for various preparation methods are given in Figure 7.34. These results indicated that there was rapid hydrogenation of citral in the first 30 min using the catalyst prepared by ion exchange method. After 30 min the selectivity and yield of citronellal decreased and citronellal was converted to acetal.

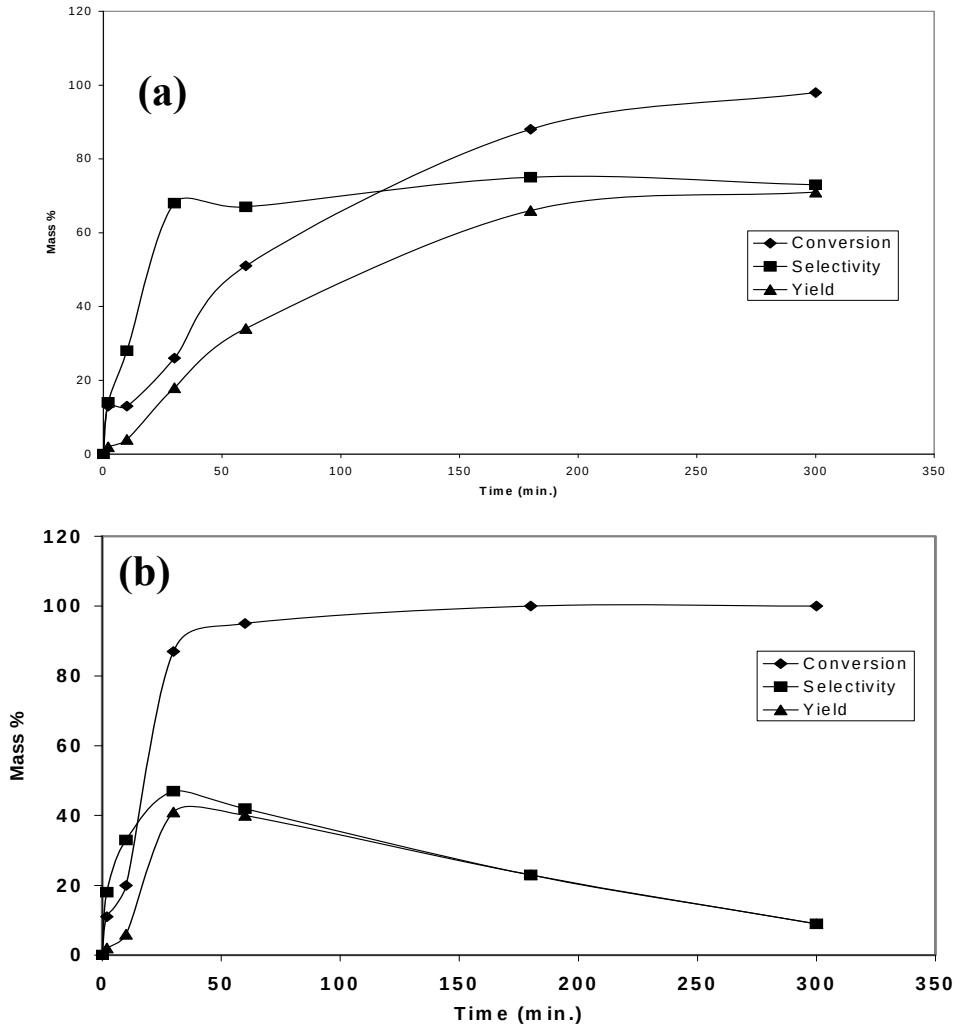

Figure 7.34. Conversion, selectivity to citronellal, yield of citronellal for different catalyst preparation methods; impregnation (a) and ion exchange (b) at 100°C, 6 bar and 400 rpm

With catalyst prepared by impregnation method, higher conversion, selectivity to citronellal and the yield of citronellal were obtained. The rate of hydrogenation was much slower than the catalyst prepared by ion exchange method. This could be due to

metal support interactions. The metal support interaction is weaker and large metal particles are obtained when impregnation is used. On the other hand, the ion exchange technique normally brings about a strong metal-support interaction, which favours the isomerization reaction as discussed by Canizares et al. [22]. The clinoptilolite rich natural zeolite, contains Ca, K, Fe and other minor components which may effect the activity and selectivity of the catalysts as discussed by Mercandante et. al. [43].

7.2.9. Catalyst Deactivation Tests

Three experiments were carried out with 2.42 Pd/CLI-430-IM catalyst in order to study the catalyst deactivation at 80°C, 6 bar and 400 rpm. In the first experiment, the catalyst was calcined under O_2 at 430°C for 2.5 hours and then reduced under H_2 at 400°C for 2 hours prior to the experiment (fresh catalyst). In the second experiment the used catalyst was tested without regeneration (used catalyst). In the third experiment, the used catalyst was regenerated at the same conditions as the fresh catalyst (regenerated catalyst).

Figure 7.16 (b) and Figure 7.35 show a typical product distribution of citral, up to the reaction time of 300 min for the catalysts described above.

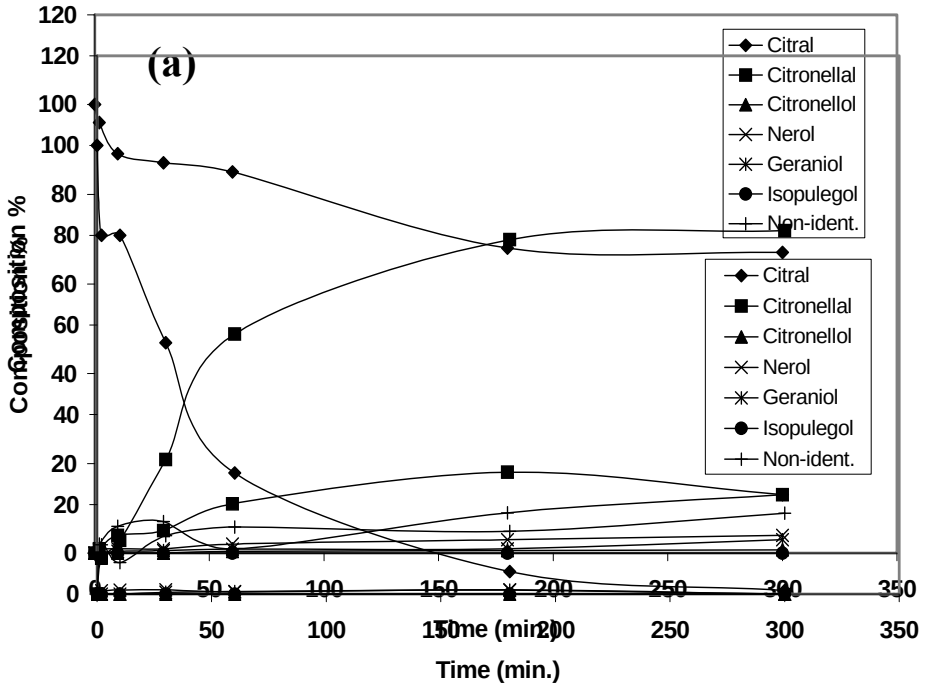

(b)

Figure 7.35. Hydrogenation of citral over 2.42Pd/CLI-430-IM catalyst at 80°C, 6 bar, 400 rpm and m=250 mg for used (a) and regenerated catalysts (b)

Fresh and regenerated catalysts showed similar activity. The formation of citronellal increased to 82 % with time. However used catalyst provided a very slow activity. The amount of citronellal attained its maximum (18 %) after 180 min. Thus this catalyst showed deactivation. Catalyst deactivation by coking is common to reactions involving in hydrocarbons. It may result from a carbonaceous (coke) material being deposited on the surface of a catalyst [1]. The used catalyst was reactivated by regeneration; by burning of the carbon that have been deposited on the catalyst. These results showed that the used catalysts can be regenerated and used again.

The plot of conversion, selectivity to citronellal and yield of citronellal for the hydrogenation of citral for different catalysts are given in Figure 7.36. The conversion (99 %), selectivity to citronellal (82 %) and yield of citronellal (82 %) in the fresh catalyst were as same as the regenerated catalyst. On the other hand, for the used catalyst, the low conversion (33 %), low selectivity to citronellal (38 %) and the low yield of citronellal (13 %) were obtained.

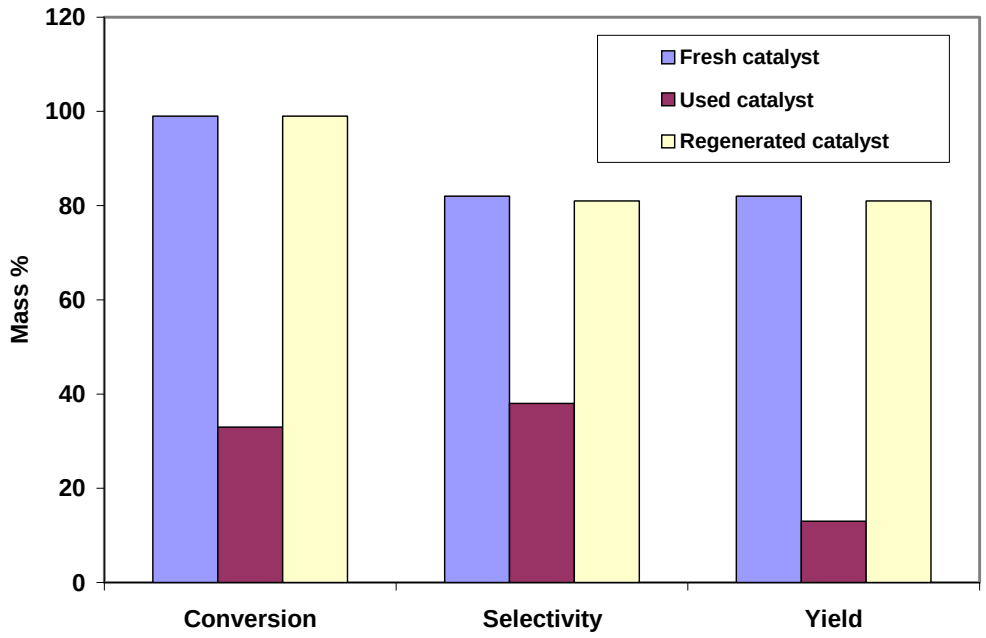

Figure 7.36. Conversion, selectivity to citronellal and yield of citronellal as a function of deactivation effects over 2.42Pd/CLI-430-IM catalyst at 80°C, 6 bar, 400 rpm and m= 250 mg

7.2.10. The Hydrogenation of Citral over Ni/Clinoptilolite Catalysts

The hydrogenation of citral over the 3.12Ni/CLI-430-IM catalyst prepared by impregnation was also investigated. The product distribution of the hydrogenation of citral for this catalyst is shown in Figure 7.37.

This catalyst showed high activity. The formation of citronellal increased to 76 % up to 180 min. At higher reaction time, where citral was completely consumed citronellal began to transform to citronellol. The results showed that Ni catalyst was selective to the citronellal and citronellol; only small amounts of nerol and geraniol were detected. Salmi et. al. [4] reported that nickel catalysts favour the hydrogenation of conjugated double bond and the carbonyl group giving citronellal and citronellol as the main products.

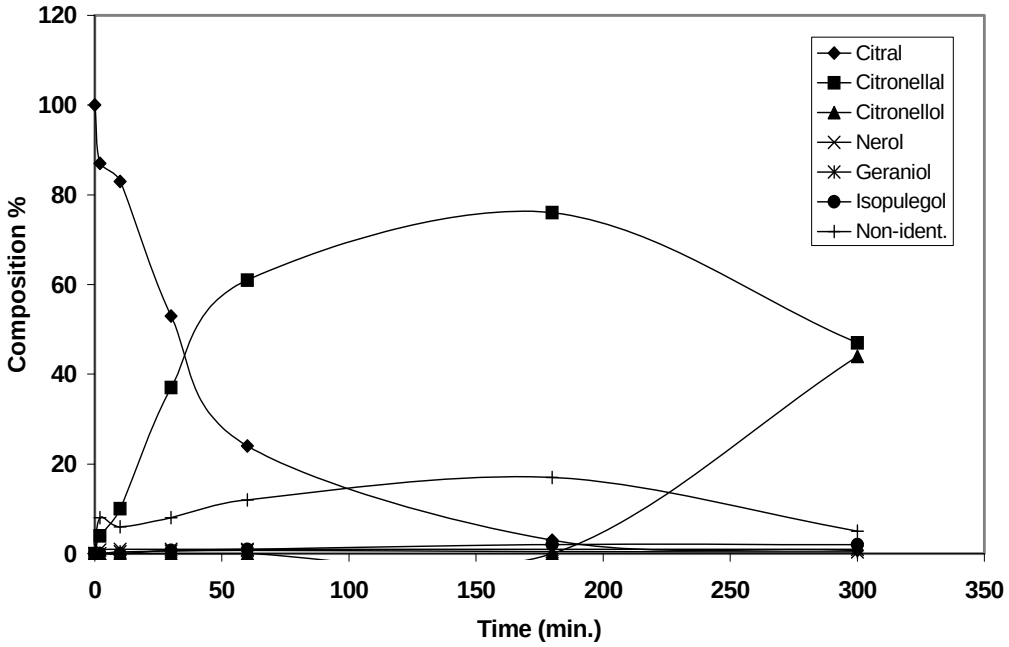

Figure 7.37. Hydrogenation of citral over 3.12Ni/CLI-430-IM catalyst at 100°C, 6 bar, 400 rpm and m=250 mg

The plot of conversion, selectivity to citronellal and yield of citronellal versus time over the 3.12Ni/CLI-430-IM catalyst are given in Figure 7.38. The yield of citronellal attained its maximum (76 %) after 180 minutes.

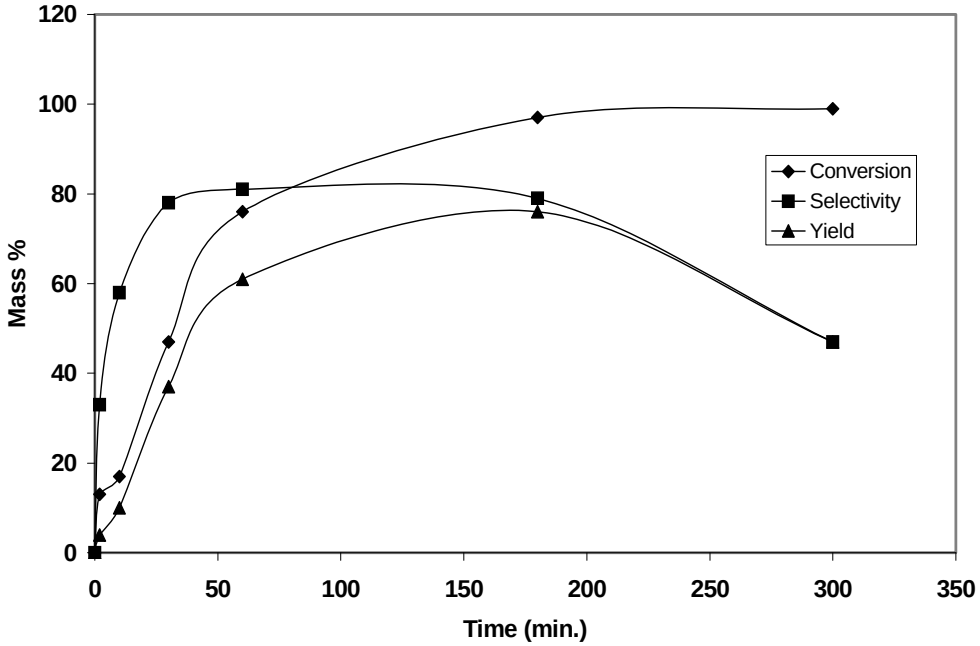

Figure 7.38. The conversion, selectivity to citronellal and yield of citronellal versus time over 3.12Ni-CLI-430-IM at 100°C, 6 bar, 400 rpm and m=250 mg

This catalyst is extremely selective to citronellol once citral is completely consumed. It give little amount of by products (less than 3 %) at reaction time of 300 min. It also indicated that, if the reaction time is extended further close to 100 % selectivity to citronellol could be reached.

7.2.11. Comparation of the Present Study Results with Literature Data on Citral Hydrogenation

Conversions, selectivities to citronellal and unsaturated alcohols reported in the literature and in the present study are given in Table 7.10.

The catalyst prepared in the present study showed better selectivity and conversion compared to the most of the catalysts given in the literature.

Table 7.10. Conversions, selectivities to citronellal and unsaturated alcohols reported in literature and in the present study

Catalyst	P (H_2) (bar)	T (°C)	Time (min)	Conversion (%)	Citronellal Selectivity (%)	Unsaturated Alcohols Selectivity (%)	Reference
2.42Pd/CLI-430-IM	6	80	180	93	98	0	Present Study
3.12 Ni/CLI-430-IM	6	100	300	99	47	44	Present Study
Ru/C	1	60	240	90	32	51	[6]
Ru-Sn/C	1	60	60	30	5	80	[38]
Ru/Al_2O_3	1	60	60	80	45	42	[43]
Pt-Sn/C	1	60	240	90	10	85	[40]
Pt/SiO_2	20	100	120	10	40	47	[45]
Pt/TiO_2	20	100	-	75	7	88	[45]
Ru/Al_2O_3	1	60	350	70	<10	54	[39]
$Ru-Ce/Al_2O_3$	1	60	1000	70	<5	68	[39]
Ru/C	1	60	350	70	<10	38	[39]
Ru-Ce/C	1	60	100	70	<5	82	[39]
$Pd/SiO_2/AlPO_4$	4	30	-	25	81	3	[44]
Pd/Sepiolite	4	30	-	25	73	5	[44]
Rh/SiO_2	1	35	-	100	-	5,2	[42]
$Rh-Sn/SiO_2$	1	35	-	57	-	70	[42]
Rh/MgO	1	35	-	100	-	0	[42]
Rh-Sn/MgO	1	35	-	45	-	10	[42]
$Rh-Ge/SiO_2$	30	70	-	50	45	5	[58]
$Rh-Ge/Al_2O_3$	30	70	-	50	10	80	[58]
Pt-Sn/MgO	20	100	-	90	0	97	[41]

CHAPTER 8

CONCLUSIONS

The following conclusions were drawn from this study.

The main cations in clinoptilolite rich natural zeolite was found to be K and Ca and Si/Al ratio was determined as 5.34. It had platelike crystals. It was verified that the natural zeolite sample was crystalline and rich in clinoptilolite. All samples showed characteristic vibrations of the clinoptilolite framework. With Pd and Ni loading slight shift in the peaks were observed which was attributed to the Pd and Ni interactions.

It was found that, as the Pd content of the catalyst increased its thermal stability improved. 0.72Pd/CLI-430-IM was found to be stable up to 440°C while other Pd catalysts were stable up to 500°C. 3.12Ni/CLI-430-IM was found to be stable up to 450°C.

Catalyst surface area changed with metal loading, catalyst preparation method and catalyst calcination temperature. Highest surface area was found for the impregnated samples calcined at 430°C and for the sample loaded 2.42 % Pd. Ion exchange method provided much more larger surface area catalysts than impregnation method.

Palladium catalysts prepared by impregnation formed unsaturated alcohols (citronellol, nerol and geraniol) in small amounts and citronellal as a major product. Palladium was found to be an effective catalyst for the hydrogenation of the conjugated C=C double bond and a poor catalyst for the hydrogenation of the C=O double bond. Impregnation method created active sites suitable for the formation of saturated aldehydes

The calcination temperatures were very important for high citronellal selectivity and yield. The highest conversion, the selectivity to citronellal and the yield of citronellal were obtained at a calcination temperature of 430°C.

Increasing the amount of the catalyst increased the reaction rates, the selectivity to citronellal and the yield of citronellal. The yield of citronellal attained its maximum value (91 %) fastest at highest amount of catalyst for 400 mg-catalyst/100mL. At higher reaction time, citronellal and citral were transformed to non-identified products.

The ethanol source composition was found to influence the product distribution. Higher yields and selectivities were obtained with a much more pure solvent.

Product distribution changed with metal loading. Catalyst activity increased as active metal loading increased. This was attributed to active metal surface area and its dispersion. Method of metal loading influenced the catalyst activity and selectivity. Pd loaded by impregnation showed better selectivity and activity compared to Pd loaded by ion exchange. Higher metal support interaction in the case of ion exchange could also be responsible for the activities and selectivities observed.

The nature of active metal affected the product distribution. Ni impregnated catalyst showed lower activity compared to Pd impregnated catalyst. With Ni catalysts citronellal and citronellol were the major products. Only small amounts of nerol and geraniol were detected. However their overall selectivities (~90) were similar considering citronellol as citronellal; citronelol is a valuable material as citronellal.

The results of the tests at different pressures, stirring rates, amount of catalyst and catalyst metal loading suggested the reactions were performed in absence of diffusional limitations.

Higher conversion and selectivity to citronellal were obtained when active metals were loaded by impregnation method.

Pd catalysts regained their activities after they were regenerated.

Finally, all of these results showed that the clinoptilolite rich natural zeolites can be used as catalyst and catalyst support for citral hydrogenation.

REFERENCES

1. Luengo, M., A. and Yates, M., "Zeolitic materials as catalysts for organic syntheses"" Journal of Materials Science, 10, 4483-4491, 1995.

2. Singh, U.K. and Vannice, M.A., "Liquid-Phase Hydrogenation of Citral over Pt/SiO_2 Catalysts", Journal of Catalysis, 191, 165-180, 2000.

3. Blackmond, D.G., Oukaci, R., Blanc, B. and Gallezot, P., "Geometric and Electronic Effects in the Selective Hydrogenation of α, β-Unsaturated Aldehydes Over Zeolite-Supported Metals", Journal of Catalysis, 131, 401-411, 1991.

4. Tiainen, L.P., Arvela, P.M. and Salmi, T., "Modelling of citral hydrogenation kinetics on an Ni/Al_2O_3 catalyst", Catalysis Today, 48, 57-63, 1999.

5. Coupe, J.N., Jordao, E., Fraga, M.A. and Mendes, M.J., "A comparative study of SiO_2 supported Rh-Sn catalysts prepared by different methods in the hydrogenation of citral", Applied catalysis A: General, 199, 45-51, 2000.

6. Galvagno, S. and Milone, C., "Influence of metal particle size in the hydrogenation of citral over Ru/C", Catalysis Letters, 18, 349-355, 1993.

7. Gallezot, P. and Richard, D., "Selective Hydrogenation of α,β-Unsaturated Aldehydes", Catal. Rev. – Sci. Eng., 40(1&2), 81-126, 1998.

8. Malathi, R. and Viswanath, R.P., "Citral hydrogenation on supported platinum catalysts", Applied Catalysis A: General, 208, 323-327, 2001.

9. Davis, M.E., "Zeolite-based catalysts for chemical synthesis", Microporous and Mesoporous Materials, 21, 173-182, 1998.

10. Stead, K., Ouki, S.K. and Ward, N.I., "Natural Zeolites – Remediation Technology for the 21st century?" 1-4.

11. Ponec, V., "On the role of promoters in hydrogenations on metals; α,β-unsaturated aldehydes and ketones", Applied Catalysis A: General, 149, 27-48, 1997.

12. Salmi, T., Arvela, P.M., Toukoniitty, E., Neyestanaki, A.K., Tiainen, L.P., Lindfors, L.E., Sjöholm, R. and Laine, E., "Liquid-phase hydrogenation of citral over an immobile silica fibre catalyst", Applied Catalysis A: General, 196, 93-102, 2000.

13. Delbecq, F. and Sautet, P., "Competitive C=C and C=O Adsorption of α-β Unsaturated Aldehydes on Pt and Pd Surfaces in Relation with the Selectivity of

Hydrogenation Reactions: A Theoretical Approach", Journal of Catalysis, 152, 217-236, 1995.

14. Noller, H. and Lin, W.M., "Activity and Selectivity of Ni-Cu/Al_2O_3 catalysts for Hydrogenation of Crotonaldehyde and Mechanism of Hydrogenation", Journal of Catalysis, 85, 25-30, 1984.

15. Sinfelt, J.H., "Role of surface science in catalysis", Surface Science, 500, 923-946, 2002.

16. Satterfield, C., N., "Heterogenous Catalysis in Industrial Practice", McGraw-Hill, 1991.

17. Gates, B., C., "Catalytic Chemistry", John Wiley & Sons, 1992.

18. Zaera, F., "The surface chemistry of catalysis: new challenges ahead", Surface Science, 500, 947-965, 2002.

19. Blaser, H., U., "Heterogeneous catalysis for fine chemicals production", Catalysis Today, 60, 161-165, 2000.

20. Richardson, J.T., "Principles of catalyst Development", University of Houston, Houston, Texas, 1989.

21. Fogler, H., S., "Elements of Chemical Reaction Engineering", The University of Michigan, Michigan, 1999.

22. Canizares, P., Lucas, A., Dorado, F., Duran, A. and Asencio, I., "Characterization of Ni and Pd supported on H-mordenite catalysts: Influence of the metal loading method", Applied Catalysis A: general, 169, 137-150, 1998.

23. Perego, C. and Villa, P., "Catalyst preparation methods", Catalysis Today, 34, 281-305, 1997.

24. Breck, D., W., "Zeolite Molecular Sieves", Wiley-Interscience Publication, 1974.

25. Armenta, G., A., Ramirez, G., H., Loyola, E., F., Castaneda, A., U., Gonzales, R., S., Munoz, C., T., Lopez, A., J. and Castellon, E., R., "Adsorption Kinetics of CO_2, O_2, N_2, and CH_4 in Cation-Exchanged Clinoptilolite", J. Phys. Chem. B, 105, 1313-1319, 2001.

26. Zhedrine, J., Q., "General overview of the characteriation of zeolites", Zeolite Microporous Solids: Synthesis, Structure and Reactivity, 1992.

27. Naccache, C. and Taarit, Y., B., "Transition Metal Exchanged Zeolites: Physical and Catalytic Properties", Zeolites: Science and Technology, 80, 373-396, 1984.

28. Denkewicz, R., P., "Zeolite Science: An Overview", The Pennsylvania State University, University Park.

29. Inglezakis, V.J., Hadjiandreou, K.J., Loizidou, M.D. and Grigoropoulou, H.P., "Pretreatment of Natural Clinoptilolite in a Laboratory-Scale Ion Exchange Packed Bed", Wat. Res., 35, 2161-2166, 2001.

30. Hernandez, M.A., "Nitrogen-Sorption Characterization of the Microporous Structure of Clinoptilolite-Type Zeolites", Journal of Porous Materials, 7, 443-454, 2000.

31. Zhao, D., Cleare, K., Oliver, C., Ingram, C., Cook, D., Szostak, R. and Kevan, L., "Characteristics of the synthetic heulandite-clinoptilolite family of zeolites", Microporous and Mesoporous Materials, 21, 371-379, 1998.

32. Gottardi, G. and Galli, E., "Natural Zeolites", Springer-Verlag, Berlin, 1985.

33. Choo, H. and Kevan, L., "Catalytic Study of Ethylene Dimerization on Ni(II)-Exchanged Clinoptilolite", J. Phys. Chem. B., 105, 6353-6360, 2001.

34. Ackley, M.W. and Yang, R.T., "Adsorption Characteristics of High-Exchange Clinoptilolites", Ind. Eng. Chem. Res., 30, 2523-2530, 1991.

35. Ackley, M.W. and Yang, R.T., "Diffusion in Ion-Exchanged Clinoptiololites", AIChE Journal, 37, 1645-1656, 1991.

36. Iznaga, I., R., Gomez, A., Fuentes, G., R., Aguilar, A., B. and Ballan, J., S., "Natural clinoptilolite as an exchanger of Ni^{2+} and NH^{++} ions under hydrothermal conditions and high ammonia concentration", Microporous and Mesoporous Materials, 53, 71-80, 2002.

37. Arcoya, A., Gonzales, J.A., Llabre, G., Seoane, X.L. and Travieso, N., "Role of the countercations on the molecular sieve properties of a clinoptilolite", Microporous Materials, 7, 1-13, 1996.

38. Galvagno, S. and Milone, C., "Hydrogenation of citral over Ru-Sn/C", Catalysis Letters, 17, 55-61, 1993.

39. Baeza, B.B., Ramos, I.R. and Ruiz A.G., "Influence of Mg and Ce addition of ruthenium based catalysts used in selective hydrogenation of α,β-unsaturated aldehydes", Applied Catalysis A: General, 205, 227-237, 2001.

40. Neri, G., Milone, C., Donato, A., Mercadante, L. and Visco, A.M., "Selective Hydrogenation of Citral over Pt-Sn Supported on Activated Carbon", J. Chem. Tech. Biotechnol., 60, 83-88, 1994.

41. Recchia, S., Dossi, C., Poli, N., Fusi, A., Sordelli, L. and Psaro, R., "Outstanding Performances of Magnesia-Supported Platinum-Tin Catalysts for Citral Selective Hydrogenation", Journal of Catalysis, 184, 1-4, 1999.

42. Sordelli, L., Psaro, R., Vlaic, G., Cepparo, A., Recchia, S., Dossi, C., Fusi, A. and Zanoni, R., "EXAFS Studies of Supported Rh-Sn catalysts for Citral Hydrogenation", Journal of Catalysis, 182, 186-198, 1999.

43. Mercandante, L., Neri, G., Milone, C., Donato, A. and Galvagno, S., "Hydrogenation of α,β-unsaturated aldehydes over Ru/Al_2O_3 catalysts", Journal of Molecular Catalysis A: Chemical, 105, 93-101, 1996.

44. Aramendia, M.A., Borau, V., Jimenez, C., Marinas, J.M., Porras, A. and Urbano, F.J., "Selective Liquid-Phase Hydrogenation of Citral over Supported Palladium", Journal of Catalysis, 172, 46-54, 1997.

45. Singh, U.K. and Vannice, M.A., "Influence of metal-support interactions on the kinetics of liquid-phase citral hydrogenation", Journal of Molecular Catalysis A: Chemical, 163, 233-250, 2000.

46. Singh, U.K., Sysak, M.N. and Vannice, M.A., "Liquid-Phase Hydrogenation of Citral over Pt/SiO_2 Catalysts", Journal of Catalysis, 191, 181-191, 2000.

47. Tsitsishvili, G.V., Andronikashvili, T.G. and Kirov, G.N., "Natural Zeolites", Ellis Horwood Limited, 1st Edition, New York, 40, 1992.

48. Knowlton, G.D. and White, T.R., "Thermal Study of Types of Water associated with Clinoptilolite", Clays and Clay Minerals, Vol. 29, No. 5, 403-411, 1981.

49. Aramendia, M.A., Borau, V., Jimenez, C., Marinas, J.M., Porras, A. and Urbano, F.J., "Chemoselective and regioselective reduction of citral (3,7-dimethyl-2,6-octadienal) by gas-phase hydrogen transfer over acid-basic catalysts", Applied Catalysis A: General, 172, 31-40, 1998.

50. Aramendia, M.A., Borau, V., Jimenez, C., Marinas, J.M., Ruiz, J.R. and Urbano, F.J., "Liquid-phase heterogeneous catalytic transfer hydrogenation of citral on basic catalysts", Journal of Molecular Catalysis A: Chemical, 171, 153-158, 2001.

51. Aramendia, M.A., Borau, V., Jimenez, C., Marinas, J.M., Ruiz, J.R. and Urbano, F.J., "Catalytic transfer hydrogenation of citral on calcined layered double hydroxides", Applied Catalysis A: General, 206, 95-101, 2001.

52. Blackmond, D., G., Waghray, A., Oukaic, R., Blanc, B. and Gallezot, P., "Selective Hydrogenation of unsaturated aldehydes over zeolite-supported metals", Heterogenous Catalysis and Fine Chemicals II, 145-152, 1991.

53. Neri, G., Mercadante, L., Milone, C., Pietropaolo, R. and Galvagno, S., "Hydrogenation of citral and cinnamaldehyde over bimetallic $Ru\text{-}Me/Al_2O_3$ catalysts", Journal of Molecular Catalysis A: Chemical, 108, 41-50, 1996.

54. Reyes, P., Rojas, H., Pecchi, G. and Fierro, J., L., G., “Liquid-phase hydrogenation of citral over Ir-supported catalysts”, Journal of Molecular Catalysis A: Chamical, 3398, 1-7, 2001.

55. Singh, U.K. and Vannice, M.A., “Kinetics of liquid-phase hydrogenation reacions over supported metal catalysts – a review”, Applied Catalysis A: general, 213, 1-24, 2001.

56. Tin, K.C., Wong, N.B., Li, R.X, Li, Y.Z. and Li, X.J., “Studies on catalytic hydrogenation of citral by water-soluble palladium complex”, Journal of Molecular Catalysis A: Chemical, 137, 113-119, 1999.

57. Esenli, F., Kumbasar, I., “Clays and Clay Mineralogy”, 46, 679-686, 1998.

58. Reyes, P., Rojas, H., Pecchi, G. and Fierro, J.L.G., “Liquid-phase hydrogenation of citral over Ir-supported catalysts”, Journal of Molecular Catalysis A: Chemical, 137, 1-7, 2001.